UNIVERSITY OF GHANA

COLLEGE OF BASIC AND APPLIED SCIENCES

Radiation Dose and Image Quality in Computed Tomography Examinations: A Comparison between Automatic Exposure Control (AEC) and Fixed Tube Current (FTC) Techniques.

BY

HAMZA SULEMANA

(10506581)

THIS THESIS IS SUBMITTED TO THE UNIVERSITY OF GHANA, LEGON IN PARTIAL FULFILLMENT OF THE REQUIREMENT FOR THE AWARD OF MPHIL MEDICAL PHYSICS DEGREE

DEPARTMENT OF MEDICAL PHYSICS

GRADUATE SCHOOL OF NUCLEAR AND ALLIED SCIENCES

JULY, 2016

DECLARATION

I hereby declare that with the exception of references to other people's work which have been duly acknowledged, this thesis is the results of my own research work and no part of it has been presented for another degree in this university or elsewhere.

Sign……………………………........ Date ………………………………

Hamza Sulemana

(Candidate)

I hereby declare that the preparation of this thesis was supervised in accordance with the guidelines of the supervision of Thesis work laid down by the University of Ghana.

Sign………………………….. Sign……………………………

Prof. Cyril Schandorf Dr. Stephen Inkoom

(Principal Supervisor) (Co – Supervisor)

Date ……………………………. Date…………………………..

Sign………………………………

Mr. Edem Sosu

(Co – Supervisor)

Date …………………………….

ABSTRACT

The aim of this study was to evaluate and compare the radiation doses imparted to patients undergoing computed tomography (CT) examinations and image quality with the use of automatic exposure control (AEC) and fixed tube current (FTC) techniques using a head and body phantom in a Siemens emotion 16-slice multidetector computed tomography (MDCT) scanner. The head and body phantoms were scanned with AEC activated and with FTC for routine head, chest, abdomen and pelvis CT examinations. All parameters were kept constant for each technique except with varying tube current time product (mAs) for the FTC technique. Dose measurements were performed using RTI barracuda system with electrometer, and CT dose Profiler probe. Organ and effective doses were calculated using CT-Expo software. Subsequently image quality between the AEC and FTC technique were assessed using the Catphan 700 image quality phantom. The volume computed tomographic dose index ($CTDI_{vol}$) values estimated with the AEC technique were; 32.8 mGy, 6.7 mGy, 14.3 mGy, and 11.7 mGy for head, chest, abdomen and pelvis respectively. The estimated volume CTDI values with the FTC technique had a range of 32.9-53.0 mGy for head, 9.5-26.2 mGy for chest, 9.5-24.2 mGy for abdomen and 9.5-26.0 mGy for pelvis respectively. The DLP values for the AEC technique were; 593 mGy.cm, 108 mGy.cm, 240 mGy.cm, and 190 mGy.cm for head, chest, abdomen and pelvis examinations respectively. With the FTC technique, the DLP values had a range of 571-946 mGy.cm for head, 284-780 mGy.cm for chest, 165-543 mGy.cm for abdomen, and 250-690 mGy.cm for pelvis respectively. Compared with the FTC technique, the use of AEC resulted in a mean dose reduction of up to 19.4% for CTDIvol and 18.2% for DLP for the head phantom and a mean dose reduction range of 12% - 59.4% for $CTDI_{vol}$ and 7.1% - 78.3% for DLP for the body phantom. The overall image quality test between AEC

and FTC techniques for spatial resolution and low contrast detectability show no statistical significant differences ($P > 0.05$). There was statistical significant difference in the contrast to noise ratio scores between the AEC and FTC techniques($P = 0.008$) with about 35% noise in the AEC images than the FTC images acquired. From the study results, the use of AEC showed a considerable dose reduction compared with the FTC technique with adequate image quality performance. Thus the use of AEC technique is promising and will benefit patients with less radiation being delivered to them in CT examinations.

DEDICATION

I dedicate this work to my late father Chief Moses Sulemana and my mother for been parents in the first place, for their care and endless support throughout my life.

I will also like to dedicate this work to my two lovely sisters Rosemary and Margret, my siblings', my late grandfather and grandmother, family members, friends and love ones for their support, care and well wishes.

My final dedication goes to my fiancé for her continuous care, tolerance and support for all this while.

ACKNOWLEDGEMENTS

I would like to express my deepest gratitude to my thesis supervisors **Prof. Cyril Schandorf, Dr. Stephen Inkoom and Mr. Edem Sosu** for their sympathetic comments and consistent guidance throughout the preparation of this thesis. I am especially grateful for their advice on ingenuity and leadership, which will without doubt help me throughout the thesis work.

I am also very appreciative to all the lecturers, students and workers of the School of Nuclear and Allied Sciences. I would like to express sincere gratitude to the management, staff and all members of the oncology department at Sweden Ghana Medical Centre for their hospitality during my time at the facility. My special thanks and appreciation goes to the Mr. George Felix Acquah (Chief medical physicist) for his tremendous support, help and guidance during my data collection.

I am honoured to share this distinguished degree to all my siblings, family members and friends who have been my support for all this while. It is with great comfort that I share my happiness from this accomplishment with my two sisters **Rosemary** and **Margaret** who are so dearest to my heart for their tremendous support throughout the whole period of this study. It is always good to think big and try hard.

Finally, my special thanks goes to my head of department Prof. Augustine Kwame Kyere for his kindness and fatherly advice he showed me throughout the period of my study in SNAS. This thesis would not have been completed without the help and support from my family and friends. Thank you, I love you all very much.

TABLE OF CONTENTS

LIST OF FIGURES

LIST OF TABLES

LIST OF ABBREVIATIONS

ACS	Automatic Current Selection
AEC	Automatic Exposure Control
ALARA	As Low As Reasonable Achievable
ATCM	Automatic Tube Current Modulation
BB	Ball Bearing
CAT	Computed Axial Tomography
CNR	Contrast to Noise Ratio
CAP	Chest, Abdomen Pelvis
CR	Contrast Resolution
CT	Computed Tomography
CTA	Computed Tomography Angiography
CTDI	Computed Tomography Dose Index
$CTDI_{vol}$	Volume Computed Tomography Dose Index
$CTDI_{w}$	Weighted Computed Tomography Dose Index
CTDP	Computed Tomography Dose Profiler
CTP	Catphan Phantom
D-DOM	Dynamic Modulation
DLP	Dose Length Product
DR	Dose Reduction
DRLs	Diagnostic Reference Levels
EBM	Electronic Beam Tomography
FOV	Field of View
FTC	Fixed Tube Current
HU	Hounsfield Unit
IAEA	International Atomic Energy Agency

ICRP	International Commission on Radiological Protection
IEC	International Electro technical Commission
KVp	Kilo voltage Potential
mA	MilliAmperage
mAs	MilliAmperage seconds
MCDT	Multi Computed Detected Tomography
MDCT	Multi Detector Computed Tomography
MRI	Magnetic Resonance Imaging
MSAD	Multi Scan Average Dose
MSCT	Multi Slice Computed Tomography
MTF	Modulation Transfer Function
NRA	Nuclear Regulatory Authority
NRPB	National Radiological Protection Board
NI	Noise Index
RDLs	Reference Dose Levels
ROI	Region of interest
SD	Standard Deviation
SNR	Signal to Noise Ratio
SPR	Scan Projection Radiography
SPSS	Statistical Package for Social Sciences
SR	Spatial Resolution
SSCT	Single Slice Computed Tomography
UNSCEAR	United Nations Scientific Committee on the Effects of Atomic Radiation
VGA	Visual Grading Analysis
Yrs.	Years
Z-DOM	Longitudinal Dose Modulation

LIST OF SYMBOLS AND CONSTANT

$\frac{I_o}{I}$	attenuation factor of an object
U_{en}/p	Mass energy absorption coefficient
C	Chamber correction factor
$D\ (Z)$	Dose measured along the z-axis
$D_{org.T}$	Organ dose
E	Effective dose
E_{DLP}	Effective dose conversion factor
f	Exposure to dose conversion factor
f_A	Effect of reconstruction algorithm
K	Conversion factor
n	Number of tomographic slice
P	Statistical Value of significant difference
T	Slice thickness
σ	Standard deviation
ε	System efficiency

CHAPTER ONE

1.0 INTRODUCTION

OVERVIEW

This chapter gives the general background of the thesis and a general overview of the research problem. The research objectives, justification, scope and limitations are also stated and finally end with organization of the thesis.

1.1 BACKGROUND

Computed tomography (CT) was introduced in medical imaging in 1974. Its usage has largely replaced other imaging modalities such as ultrasound and magnetic resonance imaging (MRI) that are limited in demonstrating anatomical and pathological structures for accurate diagnosis (Livingstone et al., 2009). The clinical applications of CT has increased in recent years due to the rapid technological developments and innovations in the imaging field.

The advent of multislice CT (MSCT) makes it possible for rapid volume acquisition and has opened new diagnostic fields such as CT angiography and CT colonography. The use of MSCT has resulted to about 30 to 50% increase in radiation dose to patients primarily due to scan overlap, positioning of the x-ray tube closer to the patient, over beaming, increased significance of over scanning and possibly increased scattered radiation with wider x-ray beams (McCollough & Zink, 1999; Hidajat et al., 1999). This has raised concerns about the radiation dose that patients are exposed to during CT examination. The use of imaging modalities utilizing ionizing radiation for diagnosis is on the increase and has resulted in an increase in the collective radiation exposures.

According to the United Nations Scientific Committee on the Effects of Atomic Radiation (UNSCEAR) survey report on Medical Radiation Usage and Exposures, the contribution of CT to total global collective dose is about 43% of the total collective dose due to diagnostic medical radiology (UNSCEAR, 2008). It was estimated in 2005-2006 in the United Kingdom that, about 60% of the total radiology collective effective dose came from CT scanning (Hall & Brenner, 2008). In Germany, about 82% of the collective effective dose for cancer patients from all X-ray procedures was due to CT examination (Brix et al., 2009) and in the United States of America, despite comprising only 11 - 13% of all diagnostic ionizing radiation exams, CT is estimated to contribute up to 67% of the collective dose (Mettler et al., 2000). The increase in CT collective doses has raised concerns about the potential radiation risks which must be considered in relation to the benefits of performing a CT examination. It is therefore imperative for optimization of patients radiation doses to be in line with the as-low-as-reasonable achievable (ALARA) principle consistent with clinical requirements, (ICRP, 2006).

Estimation of radiation dose in CT can be quantified in terms of scanner radiation output, organ doses or effective doses. Several CT-specific dose descriptors have been developed to quantify radiation dose in CT. The volume CT dose index ($CTDI_{vol}$), is the fundamental dosimetric quantity that describes the radiation output of the scanner and can be measured experimentally by using the head and body CT phantoms. The dose measurements are normally made at the core and the periphery of the CT phantoms with ionization chamber and these values are combined to give a weighted average CT dose index ($CTDI_w$) which represent a single estimate of radiation dose to the phantom. The CT head phantom is used as a reference for paediatric body by some manufactures whereas the body CT phantom is used as a reference for adult CT in the torso (chest, abdomen, and pelvis) and also for adult reference body CT (Shrimpton, 2004).

Image quality in CT imaging has many components and these are affected by many technical parameters. Several metrics describe the different aspects of image quality; these includes image noise: which describes the variation of CT numbers in a physically uniform region. High-contrast spatial resolution, which quantifies the minimum size of high-contrast object that can be resolved. Low-contrast spatial resolution which quantifies the minimum size of low-contract object that can be differentiated from the background, which is related both to the contrast of the material and the noise-resolution properties of the system. Contrast-to-noise ratio (CNR) and signal-to-noise ratio (SNR) are also some common metrics that often quantify the overall image quality (Callstrom et al., 2001). Optimizing of scan parameters, improving the image reconstruction and improved data processing procedure, reduces image noise which allows radiation dose reduction.

Dose reduction in CT has become an important issue and various dose reduction and optimization techniques have been formulated aimed at increasing the benefit to risk ratio. Modulation of the x-ray tube current during scanning is one of the best way of reducing the dose. Automatic tube current modulation is one of the available tools in modern CT scanners used for radiation dose reduction. This technique adjusts the tube current (mAs) in either the x-y plane (angular modulation technique) or z-plane (z-axis modulation technique) to provide a constant level of image noise on the basis of patient size, attenuation profile, and the scanned parameters (Kalra et al., 2005).

The dose-modulation technique, decreases the mAs automatically for regions with lower attenuation and increases the radiation dose literally (higher attenuation parts) whilst maintaining an acceptable level of image noise (Rizzo et al., 2006). The angular-modulation technique involves varying the tube current as the x-ray tube rotates about the patient, while the z-axis modulation involves varying the tube current along the z-axis of the patient (McCollough et al., 2006). A combination of the angular and z-axis modulations involves varying the tube current both during gantry rotation and along the z-axis of the patient. This study is aimed at comparing the radiation dose and image quality achieved with the use of automatic exposure control (AEC) and fixed tube current (FTC) techniques for some CT examinations performed on a 16 – slice Siemens CT scanner.

1.2 PROBLEM STATEMENT

The amount of radiation dose delivered to patients and the quality of the images acquired in CT examination are determined by the selection of the tube voltage and the tube current. However, there are other imaging parameters that have influence on the radiation dose and image quality which sometimes leads to nosier or poorer images for accurate diagnosis. In CT examination, finding the right balance between image quality and radiation dose delivered to patient is not always in harmony due to lack of optimized scan parameters. This has been a major concern to the medical physicist, radiologist and medical practitioners since the inception of CT in clinical use.

With recent advancement in CT scanner technology, radiation dose to patients in CT examinations has increased. Thus, optimization of scanning techniques to maintain optimal diagnostic image quality at the lowest possible radiation dose has become very important. The determinant of radiation dose and image quality in CT examination is the tube current and manual adjustment of it based on patient weight helps in establishing an appropriate balance between image noise and radiation dose. Studies have suggested the use of FTC to obtain a good quality image for accurate diagnosis, but this does not guarantee constant image quality throughout an examination couple with high radiation dose to the patient.

In an effort to address this concerns, CT manufacturers have implemented AEC to appropriately manage or reduce radiation doses to patients whiles maintaining consistent image quality for accurate diagnosis (Sookpeng et al., 2013). Some research work has been conducted to assess the diagnostic acceptability in terms of radiation dose and image quality between automatic tube current modulation and fixed tube current for some CT examinations(Jen-Pai et al., 2010). However, there is inadequate information published on the subject matter particularly in Ghana. It is therefore expedient that, radiation dose and image quality with the use of AEC system and FTC be assessed. This study seeks to investigate this matter using the CT system at Sweden Ghana Medical Centre as case study. And will also serve as a pedestal towards establishing optimized national dosimetry scan protocols and reference dose levels.

1.3 STUDY OBJECTIVE

The main objective is determine radiation dose to patients and compare the dose delivered using automatic exposure control (AEC) and fixed tube current (FTC) techniques in CT examinations.

1.3.1 Specific Objectives

The specific objectives of the research were to;

1. To evaluate the radiation dose delivered to patients with the use of AEC and FTC techniques.
2. To estimate organ and effective doses for the radiosensitive organs in the head and trunk (chest, abdomen, pelvic) regions.
3. To assess the image quality by examining the spatial resolution, low contrast resolution and the contrast to noise ratio.
4. To make appropriate recommendations from the findings of this work

1.4 RELEVANCE AND JUSTIFICATION

CT has become an important medical tool since its inception over 40 years ago. CT scanning has been recognized as a high radiation dose modality and it is therefore considered as a potential source of increased cancer risk. This is a source of major concern since the dose delivered to the patient in CT scan procedure is considered as high as compared to other imaging modalities. Over the years CT machines used a constant tube current throughout the scan procedure. The key problem with these constant tube current machines is that, they produce more dose to the patient than necessary since areas in the scan region with low attenuation are irradiated with the same tube current value as areas with high attenuation. To address this problem, CT manufactures have implemented a tube current modulation techniques that vary tube current throughout a scan to account for patient attenuation while maintaining acceptable image quality. However, the tube current modulation technique can increase the radiation dose to larger patients. With the rapid development of multi detector CT (MDCT) technology and increasing concern over the associated radiation dose, optimization of scanning techniques to maintain diagnostic image quality at the lowest possible radiation dose has become very important.

Based on this perspective, it is of interest to quantify the amount of radiation dose imparted to patients undergoing a CT examination, with the use of AEC and manual FTC techniques. This work will therefore provide an opportunity to assess and evaluate the radiation dose and image quality with the used of AEC and FTC techniques towards producing an optimized working protocol for routine examination. The results will provide information on the status of radiation protection of .the patient at the Sweden Ghana Medical Centre and will also add significant information to the body of knowledge on the subject matter for the scientific community.

1.5 SCOPE AND DELIMITATION OF THE RESEARCH

The research primarily aimed at evaluating and comparing the radiation dose and image quality with the use of AEC modulation and FTC techniques using the head and body phantom in a 16-slice multidetector CT scanner and as well estimate the organ and effective doses associated with the two techniques. In this study dose measurements were performed using a standard cylindrical dosimetry head (16 cm diameter) and body (32 cm diameter) phantoms respectively. Organ and effective doses were estimated for the radiosensitive organs covering the head and trunk regions using the CT Expo software V2.3.1 (E) (G. Stamm, Hanover. Germany 2014). Subsequently, analysis of image quality was done for spatial resolution test, low contrast detectability test and contrast to noise ratio using Catphan 700 phantom.

1.6 THESIS STRUCTURE

The thesis contains five chapters. Chapter one is an introduction to the research that provides an overview of the current state of knowledge relevant to the study. Chapter two reviews the existing literature relevant to the research problem. The experimental and theoretical framework for the study is in chapter three. The results and discussions are in presented in chapter four. Chapter five provides the conclusions of the study, recommendations and suggestions for further research.

CHAPTER TWO

2.0 LITERATURE REVIEW

OVER VIEW

This chapter provides details background regarding basic knowledge in CT, CT image quality, and CT dosimetry. The chapter also contains detailed of the principles of operation of the AEC systems employed by the different CT scanners and relevant literature pertinent to the research study.

2.1 INTRODUCTION

Computed tomography (CT) also known as computed axial tomography (CAT) was invented and introduced in to clinical used in the 1970s. By then, it was considered as the most advanced machine since the development of x-ray machine (Goergen et al., 2009). Initial CT scanners were single slice axial, but technological development has seen the introduction of helical and multi-slice models. The use of CT has been increasing rapidly; there have been a 12-fold and 20-fold increase used in CT in some European countries and the United States over the last 20 years (Hall & Brenner, 2008).

CT scanners start to take a centre stage in the imaging world with the inception of single detector CT scanner that takes an image one at a time, with the x-ray tube and detector rotating 360 degrees or less with the patient and the table staying fixed (Seerman, 2016). This cross-sectional imaging modality supplies diagnostic radiology with better visualization into the pathogenesis of the body, exhibiting smaller contrast differences than conventional x-ray images and increasing the chances of recovery. From the early part of 1990s until present, CT ability to acquire multiple slice at a time has led CT scans to be one of the most important methods of radiological diagnosis (Siemens, 2000).

The number of slices ranges from four, six, to 64 and up to 640 slices for the more modern CT scanner machines. This is normally referred to as multi-slice computed tomography (MSCT) or multi-detector computed tomography (MDCT) technology (Marchal et al., 2005).The techniques and procedures of CT have been expanded in the past few years, leading to an increase in the use of this imaging modality and similarly the radiation dose to the patient. CT scanning is capable of providing high quality images valuable for adequate diagnostic information, however it is also described and perceived as a high dose procedure (Kulama, 2004). During a CT examination, the radiation dose imparted to the patient can be high, for that matter it is important to keep the radiation exposure as low as possible, paying much attention to the image in order to maintain a clear image quality that is suitable for the diagnostic task (Jurik et al., 1997).

Many international associations have set guidelines to regulate CT examination in order to reduced radiation dose delivered to patients. The European guidelines has compiled image quality criteria for most CT examinations, high-quality imaging procedures and the use of Diagnostic Reference Levels (DRLs) (Tsapaki & Rehani, 2007). DRL is aimed at setting dose levels in different CT examinations and allow assessment to be made between different scanners and techniques, and make it easy for comparison. All of this helps in improving patient protection by reducing the patient dose while maintain image quality and providing advice to use and select the right dose for a particular CT examination.

The increasing use of CT facilities has also raised concerns about the radiation dose to workers. Due to this, continuous efforts should be made in the area of decreasing doses to staff and the general population. There are many methods used for optimizing patient dose whiles maintaining the quality of the image good enough for diagnosis (Aweda & Arogundade, 2007).The use of different models of CT scanners, vary the radiation dose to the patients substantially due to varying CT geometry and filtration. Evidence have showed that the image quality acquired from CT scanners is much higher than really necessary to produce precise clinical diagnosis (Tsapaki & Rehani, 2007).

Thus, CT manufacturers, radiologists and physicists together should put measures in place aimed at decreasing patient dose, and expand and develop CT scanners to provide the needed image quality with low radiation dose to the population (Kalra et al., 2004). If CT examination is clinically acceptable, justified and doses remain optimized then CT can be a very useful tool. While the use of CT scanners has increased recently, the effect of radiation doses to patients has also increased and this has raised concerns for the need to decrease radiation exposure from CT procedures. The radiology society has applied CT dose reduction applications that match the standard of as low as reasonably achievable (ALARA) in response to the growing awareness from the population (McCollough et al., 2009).

Due to this public awareness, dose reduction has become a major concern in the use of CT. Because of inadequate guidelines and a limited research foundation on the topic of CT examination and scanning techniques, different methods have been used towards optimizing of radiation dose (Kulama, 2004).

Rehani and Berry (2000) pointed out that, CT tests are hazardous and that there should be a guarantee that the examinations asked for are justified and most suitable for patient need and diagnosis. This is to ensure a decrease in patient exposure and in compliance to the recommendations of the International Commission on Radiological Protection (ICRP) which advises that all exposures should be ALARA (Catalano et al., 2007). The major dose reduction tool in radiation protection is the process of proper justification of a study. However, where an examination is undertaken, the focus must be on dose optimization and This can be reached in two ways: first, is during the design of the equipment, and secondly is optimization of the scan protocols (M a Lewis & Edyvean, 2005).

2.2 THE EVOLUTION OF CT SCANNING

Historically, CT scanners has undergone a series of transformation from generation to generation. CT scanner generation started with pencil- thin beam, to small fan, to fan beam with rotating detector, and fan beam with stationary detector (Kalender, 2005). The differentiable feature among different scanners is the detector width and the gantry opening size. Today, the general scanner design for clinical CT appears standardized to some level. A number of dedicated scanners using flat-detector technology are on the increased such as dedicated scanners for the breast, for the faciomaxillary skull and the extremities as well as the use of C-arm based scanning for interventional and intraoperative imaging using flat detectors is also showing some increase.

2.2.1 First Generation CT Scanners

The first CT scanner was developed in the early 1970s by Hounsfield, a computer engineer in England (Kalender, 2005). The first generation of CT scanners utilizes a pencil beam x-ray source position at a fixed source interval with only one detector acquired image data by a ‘translate-rotate’ method. The combination of the x-ray tube and detector moved in a linear motion across the patient (translate) and this system motion was repeated until the beam and detector reached 180 degrees.

When the x-rays were emitted from the source and penetrated through the patients, the intensity of x-rays was evaluated from a sequence of transmission measurements made by the detector. This process is repeated for an acquisition of 180 projections at one degree interval surrounding the patient generating 28,800 x-ray of total measurements. From these measurement an image was created. The first generation CT scanners projected a succession of parallel beams at different locations through the patient as it’s translate linearly across a specific field of view (FOV). When the system has completed the appropriate field of view for a particular accusation, it rotates one degree and the translation process is repeated in the following projection (Bushberg et al., 2011a).

One advantage of the first-generation CT scanner was that it employed pencil beam geometry-only two detectors measured the transmission of x-rays through the patient. The pencil beam allowed very efficient scatter reduction, because scatter that was deflected away from the pencil ray was not measured by a detector. With regard to scatter rejection, the pencil beam geometry used in first-generation CT scanners was the best (Bushberg et al., 2011b). However, the disadvantage of these scanners was the scan time, which took approximately 4 - 5.5 minutes to produce an image, and the limitation of the device to the head only (Cunningham & Judy, 2000). Figure 2.1 below shows the first-generation CT scanner, which used a parallel x-ray beam with translate-rotate motion to acquire data.

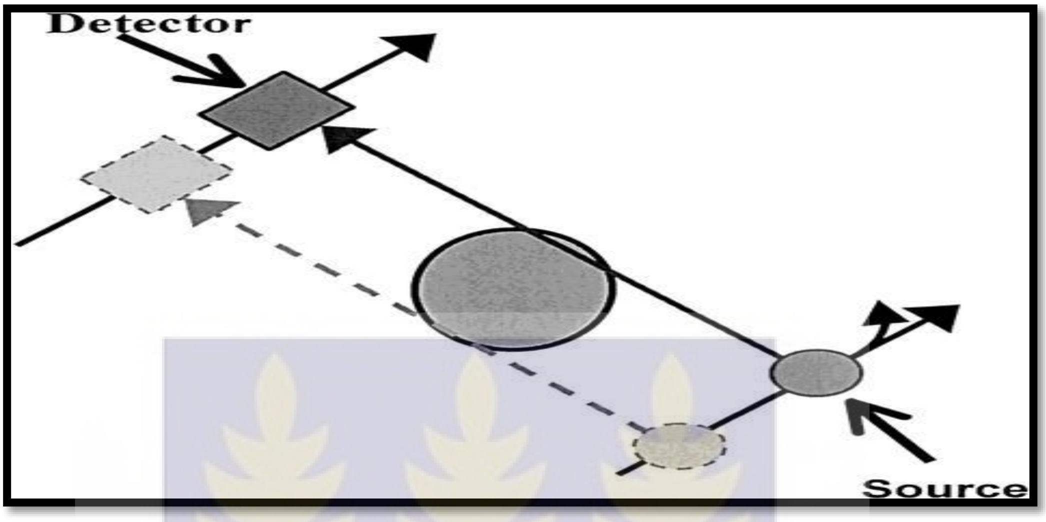

Figure 2.1: Diagram of the second-generation CT scanner (Mahesh, 2009)

2.2.2 Second Generation CT scanner

The second generation of CT was introduced in 1972 for the purpose of improving image quality and scan time. The x-ray source was changed from the pencil beam to a narrow fan shaped beam geometry (10 to 15 degrees) together with multiple detectors. These scanners decreased the scan time and improved the image quality, but increased the amount of scatter radiation (Carlton et al., 2005). With improvement made from first to second generation CT scanners, the average scan time was reduce from few minutes to few tens of seconds. The angle of rotation between the translation motions increase considerably as a result of the narrow fan beam and multiple array of detector system used.

Data analysis and processing efficiency was improved per rotation through the multi detector system, minimizing the total number of revolution required to produce an image and the increase in detector number from 2 to 30 improve the x-ray beam use to produce the image. The clinical used of the first and the second generation CT scanners were only restricted to head scan protocols due to prolong image acquisition time. However, with the improvement made on the second generation CT scanners, a few body scan were executed. Figure 2.2 below shows the second-generation CT scanner, which used translate-rotate motion to acquire data.

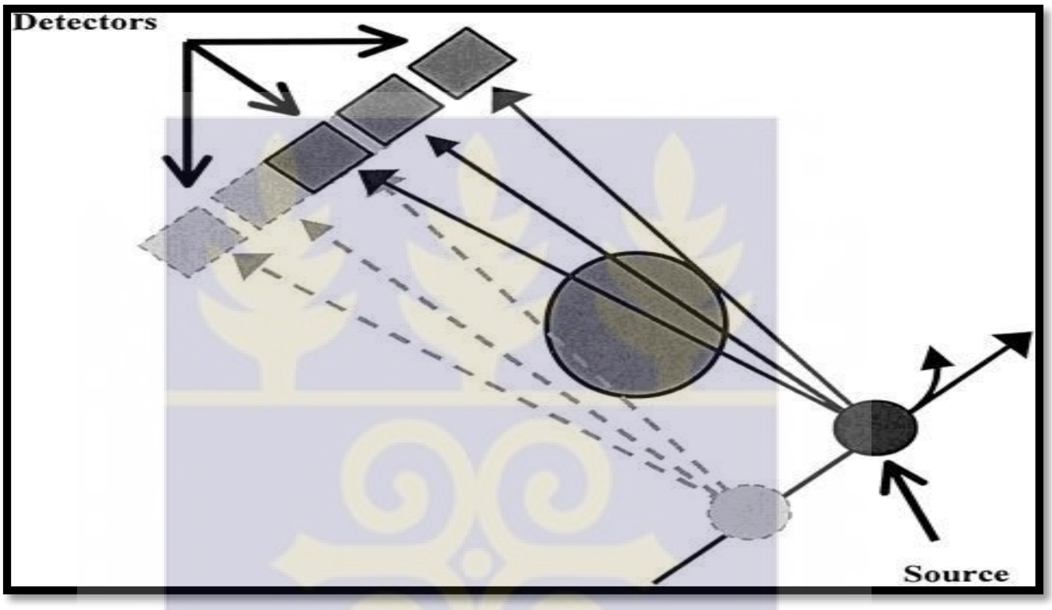

Figure 2.2: Diagram of the second-generation CT scanner (Mahesh, 2009)

2.2.3 Third Generation Scanner

The number of detectors used in third-generation scanners was increased substantially, and the angle of the fan beam was also increased so that, the detector array formed an arc wide enough to allow the x-ray beam to interact with the entire patient. Third generation CT scanners saw the evolution of elements of the modern CT scan, which uses a wide fan shaped beam and a curved detector array with up to 750 detectors. The wide fan beam was wide enough to include the whole patient in an individual exposure. These scanners decreased the scan-time to nearly one seconds for a single image and improved the image quality, but the use of a moving detector created a problem called a ‘ring artefact’ (Carlton et al., 2005). Figure 2.3 below shows the third-generation CT scanner, which acquires data by rotating both the x-ray source with a wide fan beam geometry and the detectors around the patient.

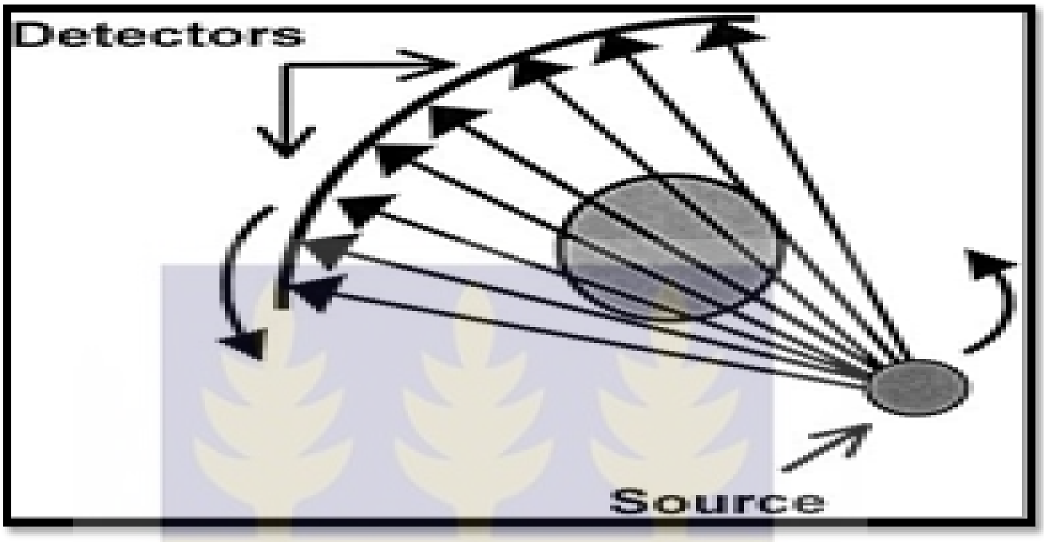

Figure 2.3: Diagram of the third-generation CT scanner (Mahesh, 2009)

2.2.4 Fourth Generation CT scanner

Fourth-generation CT scanners were designed to overcome the problem of ring artefacts. With this CT scanners, the detectors are removed from the rotating gantry and are placed in a stationary 360-degree ring around the patient, requiring many more detectors. Modern fourth-generation CT systems use about 4,800 individual detectors. Because the x-ray tube rotates and the detectors are stationary, fourth-generation CT is said to use a rotate/stationary geometry**.** The design was based on a rotating x-ray source and stationary detector and achieved scan-time ranges from 2 to 10 seconds (Carlton et al., 2005). Figure 2.4 below shows the fourth-generation CT scanner, which uses a stationary ring of detectors positioned around the patient.

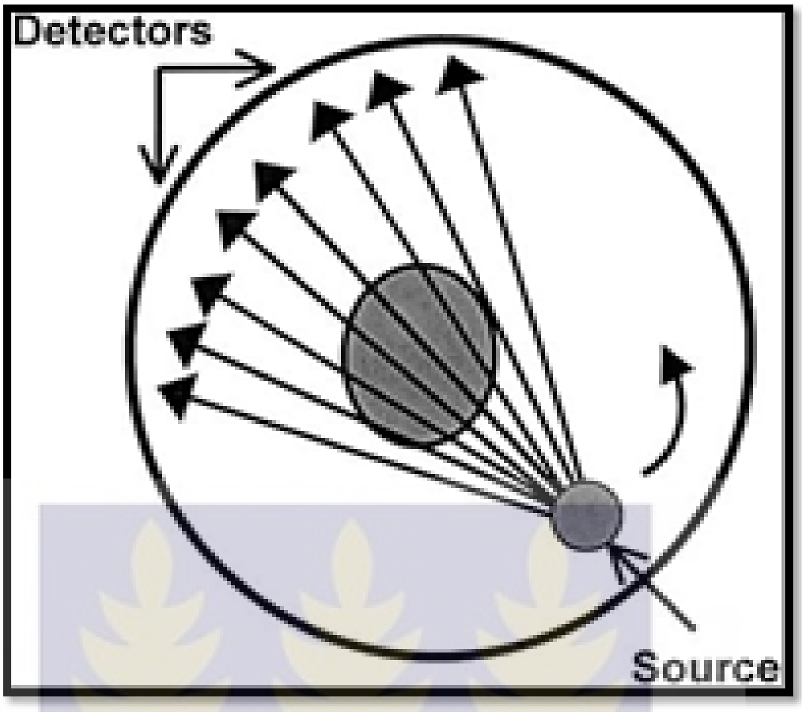

Figure 2.4: Diagram of the fourth-generation CT scanner (Mahesh, 2009)

2.2.5 Five Generation CT Scanner

This generation of scanners is referred as cardiac cine CT or Electronic Beam Tomography (EBT). The parts in these systems are stationary for which; the x-ray source and detectors are both fixed. These group of scanners do not look like that of the conventional x-ray tube, but consist of a large semi-circle ring that surrounds the patient, allowing high speed CT scanning to acquire up to 17 images per second (Carlton et al., 2005; GE Health care, 2003).

2.2.6 Sixth Generation CT scanner

This generation of scanners are also Helical/Spiral CT, that uses slip ring technology, where many images are acquired while the patient is moved through the gantry (Fishman & Jeffrey, 1998). Normally in helical CT, the x-ray tube is continuously rotating while the table (couch) is fixed during the examination, allowing patient images to be acquired within one single breath hold (Cunningham & Judy, 2000). The design of slip ring technology comprises of many sets of matching rings to allow the current and voltage to the x-ray tube, without cables connecting directly to the tube. This avoids the x-ray tube from stopping during its continuous rotation. The main advantages of these scanners include the shorter scan time, avoiding overlap and reduction in the motion 'artefact' (Carlton et al., 2005).

2.2.7 Seventh Generation

In this generation, CT scanning improved with the introduction of multiple detectors and has been referred to as Multi detector Computed Tomography (MDCT), Multi-slice Computed Tomography (MSCT) and Multiple Computed Detector Arrays (MCDA) (Carlton et al., 2005). The main feature of these scanners is the number of detectors, which varies from two to 320 rows of detectors (Topics, Katada, Ct, & Ct, 2002). The number of detectors impacts on the total time of examinations for the body and chest being completed in 15 to 20 seconds.

2.2.8 Helical /Spiral CT

Technological development has seen the introduction of helical CT in the early 1990s which led to good image quality and faster scan times; this is considered as a major advancement in CT scanning (Cunningham & Judy, 2000). Helical CT utilizes slip-ring technology to acquire data continuously as the patient is translated through the gantry (Fishman & Jeffrey, 1998). The Slip rings are electro-mechanical devices consist of a sets of parallel conductive rings concentric to the gantry axis which connect to the x-ray tube, detectors and control circuit by sliding contactors. By using slip-ring technology in spiral CT, the gantry performs multiple 360° rotations constantly while the patient is moved continuously through the scan field in the z-direction through the gantry during the scanning and data acquisition process. This technique eliminate the need for the cables that supply the kVp and mAs to the tube, which would otherwise have to be rewound between scans (Cunningham & Judy, 2000). The helical CT is referred to as volume scanning. The major advance in helical CT in comparison to earlier machines is the faster scan time, taking just a minute to complete an abdomen and chest scan which can be done in a single breath-hold. Also it reduction in patient movement during exam and is ideal for three-dimensional imaging (Fishman & Jeffrey, 1998).

2.3 MULTI-SLICE CT

Multi-slice CT (MSCT) also known as multi row CT or multi detector row CT (MDCT) has been introduced in to the imaging realm by Elscint since 1992 (Kalender 2005). MSCT is a CT system designed with multiple rows of CT detectors, combined with helical/spiral scanning to produce images made up of multiple slices. MSCT has noticeably enhanced the performance of CT in terms of image resolution, production of thinner sections and a reduction in the time taken for examinations. Recently, the multi-slice CT systems appears with two, four, eight, 16, 32 and 64 detectors, and more recently a 320 row system (Katada, 2002). Radiation doses associated with a 64-slice CT was investigated by Fujiiet et al. (2009) in phantom study. Their study showed that a 64-slice CT provides the same organ and effective doses for adults and children, similar to those with 4, 8 and 16-slice CT scanners, which gives an indication of high doses from MSCT scanners (Fujii et al., 2009).

2.3.2 MSCT Detector

The detector system in MSCT is different from single slice CT (SSCT) in terms of the detector configuration. MSCT detectors are in an array, segmented in the z axis which means there are more rows of detectors next to each other allowing for simultaneous acquisition of multiple images in the scan plane with one rotation (Goldman, 2008; Bongartz et al., 2004). In 2002, 16-slice CT scanners was introduced in to the medical world, providing 16 data channels to obtain 16 slices in one rotation. In 16-slice CT, the detectors are joined together to allow smaller slices to be obtained. This design works because the innermost 16 detectors are half the size of the external elements, allowing the attainment of 16 thin slices that range from 0.5 - 0.75 mm thick. MSCT companies started to introduce 16-slice and 8-slice models in 2003 and 2004. Around the same time, 32-slice and 40-slice scanners were being introduced.

In 2005, 64-slice scanners were introduced, with different companies using different designs for the detector array. They use a periodic motion of the focal spot in the longitudinal direction (z-flying focal spot) to double the number of simultaneously acquired slices. Each of the 32 detectors collects two measurements separated by 0.3 mm, therefore the net result gives a total of 64 slices (Goldman, 2008). Today, modern CT scanners are capable of imaging simultaneously 128 or even 320 parallel slices in one rotation(Geleijns et al., 2009).The Beam width has increased significantly from a standard of 10 mm to current beam widths of up to 160 mm. Figure 2.5 shows detector array configurations of some manufacturers.

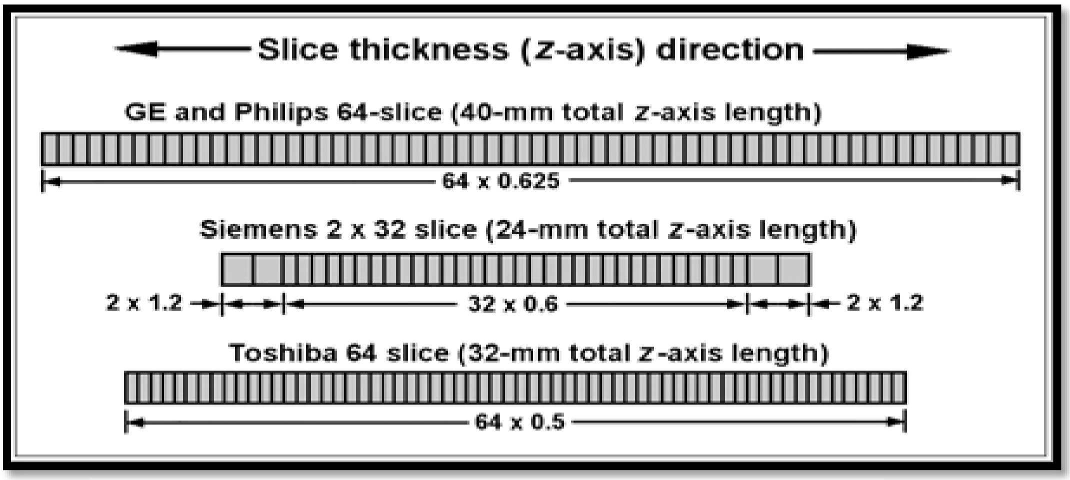

Figure 2.5: Diagrams of 64-slice detector designs in z-direction for different CT scanner manufacturers (Goldman, 2008).

2.4 SINGLE VERSUS MULTI-SLICE CT

The main differences between single-slice CT (SSCT) and MSCT hardware is how the thickness represented by an image, or slice, is determined or design of the detector arrays. The SSCT consist of 750 or more detectors arranged in a single row. For MSCT, the slice width is determined by detector configuration using x-ray beam collimation. The x-ray beam width in MSCT is created to cover larger area in order to ensure that the penumbra reclines further than the active detector area as shown in Figure 2.6 below. MSCT, allows for four extra rotations, while for SSCT scanners only one further rotation is allowed.

The beam thickness in MSCT scanners usually varies from 2.4 to 4 cm, while in SSCT the characteristic highest beam thickness is 1 cm. MSCT scanners gives large over scan input particularly when small lengths are scanned which consequently increased the patient dose(Tsalafoutas & Koukourakis, 2010). The main difference between SSCT and MSCT is the design of the detector arrays. MSCT has lower geometric efficiency compared to SSCT, and gaps between the detectors elements in the detector array result in a relatively higher dose from MSCT systems (Health care human factor

Group, 2006).

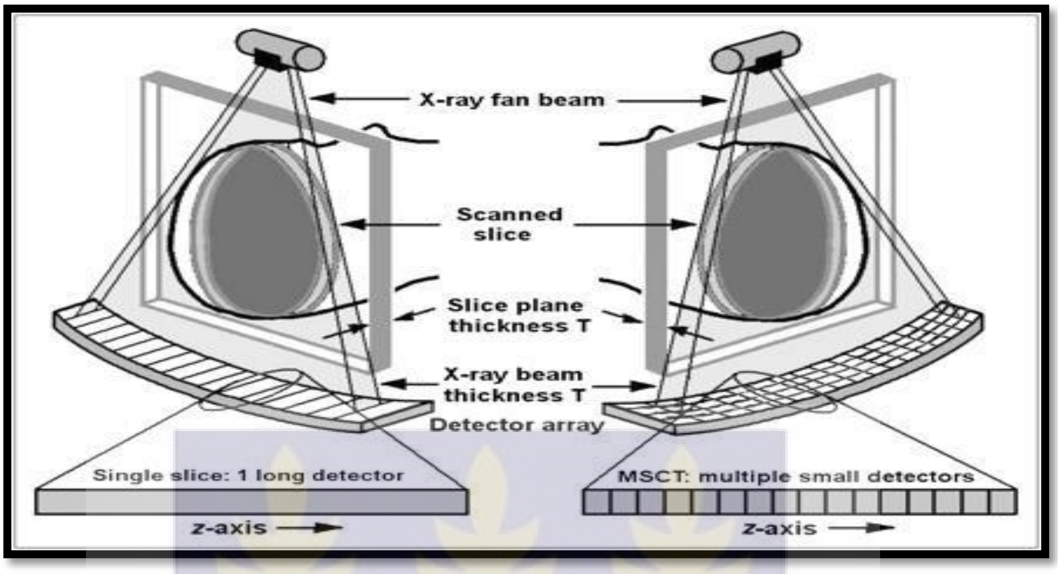

Figure 2.6: Left: SSCT arrays with single row detector elements along the z-axis; Right: MSCT arrays with several rows of small detector elements along the z-axis (Goldman, 2008).

In a study conducted by Lewis (Lewis, 2005) on variation between single and multi-slice systems and the patient dose from both single and multi-slice CT scanners, pointed out that, the dose on a multi-slice scanner is higher compared to a single-slice CT scanner. He also described the fundamentals of radiation dose and the methods for dose reduction.

2.5 CT DOSIMETRY

With the introduction of spiral CT in the early 1990s and the subsequent introduction of four slice CT has change the dynamics of modern CT scanning capable of providing high quality diagnostic information. However, this modality is generally describe as being a high dose procedure (Kulama, 2004). Now with 16 and 64 slice CT scanners available as well as other models capable of providing 320 slices with large area, have greatly change the clinical applications of CT. For instance, the use of vascular and cardiac examinations, perfusion imaging and whole body imaging.

In CT imaging, radiation dose delivered to patients is been influence by a number of factors. These includes; the radiologist, application specialist and technician who choose the parameters for the tube current (mA), tube potential (KVp) and the differences in scanning parameters (Catalono, et al., 2007). In MSCT examination, the radiation dose delivered to patients are quite high, and therefore call for the need to keep radiation ALARA. In addition, extra carefulness is also needed in reducing radiation dose and whiles maintaining an image quality that is acceptable for diagnosis (Jurik et al., 1997).

The radiation dose to patients in CT differ depending on the design and model of MSCT scanner and also the variations in MSCT geometry, filtration and the awareness of the image quality from the CT scanner. This is where the needs are to be balanced between radiation dose and image quality (Tsapaki & Rehani, 2007). This calls for the need for manufacturers, radiologists, technologists and physicists to collaborate to find a plan to decrease patient dose in accordance with the ALARA principle. Many advances in the use and development of MSCT scanners have resulted in the ability to provide images of good quality, with a resultant low radiation dose to the population (Kalra et al., 2004a), however this is not easily understood in the practical medical imaging field.

Parameters used to acquire images in CT scanners have been briefly studied, and manufacturers have adopted an auto mA protocol for minimizing the radiation dose whiles keeping image quality constant. It is commonly believed that a change in the kVp is difficult, because any change in the kVp would have major impact on the image quality and dosage (McNitt-Gray & Geffen, 2006). The reason for optimization in diagnostic radiology is to achieve optimal parameters and protocols needed to create high image quality with the lowest possible dose to patients. As a result of this, dose optimization is therefore, necessary for each particular x-ray unit and for each x-ray examination. This optimization procedure requires an evaluation of patient dose and image quality (Mahesh, 2009).

According to a research conducted by Yu et al. (2009) indicated that, radiation dose from CT scanners gives rise to radiation risk and therefore recommend ways by which the radiation dose can be reduced as much as possible. They recommended that, any examination involving the use of CT should be justified and that radiologists and technologies should agree on whether CT is the most suitable examination and if so the exposure parameters should be adjusted to optimize the examination and minimize the radiation dose to the patient. They further suggested that, radiologist should avoid unnecessary CT examination where possible and further clinical studies be carried out on CT doses.

Also, Yu et al. (2009) recommended the used of ALARA principle as a guideline for dose reduction on CT scans, suggesting that all CT examinations should be justified with appropriate settings by the user to reduce the doses, as all CT manufacturers supply CT scanners with dose reduction systems such as AEC.

Furthermore, a study by smith et al., (2007) discussed various strategies by which radiation dose associated with neuroradiology CT protocols can be reduced. In their study they concluded that, the tube current, tube rotation time, peak voltage, pitch, and collimation are major factors affecting the radiation dose received by the patient during a CT examination. They however found that, if one of these parameters is reduced, another parameter needs to be increased in order to keep the image quality acceptable. They therefore suggest a dose modulation, that will adjusts the tube current in reaction to the 'patient's attenuation to keep the same image quality for the smallest amount probable tube current, decreases the radiation dose to patients without major image compromise.

Additionally, a study conducted by Huda. (2002), on radiation dose and image quality in CT scanning and the relationship between tube voltage and dose. His results show that, the option of tube voltage and productivity in CT examinations have a direct effect on both image quality and patient dose.

Many efforts have been made towards optimizing of image acquisition parameters or protocols in order to attain a lower radiation dose whiles maintaining an acceptable image quality for accurate diagnosis (Wade et al., 1997). CT dose can be decrease effectively by justification of each individual examination by a radiologist, a reduction of the scanned volume and optimum selection of technique factors (KVp, mA, rotation time, slice width) and pitch or couch increment (Crawley et al., 2001).

2.5.1 CT dose index (CTDI)

CTDI is the primary dose measurement concept in CT. Its represent the average absorbed dose in air along the z-axis from a series of contiguous irradiation. It is the main dose quantity concept in CT as documented by CT manufactures (McCollough et al., 2008).The CTDI is defined for axial scanning and is measured during a single rotation using a pencil ionization chamber aligned parallel to the z- axis of the CT scanner. Although CTDI has significantly change clinical radiation dosimetry and knowledge regarding CT practice (Food & Drug Administration, 2006). It is however, does not represent the patient dose but used to measure the CT output and also for comparison of the radiation output levels between different CT scanners. This concept was introduced over thirty years ago in the era of single slice CT scanners with beam widths of 10 mm or less (Brenner et al., 2006). CTDI is defined by the relationship given in the equation below.

$$CTDI = \left(\frac{1}{nT}\right) \int_{-\infty}^{+\infty} D(z)dz \quad (Gy) \tag{2.1}$$

Where*:* *n* is the number of tomographic slices acquired in a single scan, *D (z)* is the radiation dose measured along the z-axis and *T* is the slice thickness. The CTDI is measured in gray (Gy), but can also be measured in submultiples such as centigray (cGy) and milligray (mGy) respectively (Seeram, 2009).

2.5.2 CTDI$_{100}$

It is a calculated parameter of radiation dose that represent a collection of several scan doses at the core of a 100 mm scan, which is able to collect doses for a longer scan lengths. It is introduced to overcome the limitations of the CTDI$_{FDA}$. The CTDI$_{100}$ is much longer than CTDI$_{FDA}$ but however smaller than the MSAD, with incorporated limits of -50 mm to +50 mm which match to the 100 mm (McCollough et al., 2008). The CTDI$_{100}$ is given the equation;

$$CTDI100 = \frac{1}{NT} \int_{-50}^{+50} D(Z)dz \quad (Gy) \tag{2.2}$$

Where*; D (z)* is the dose profile along the *Z-* axis, *N* is the number of slice image in a single axial scan and T is the slice thickness.

2.5.3 CTDI$_{FDA}$

Theoretically, the equivalence of the MSAD and the CTDI requires that all contributions from the tails of the radiation dose profile be included in the CTDI dose measurement. The exact integration limits required to meet this criterion depend upon the width of the nominal radiation beam and the scattering medium (McCollough et al., 2008).The CTDI was first introduced by the U.S food and drugs authority (FDA) known as the $CTDI_{FDA}$ that introduced the integration limits of ±7T where T represents the nominal slice width. The used of $CTDI_{FDA}$ in dose measurement was limited to approximately fourteen slices (McCollough et al., 2008).this limitation was solve by the introduction of another dose index, the $CTDI_{100}$ (Seeram, 2009). The $CTDI_{FDA}$ is determined using the relation;

$$CTDI_{FDA} = \frac{1}{nT}\int_{-7}^{+7} D\,(Z)dz \qquad (2.3)$$

2.5.4 Multiple Scan Average Doses (MSAD)

MSAD is the average dose along the z-axis from multiples slices. It represents the average dose across the central slice from a series of N slices (each of thickness T) when there is a constant increment between successive slices (Edyvean et al., 2003). The MSAD primarily describe the CT dose and the sequence of CT scans achieved on a patient (Seeram, 2009). The MSAD can be calculated using the following equation;

$$MSAD = \frac{N*T}{I} * CTDI \qquad (2.4)$$

Where, *N* is the number of scans, *T* is the nominal slice width (mm) and *I* is the distance between scans (mm).

For *MSCT* system *N*T* is the total beam width, and *I* correspond to the patient table advance during one gantry rotation. Thus for spiral scan, the MSAD is given by;

$$MSAD = {}^{1}/_{pitch} * CTDI \qquad (2.5)$$

The MSAD and CTDI are equivalent theoretically when the pitch is equal to one (Edyvean, et al, 2003). This indicates that all the scatter tails are included and the scan interval (I) is equal to the nominal thickness (T). Figure 2.7 below shows a dose profile for MSAD and CTDI along the z-axis.

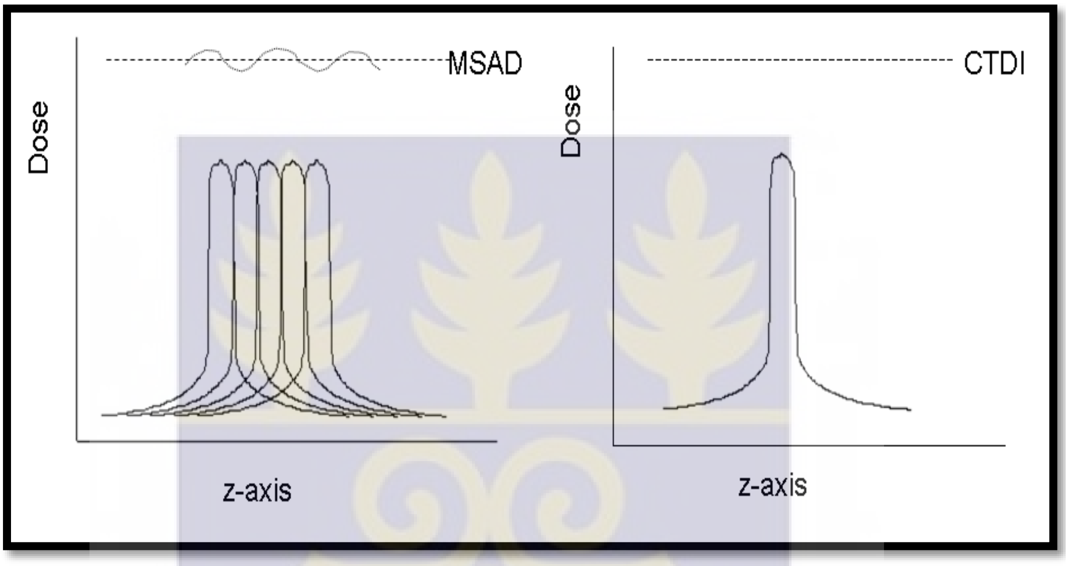

Figure 2.7: Dose Profile of MSAD and CTDI along the z – axis.

2.5.5 Weighted CTDI

The CTDI varies across the field of view (FOV).It is therefore important to note that, dose distribution within the cross section of the body imparted by a CT scan is much more homogeneous than that imparted in radiography. However, this is somewhat larger near the skin than in the body centre. Weighted CTDI (CTDIw) is the subjective standard of the $CTDI_{100}$ at the centre and the periphery of a standard PMMA phantoms (Morin et al.,2003) either a 16 cm (head) or 32 cm (body) diameters to give a measure relating to patient dose. The CTDIw is employed as a standard measure relating to patient dose (International Electrotechnical Commission, 2009) and this is given by;

$$CTDI_W = \frac{1}{3}\, CTDI_{100.center} + \frac{2}{3}\, CTDI_{100.\ periphery} \qquad (2.6)$$

2.5.6 Volume CT dose index (CTDIvol)

With advances in CT scans, dose measurements has been up dated and made easier over time. A new CTDI has been developed and approved by the International Electro technical Commission (IEC), which calculates the volume CTDI ($CTDI_{vol}$) (Morin et al., 2003). $CTDI_{vol}$ is a standardized parameter that measures scanner radiation output and is an index to track across protocols for quality control purposes. The dose received from CT examinations is recorded in the Digital Imaging and Communications in Medicine (DICOM) header and displayed on the scanner screen in term of CTDIvol and dose length product (DLP). For single-slice scanners the CTDIvol is described as (Morin et al., 2003);

$$CTDI_{vol} = \frac{N.T}{I} * CTDI_w \qquad (mGy) \qquad (2.7)$$

For MSCT, the $CTDI_{vol}$ is given by;

$$CTDI_{vol} = \frac{1}{Pitch} * CTDI_w \qquad (mGy) \qquad (2.8)$$

2.5.7 Dose-Length Product (DLP)

Dose-Length Product (DLP) is the amount of radiation dose the body receives from a whole CT examination. The DLP is described as (Morin et al., 2003);

$$DLP = CTDI_{vol} * scan\ length \qquad (mGyxcm) \qquad (2.9)$$

The DLP differs from one scanner type to another and the image quality desired. Also, a change in technique (such as varying slice thickness, kVp or mA) also affect the value of DLP. The DLP is the CTDIvol multiplied by the scan length (slice thickness

× number of slices) in centimetres. The unit for DLP is milligray (mGy) x cm (McCollough et al., 2008).

2.5.8 Effective Dose

The effective dose is a dose parameter that reflects the risk of a non-uniform exposure in terms of a whole body exposure. It is a concept used to normalize partial body irradiations relative to whole body irradiations to enable comparisons of risk. The calculation of effective dose requires knowledge of the dose to specific sensitive organs within the body, which are typically obtained from Monte Carlo modelling of absorbed organ doses within mathematical Anthropomorphic phantoms (Jones & Shrimpton, 1991),and recently also voxel phantoms based on real humans. Effective dose is expressed in the units of milliSieverts (mSv), and can be compared to the effective dose from other sources of ionizing radiation, such as background radiation level, which is typically in the range of one to three mSv depending upon the location. One equation for determining a reasonable approximation of effective dose is;

$$E = K * DLP \qquad (mSv) \tag{2.10}$$

Where, E is the effective dose, and k is the conversion factor measured in, mSv x mGy^{-1} x cm^{-1}) dependent on the body region imaged. Table 2.1 shows General values of the conversion factor, appropriate to different anatomical regions of patient (head, neck, chest, abdomen or pelvis).

Table 2.1: Conversion factors (effective dose per DLP) for various body regions in adults and children based on body weighting factors from ICRP publication 60 (Bongartz et al., 2004) and ICRP publication 103 (Deak et al., 2010).

	ICRP 60	ICRP 103				
Body Region	**Adult**	**Adult**	**10 yrs.**	**5yrs**	**1 yr.**	**New born**
Head	0.0023	0.0019	0.0027	0.0035	0.0054	0.0087
Chest	0.019	0.0146	0.0237	0.0323	0.0482	0.0739
Neck	0.0054	0.0052	0.0094	0.0121	0.0168	0.021
Abdomen	0.017	0.0153	0.0249	0.0357	0.053	0.0841
Pelvis	0.017	0.0129	0.0219	0.03	0.0446	0.0701

2.6 IMAGE QUALITY

Fundamentally, image quality in CT, as in all medical imaging, depends on 4 basic factors: image contrast, spatial resolution, image noise, and artefacts (Goldman, 2007). Depending on the diagnostic task, these factors interact to determine sensitivity (the ability to perceive low-contrast structures) and the visibility of details. However, in order to assess how well an image represents patient anatomy, two main features: detail or high-contrast resolution and contrast detectability or low-contrast resolution are employed.

2.6.1 Methods of Image Quality Evaluation

Optimal Image quality determination in CT scan is a complex task and time-consuming involving both quantitative objective physical measures linked with subjective observer perception as an indication of clinical performance(Mansson, 2000). For any clinical image quality evaluation to be measured, the requirements of the resulting image should be defined, and the clinical structures required must be contained in the image. Image quality can be defined in terms of physical, psychophysical and observer performance test. The physical measurable parameters are: uniformity, linearity and noise; whiles psychophysical variables includes; contrast resolution and spatial resolution.

2.6.1.1 Image Noise

Noise in CT is the degree of uncertainty in the measurement of the attenuation of the x-ray beam passing through the patient. Noise in CT depends on the number of x-ray photons reaching the detector (Primak et al., 2006), called quantum noise, which is considered to be the most significant issue affecting the quality of the image. The quantum noise, designated σ is determine as the standard deviation or statistical fluctuation of the pixel values (mean HU) or CT numbers from a number(N) of pixels of a homogeneous region of interest (ROI). It is normally measured in a water phantom (Kalender, 2005). The standard deviation is given by;

$$\sigma = \frac{1}{N-1} \sum_{i-1}^{N} (P_i - P) \quad . \tag{2.11}$$

Image noise limits low contrast detectability and may possibly hide anatomical details of surrounding tissues. Image noise is influence by a number of parameters such as tube voltage, mA, exposure time, collimation, reconstructed slice thickness, reconstructed algorithm and helical pitch ((McNitt-Gray, 2006; Kalendar, 2005; Barrett et al., 1976). The relationship between these parameters is given by;

$$\sigma = f_A . \sqrt{\frac{I_o/I}{\varepsilon . mAs . S}} \tag{2.12}$$

Where; σ is the standard deviation of the pixel value or CT number, Io/I is the attenuation factor of the object, ε is the efficiency of the entire system, mAs tube current scan time product, S is the slice thickness and f_A account for the effect of the reconstruction algorithm. When consider the slice thickness, noise and mAs. The relation becomes;

$$S\ x\ \sigma^2 \alpha \frac{1}{mAs} \qquad (2.13)$$

From the above equation, noise increase by √2 if the mAs is reduced by half when the slice thickness is constant and the mAs is double when the slice thickness is half at constant noise.

2.6.1.2 High Contrast/Spatial Resolution

High-contrast resolution or spatial resolution is the level of detail that is visible on the image. It is the parameter determining the system's ability to resolve high contrast objects of small sizes that are very close together (Lois, 2013). It measures the ability of a system to distinctly delineate two objects as they become smaller and closer together. The closer they are together with the image still showing them as separate, the better the SR. SR depends on the reconstruction matrix; detector width; slice thickness; object to detector distance; spot and matrix size (Bushberg, et al, 2011c). High contrast resolution can be measured directly or calculated. For the direct measurement a line pair phantom (a module inside a Catphan 600 phantom made up of closely space metal strips imbedded in it) is used where each bar plus adjacent space is termed as line pair. In principle the phantom is scanned and the number of strips that are visible are counted. The spatial frequency in the line pair per centimetre is given by (Goldman, 2007).

$$Spatial\ frequency = \frac{1}{2\ x\ bar\ width} \tag{2.14}$$

Theoretically, the spatial resolution can also be defined using the modulation transferred function (MTF). The MTF is calculated using the Fourier transform of the line spread function (Akbari et al., 2010). The MTF depends on the size or spatial frequency of the object. A smaller object of higher spatial frequency is not clearly depicted on the CT image. The MTF scale is normally from 0 to 1. If the image reproduces the object exactly, the MTF would have a value of 1. If the image contained no information about the object, the MTF would be zero. An MTF curve that extends farther to the right indicates higher spatial resolution and better ability to reproduce small objects (Joseph & Rose, 2013).

2.6.1.3 Low Contrast Resolution

Low-contrast resolution is the ability of an imaging system to differentiate between objects with similar densities. It is often determined using objects having a very small difference from the background. The visibility of low contrast objects is constrained mainly by the contrast level, image noise and window setting of the display (Cody et al., 2012). CR is highly degraded by noise. Low contrast detectability can be evaluated by subjective and objective methods using phantoms containing low contrast targets of different diameters and contrasts. To reliably identify a structure, the signal to noise ratio (SNR) needs to be better than 5:1. This requirement is known as Rose's criterion. The SNR is hence the best descriptor of CR, which is simply determined from measurements of areas of interest within the examination point and surrounding noise (Primak et al., 2006).

2.6.1.4 Observer Performance Method

Observer performance measures are obtained from images of patients in the clinical settings or phantoms (Mansson, 2000). There are several established methods to evaluate the quality of images based on set criteria which have to be fulfilled. From these methods the two most common are visibility using visual grading analysis (VGA) or mathematical calculation using Monte Carlo methods.

2.6.1.5 Relative Visual Grading Analysis (VGA)

A simple way of quantifying subjective opinions and making them useful is by visual grading analysis. This works by defining the visibility of anatomical structure in the images that need to be examine and then evaluate and range this against a similar anatomical structure called a reference image. The method of ranking depends on the observer by random ranking, where zero means a visibility equivalent to the anatomical structure with respect to the reference image and a positive or negative value means superior or inferior visibility (Zarb et al., 2010).

2.6.1.6 Absolute VGA

In this method, the images are evaluated and ranked against each other. This method generally specify an explanation assisting analysis to improve the agreement between observers (Zarb et al.,2010). The observers rank the anatomical structures visibility using 3, 5, or 7 scale (Li et al, 2010).

2.7 AUTOMATIC EXPOSURE CONTROL (AEC) IN CT

Automatic exposure control is a CT imaging technique that performs automatic modulation of tube current in the x, y plane (angular modulation), or along the scanning direction, z-axis, (longitudinal modulation), or both (combined modulation) (Kalra et al., 2005a) as shown below in figure 2.8. The modification is done with respect to the patient's size, shape, weight and attenuation of body parts being scanned. In its mode of operation, the radiologic technician is required to select the desired image quality level and the system adjust the tube current to obtain the predetermined image quality with improved radiation efficiency to produce the desired image quality, while limiting the radiation dose to the patient (Söderberg, 2008). AEC system can in most cases reduce radiation dose by typically between 10-50 percent whiles maintaining a consistent image quality (Kalender, 2005b). Results from studies have shown that, the use of AEC systems reduced patient dose by about 35%-60% for the body and 18% for the neck, across all sizes of patient, compared with fixed tube current techniques. These dose reductions vary between different studies and depend on the tube current being used for the fixed technique and the size of the patient (Lee et al., 2009; Rizzo et al., 2006).

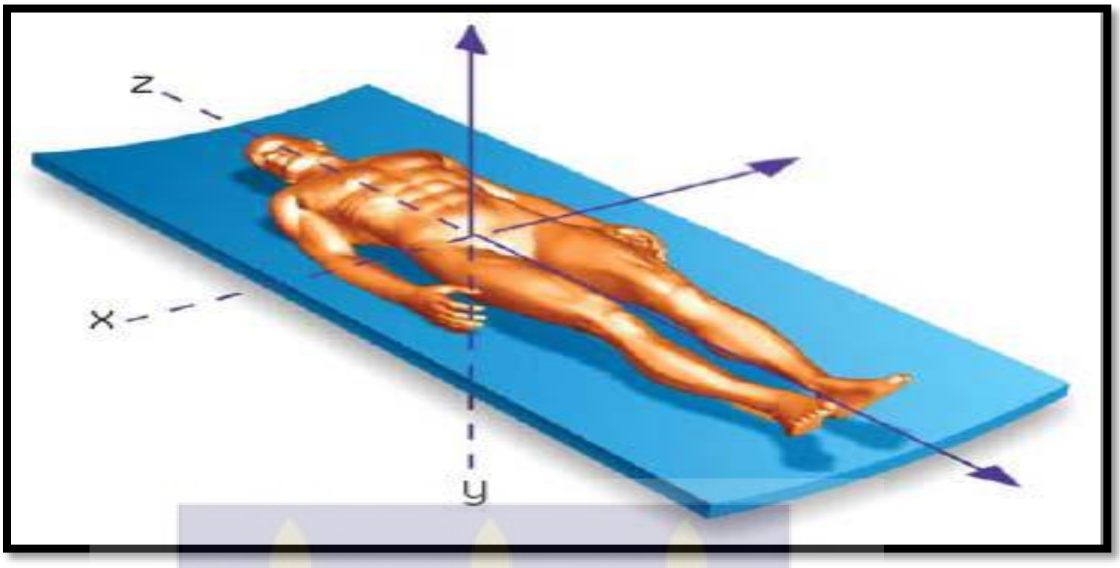

Figure 2.8: Three dimensional orientation of a body co-ordinate system (Söderberg, 2008)

Sabri et al., (2015), performed an experimental study using a thoracic phantom in comparing the radiation dose and image quality between angular automatic tube current modulation and fixed tube current CT scanning of the thorax with the aim of reducing dose by implementing an automatic tube current modulation system while attain the minimum requirement of image quality. Their result shows no significant difference for image quality between using ATCM and fixed tube current techniques. However, the images acquired with ATCM technique had a higher image noise compared with images acquired with fixed tube current. They concluded that, image quality and dose delivered to patient should be taken into consideration to ensure that the dose delivered to the patient can be reduced as much as possible.

In a study conducted by Livingstone et al., (2010) to evaluate the radiation dose and image quality using a manual protocol and dose modulation techniques in a 6-slice CT scanner. Their study was conducted on human subjects who underwent contrast enhanced CT of the chest. They pointed out that a dose reduction of up to 15% to 42%

was achieved in dose modulation techniques with acceptable image quality as compared to the manual protocol technique.

Su et al., (2010) examined comparison of radiation dose and image quality between z-axis automatic tube current modulation (ATCM) and fixed tube current techniques in CT of the liver using a multi detector row CT. Their data showed that, the average tube current of the images decreased of 8.6-22.7% with the ATCM technique as compared with the fixed tube current. However the image quality in both techniques showed no significant difference. They concluded that, using ATCM, the radiation exposure and effective radiation dose of dynamic contrast-enhanced multi-detector row CT of the liver could be effectively reduced with maintenance of the image quality Also R. Livingstone et al., (2009), examined radiation dose and image quality from six slice CT scanner using human subjects. Their study compared the radiation dose and image quality using dose modulation techniques and weight based protocols exposure parameters for biphasic abdominal CT. Their results showed that, the use of dose modulation technique resulted in a reduction of 16 to 28% in radiation dose with acceptable diagnostic accuracy. It was concluded that a reduction of current-time product of approximately three to five percent using D-DOM and 37 to 55% using Z-DOM was achieved for arterial and portal venous phases compared to the weight based protocol settings and a reduction of approximately 30 to 50% of tube current-time product was noted within D-DOM and Z-DOM respectively for arterial and portal venous phases.

Furthermore, a study by Lee et al., (2009b) assessed the variation in radiation dose and image quality between fixed tubed current and combined automatic tube current modulation on patients who underwent craniocervical CT angiography in a 64 multi detector row CT system. Their results showed no significant difference in image quality at the shoulder region but with high noise values noted at the upper neck region with ATCM technique. They also indicated that a significant radiation dose reduction of about 18% was noted with the combined ATCM technique and concluded that the combined ATCM technique for craniocervical CTA performed at 64-section MDCT substantially reduced radiation exposure dose but maintained diagnostic image quality.

Yoshinori et al., (2008) examined the possibility of obtaining adequate images at uniform image noise levels and reduced radiation exposure with automatic tube current modulation (ATCM) technique for 64-detector CT in suspected patients suffering from lungs or abdominal disorders. They concluded that, it is possible to maintain a constant image noise level with a 64-detector CT using ATCM technique.

Namasivayam et al., (2006), compared the results of two study groups performing MDCT of neck using z-axis AEC and with fixed-current technique (300 mA). They concluded that z-axis AEC resulted in similar subjective noise and diagnostic acceptability with considerable dose reduction compared with those of fixed tube current.

.

2.7.1 Angular Modulation

Angular dose modulation involves varying the tube current to equalize the photon flux to the detector as the x-ray tube rotates about the patient (e.g., from anteroposterior to lateral). In this technique, the tube current is adjusted for each projection angle relative to the size, shape and attenuation of the patient in order to minimize X-rays in the beam projection angles (i.e., x- and y-axes) that are associated with less beam attenuation and as a result contribute less to the overall image noise. For instance, in the shoulder and pelvis region, the x-rays are attenuated less in the anterior-posterior direction as compared to the lateral direction. Therefore angular modulation technique reduces unwanted radiation in the anterior- posterior direction without degrading the image quality(Kalra et al., 2005c).Also in angular modulation, more dose modulation occur in asymmetric regions and the variation in image noise throughout the examination can be optimized and also helps in reducing photon starvation artefacts, more particularly in the shoulder region(Kalender et al.,1999).

2.7.2 Longitudinal Modulation

In longitudinal modulation technique, the tube current is adjusted along the scanning direction (z axis) of the patient, based on the size, shape and attenuation of the anatomic region being scanned. This modulation technique is to produce consistent noise level in all images irrespective of the patient size and anatomy. The aim is also to reduce the variation in image quality from patient to patient. Consequently, radiologic technologist must select a required image quality level as an input to the AEC algorithm. The method varies among various CT manufacturers. But irrespective of the type, the longitudinal modulation technique uses a single localizer radiograph to determine the tube current required to produce images with required level of image noise (Kalra et al., 2005). The Figure 2.9 below shows an illustration of longitudinal (z-axis) modulation.

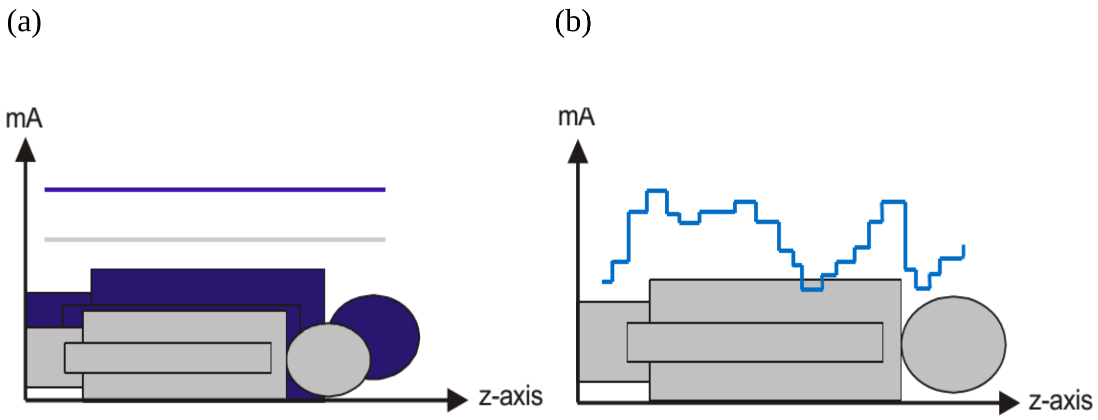

Figure 2.9: Illustration of longitudinal modulation; where (a) Represent lower mA used for a smaller patient. (b) Represent lower mA used with low attenuation along the scanning direction (keat, 2005).

2.7.3 Combined Modulation

The combined modulation technique is a simultaneous combination of angular and longitudinal (x-, y-, and z-axis) tube current modulation that modulates the tube current both during each gantry rotation and for each slice position. It is the most extensive approach to CT dose reduction, since the X-ray dose is adjusted in accordance with the patient attenuation in three dimensions (McCollough et al., 2006).

2.7.4 Principles of AEC System for Different CT Manufacturers

Each manufacturer of a CT systems has developed different AEC techniques and application capabilities (Söderberg, 2008).With their main purpose of maintaining image quality, control of patient radiation dose, avoidance of photon starvation artefacts and reduced load on the x-ray tube (Kulama, 2004). The most common systems are discussed below.

2.7.4.1 Siemens - CARE Dose 4D

Siemens use a combined tube current modulation system called CARE Dose 4D (Söderberg, 2008).The system works with automatic tube current modulation of the patient's size and shape together with real time, online, controlled tube current modulation during each tube rotation (Siemens, 2004). Based on a single CT localizer radiograph, "topogram", anterior-posterior or lateral attenuation profile (size, anatomic shape and attenuation at each position) along the patient's long axis (z-axis) is measured in the direction of the projection and estimated for the perpendicular direction with a mathematical algorithm (Söderberg, 2008). Figure 2.10 shows an anterior-posterior topogram where anterior-posterior and lateral attenuation profile is estimated.

The CARE Dose 4D has adequate image noise according to Siemens modulation, which differs depending on the patient's size and shape. The operator can choose the level of tube current, which can be selected according to the patient's size, using 'weak', 'average' or 'strong' settings to control the amount of mA supplied. The CARE Dose 4D modulations are able to provide a lower tube current to keep image noise consistent regardless of the patient size (Keat, 2005).

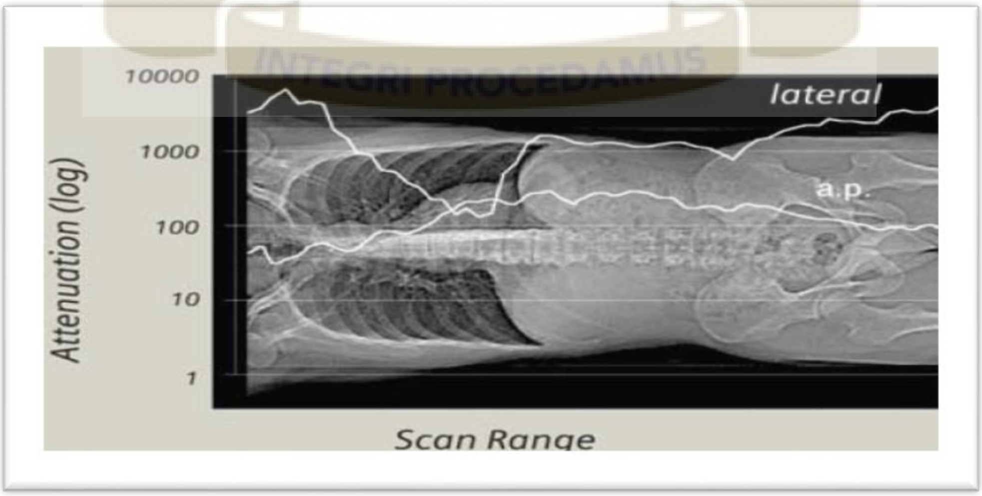

Figure 2.10: Example of an anterior-posterior topogram (Siemens, 2004).

2.7.4.2 Toshiba - Sure Exposure 3D

The Toshiba CT scanners uses a combine modulation system called Sure Exposure3D. The Sure Exposure system gives the operator two ways of setting the required image quality: standard deviation (SD) of CT numbers or image quality level (Söderberg, 2008). These methods are based on measurements of SD of pixel values measured in a patient-equivalent water phantom (McCollough et al., 2006).With the sure Exposure 3D system, the user specify the SD value for the HU image noise as well as the maximum and minimum tube current. The image noise intensifies when the tube current is low leading to very poor images and very high tube current cause high radiation exposure with minimal noise level (Söderberg, 2008). The image acquisition process is done by acquiring a frontal and a lateral localizer radiograph, known as "scanogram" of the patient as shown in Figure 2.11 below. The scanogram is then used to map the selected image quality with respect to the tube current values. The sure exposure 3D makes use of the frontal and lateral diameters and the detector intensities to determines the oscillating tube current modulation during each gantry rotation (Söderberg, 2008).

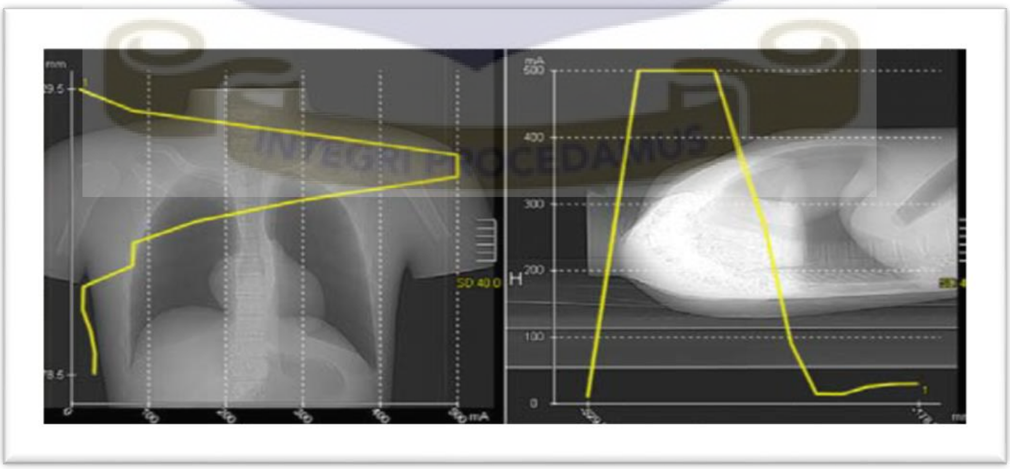

Figure 2.11: Axial and lateral scanogram used for selection of SD to tube current values (Söderberg, 2008).

2.7.4.3 GE - Auto mA

General Electric (GE) uses a combined tube current modulation system called Auto mA 3D. The system consists of two fundamentals: Auto mA that provides longitudinal AEC, and rotational AEC provided by Smart mA. It is possible to use Auto mA individual and together with Smart mA (Söderberg, 2008). The Auto mA make use of a single localizer radiograph, "scout", to determine patient size, anatomic shape and attenuation characteristics to adjust tube current for each slice position along the patient's long axis. With Smart mA the tube current is for different projection angles within each x-ray tube rotation adjusted (Kalra et al., 2005a; kalra et al., 2005b). For each rotation (4 times/turn), the system calculates each x and y mA-value from the relation between the patient's long and short axis, based on the scout image (General Electric Company, 2004).

The Auto mA method permits the operator to achieve acceptable image quality by adjusting a Noise Index (NI) value, which allows the system to permit the same noise level in each image which can be measured using a region of interest (ROI) in the image (ImPACT Scan, 2005). While in Smart mA, the tube current is meant for altered projection angles within each tube rotation motion adjusted (Söderberg, 2008). It is however indicated that, the noise index may change for different patient sizes (McCollough et al., 2005) with selected maximum and minimum tube current limited for where the tube current modulation is desired. Several studies have showed that, a dose reduction of about 60 percent can be achieved with the used of Auto mA 3D in the abdominal/ pelvic CT examination. (Kalra et al., 2005b).

2.7.4.4 Philips - Dose Right

The AEC system used by Philips is referred to as the 'Dose Right'. The Dose Right has three components; the Automatic Current Selection (ACS) that provides patient based AEC, the Z-DOM that supports longitudinal AEC and the D-DOM that supplies angular AEC. However the three dose modulation tools cannot be used concurrently, but can operate on ACS with Z-DOM or D-DOM (Söderberg, 2008). Dose Right differs from patient to patient as it depends on the size of the patients as identified on the scout view displayed on the CT scanner, which is reset by means of a 'reference image' (Kulama, 2004).

Philips uses a reference image concept to modulate tube current. After a protocol is selected and a scan projection radiography (SPR) is processed, the system calculates the attenuation coefficient of the patient, compares this to a tube current table stored for a reference average patient, and suggests suitable mAs values to produce CT scans with image noise similar to that of the reference image. For every 5-6 cm the patient is above the reference size the mAs is double, while the mAs is halved for each 7-8 cm smaller the patient is than the reference size (Supawitoo Sookpeng, 2014). There are two dose saving methods for the Philips scanner which are angular and z–axis dose modulations (DOM).

The angular modulation system modulates the tube based on the patients symmetry change in the rotational direction of the gantry (x and y-axis). The modulation is calculated online in real-time during each rotation of the gantry around the patient by using data of the previous rotation to calculate the next rotation modulation. D-DOM makes use of the detector dose and determines which part of the rotation can advantage from a reduced dose, without lost in image quality(Nicholas, 2005; Philips Medical Systems, 2008).

Z-DOM is also referred to as longitudinal modulation and consequently is the tube current modulated according to changes in the body attenuation along the longitudinal axis of the patient (z-axis). Based on a single CT localizer radiograph, surview, the mAs values are calculated to the real scanning of the patient to achieve same image quality in all slices. As the scanning process advance, the Z-DOM mAs values change and the modification is based on the scanning direction instead of adjustment based on the patients anatomic shape (PhilipsMedicalSystems, 2008).Table 2-2 below is a summary of AEC systems from different manufactures with their method of defining image quality.

Table 2-2: Lists of AEC systems from manufacturers of CT Scanners with their method of defining image quality level (Söderberg, 2008).

Manufacturer	**AEC system**	**Method to set level of image quality**
Siemens	CARE Dose 4D	Quality reference mAs
Philips	Dose Right	Reference image
GE	Auto mA 3D	Noise index
Toshiba	Sure Exposure 3D	Image quality/ standard deviation

The chapter that follows takes us through the methodology of the work, its explicitly outline the dose measuring process, organ and effective dose estimation as well as the image quality assessment processes upon which the research is based.

CHAPTER THREE

3.0 MATERIALS AND METHODS

OVERVIEW

This chapter contains the materials and methods used in this study. The chapter also gives a description of the CT facility, the methodology employed in the evaluation of the radiation dose, organ and effective doses and analysis of the quality of the images obtained.

3.1 MATERIALS

The following are the list of materials utilized for this study;

1. 16-slice Siemens CT scanner (Siemens Somatom Emotion, Forchheim, Germany).
1. CT dose profiler probe (RTI Electronics, Sweden).
2. Standard CT dosimetry Polymethyl methacrylate (PMMA) cylindrical acrylic head and body phantoms (RTI Electronics, Sweden).
3. CT-Expo software V 2.3 (G. Stamm, Hanover. Germany 2014).
4. Catphan 700 Image Quality Phantom (The Phantom Laboratory Inc., Greenwich. NY).
5. ImageJ software version 1.46r, Java 1.6.0 (National institute of mental health, Maryland U.S.A).
6. Microsoft Excel spreadsheet (2013) and SPSS version 20.0.

3.1.1 The CT Scanner

In this study dose measurements were performed on a multi detector row, Siemens Somatom Emotion CT scanner (Siemens Healthcare, Forchheim, Germany) with 16 channel detector configuration with a very small focal spot (0.8 x 0.5 mm) capable of 16 x1.2 mm multi-slice imaging which was installed in 2011. Figure 3.1 shows a diagram of the Siemens CT scanner. The CT scanner uses the CareDose4D as its automatic exposure control feature. This enables automatic adjustment of the tube current in various planes (x-y and z) axis based on the size and attenuation of the body area being scanned to achieve a constant image quality. The tube potentials available in the scanner were 80 kV, 110 kV and 130 kV with 130 kV being the most preferred in most cases because it results in good image quality without excessive tube load. Parameters such as the total time duration of the scan, field of view and pitch selection were displayed on the console. The respective default parameters recommended by the manufacturer used in this study are presented in Table 3.1.

Table 3-1: Default scanning parameters used for most common adults CT examinations.

EXAMINATION	KVp	mAs	Slice Thickness (mm)
Head cerebrum	130	270	8
Head base	130	220	5
Routine Chest	130	70	5
Routine abdomen	130	120	5
Routine Pelvis	130	120	5

Figure 3.1: Picture of the Siemens CT scanner [Field work, 2016]

3.1.2 Phantoms Used in this Study

Comparison of radiation dose and image quality with the use of automatic exposure control and fixed tube current techniques in a Siemens Somatom Emotion - 16 slice CT scanners has been investigated by using a standard CT dosimetry PMMA cylindrical acrylic head and body phantoms.

3.1.2.1 Head and Body Phantoms

The body phantom is 32 cm in diameter that mimics an adult body, and the head phantom is 16 cm in diameter that mimics an adult head or a small paediatric body as shown in Figure 3.2. Both are 15 cm thick (in the z-axis direction) and contain 1 cm diameter holes for insertion of the CT dose profiler probe. The holes on the phantoms are at the centre and at 1 cm depth at the 3-, 6-, 9- and 12- o'clock positions referred to as the peripheral sites. The two phantoms are made from Polymethyl methacrylate (PMMA) materials (Shope, et al 1982).

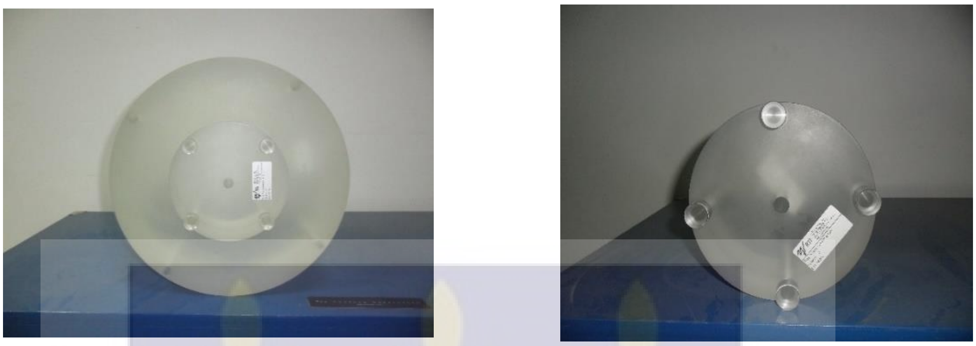

Figure 3.2: Picture of the body phantom (left) and the head phantom (right) [Field work, 2016]

3.1.2.2 Catphan 700 Image Quality Phantom

The Catphan 700 is a diagnostic imaging tool designed to test the image quality and system performance of CT scanners. It is divided into five different test modules each specific to a different image quality evaluation. Each module located within the phantom is used to evaluate different image quality parameter. Figure 3.3 showed the catphan 700 phantom.

Figure 3.3: Picture of the Catphan 700 Phantom (The Phantom Laboratory Inc., Greenwich. NY).

3.1.3 CT Dose Profiler (CTDP) Probe

The CT Dose Profiler (CTDP) is a point dose measuring detector with a solid-state sensor that is at 3 cm from the end of the probe. It contains a thin diode (of thickness: 300 µm, size: 2x2 mm) and is approximately 100 times sensitive than the existing CT pencil ion chambers. The probe is encased in an aluminium filled with Plexiglas. The probe can be extended with an extension piece (45 mm) made of PMMA to fit in to different phantoms. When the probe is placed in a 15 cm long PMMA phantom, the detector is then cantered in the middle, when the probe extension reaches the end of the phantom. The sensor is very thin (250 µm) in comparison to the beam width. This makes it completely irradiated when it is in the beam. Figure 3.4 shows a diagram of the CT dose profiler probe.

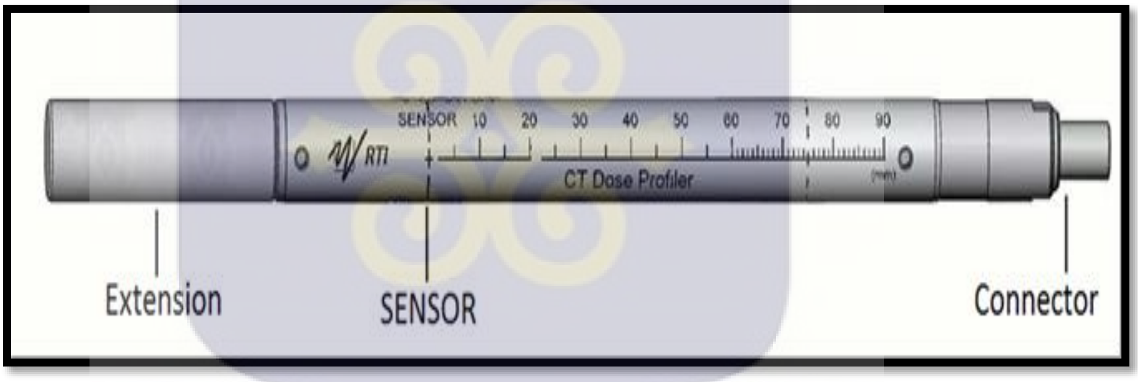

Figure 3.4: Diagram of a CT dose profiler probe (www.rti.se, RTI Electronics, Sweden).

The sensor collects the dose profile and also acts as a trigger. As radiation hits the sensor in either direction, the detector registers the dose value at that point and sends the information to the Ocean software which is used to calculate the CTDI values. A profile of the dose values is generated and display all the data points graphically. The CT dose profiler probe replaces the traditional five axial scan with a 10 cm pencil ion chamber in dose measurements with only one helical scan in a CT head or body phantom. The pencil ion chamber when used in dose measurement may results in inaccurate measurements due to its tendency to underestimate the dose profile. (www.rti.se.)

3.2 METHODS

3.2.1 Experimental Method

3.2.2 CT Protocol

Dose measurements were performed for a routine head and a routine body (chest, abdomen and pelvis) CT examination protocols as recommended by the manufacturer with automatic exposure control (AEC) and with manual fixed tube current (FTC) techniques. The scan protocols of the CT examinations conducted are presented in Tables 3.2 and 3.3.

Table 3.2: Protocol for AEC technique for routine head and body examination

Parameters	Examination			
	Head	Body		
		Thorax	Abdomen	Pelvis
kVp	130	130	130	130
Effective mAs	160	111	139	142
Rotation Time (s)	1.5	0.6	1	0.6
Acquisition (mm)	16 x 1.2	16 x 1.2	16 x 1.2	16 x 1.2
Slice Thickness (mm)	4	5	5	5
Pitch Factor	0.55	0.8	1.5	0.8
Reconstruction Slice	3 mm	3 mm	3 mm	3 mm
Kernel	H31S	B41S	B41S	B41S

Table 3.3: Scan parameters used for manual selection of fixed tube current technique (FTC) for routine head and body examination

Examination	kVp	mAs	Rotation Time (s)	Pitch	Slice Thickness (mm)
Head	130	140	1.5	0.55	4
Body	130	80	0.6, 1.0, 0.6	0.8, 1.5, 0.8	5
Head	130	160	1.5	0.55	4
Body	130	100	0.6, 1.0, 0.6	0.8, 1.5, 0.8	5
Head	130	180	1.5	0.55	4
Body	130	120	0.6, 1.0. 0,6	0.8, 1.5, 0.8	5
Head	130	200	1.5	0.55	4
Body	130	140	0.6, 1.0, 0.6	0.8, 1.5, 0.8	5
Head	130	220	1.5	0.55	4
Body	130	160	0.6, 1.0, 0.6	0.8, 1.5, 0.8	5
Head	130	240	1.5	0.55	4
Body	130	180	0.6, 1.0, 0.6	0.8, 1.5, 0.8	5
Head	130	260	1.5	0.55	4
Body	130	200	0.6, 1.0, 0.6	0.8, 1.5 0.8	5
Head	130	280	1.5	0.55	4
Body	130	210	0.6, 1.0, 0.6	0.8, 1.5, 0.8	5
Head	130	300	1.5	0.55	4
Body	130	220	0.6, 1.0, 0.6	0.8, 1.5, 0.8	5

3.2.3 Dose Measurements

In this study, dose measurements were performed by setting up the head and body phantoms in succession. The head phantom was first set up on the CT couch and centered at the isocenter of the scanner with the long axis of the phantom aligned with the z-axis of the scanner. A CT Dose profiler was connected to a barracuda via an extension cable and the barracuda connected to a computer with the modern ocean software. The CT Dose profiler was placed at the central hole of the phantom. The two horizontal CT lasers in the CT room were visible on the probe at the mid - line of it and the vertical laser also at the middle of the phantom were obtained for purposes of alignment.

A piece of tape was put along the probe, attaching it on to the phantom to ensure that the probe is not dislodged within the phantom during scanning. A topogram image of the phantom was taken and used to select the volume to be scanned. The AEC was activated for the first scan with the standard protocol of routine head examination as shown in Table 3.2. The head scan was repeated with manual selection of fixed tube current values (140 mAs, 160 mAs, 180 mAs, 200 mAs, 220 mAs, 240 mAs, 260 mAs, 280 mAs, and 300 mAs) whiles other parameters were kept constant (Table 3.3). The head phantom was scanned in spiral mode at routine CT head scan technique with the exposure factor of 130 kVp and a reference mAs of 220 mAs. These settings were chosen to provide a range of data points both above and below the default setting in order to check the functionality of the automatic exposure control (AEC) system as well as to ascertain the effects of the setting on both dose and image quality. After taking the head phantom measurement, similar scanned procedure was repeated on the body phantom. The AEC technique was scanned with the standard protocol for routine abdomen CT scan technique with exposure factor of 130 kVp at a reference mAs of

120 mAs. The body scan was repeated with manual selection of fixed tube current (80 mAs, 100 mAs, 120 mAs, 140 mAs, 160 mAs, 180 mAs, 200 mAs, 210 mAs and 220 mAs) whiles other parameters were kept constant. The volume computed tomographic dose index ($CTDI_{vol}$), weighted computed tomography dose index weighted ($CTDI_w$) and the dose length product values (DLP) values produced during the scanning were recorded after each scan for the head and body examinations. The measurement of radiation dose was automatically generated by the ocean software after the end of the examination which also includes the effective mAs or tube-current-time product values. Figure 3.5 shows the experimental setup for the dose measurements in this work.

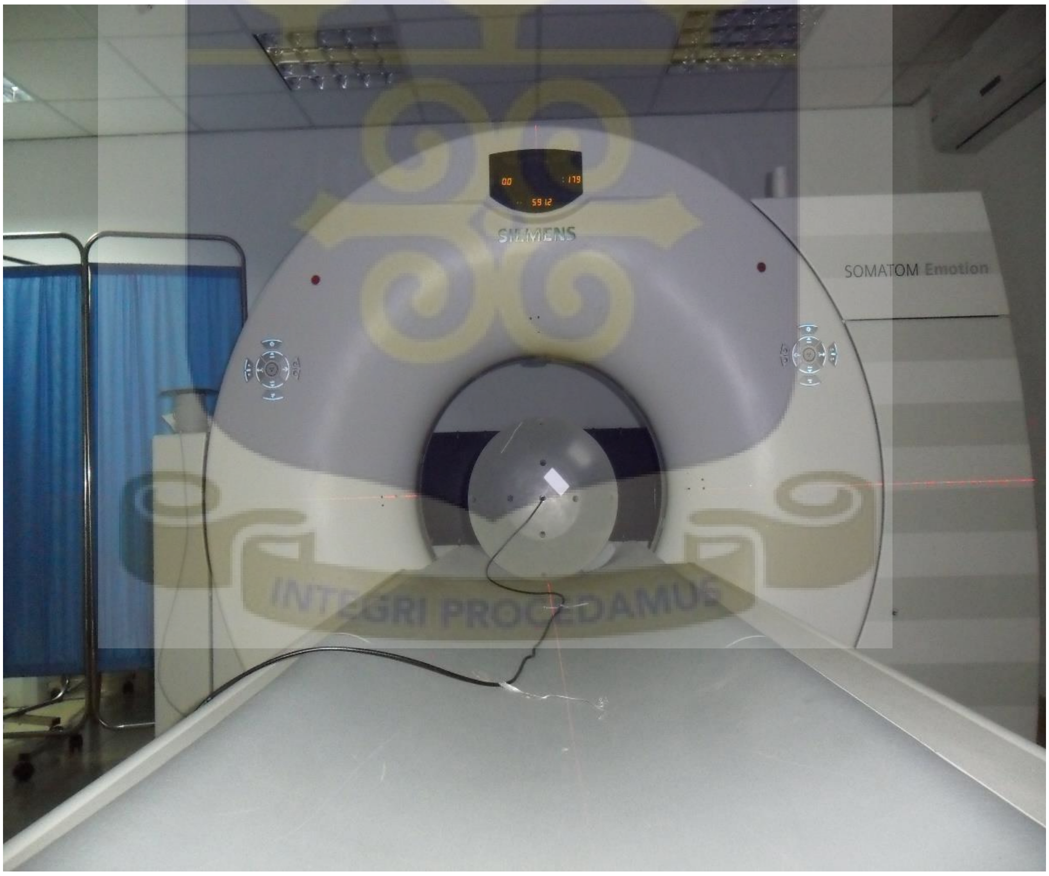

Figure 3.5: Experimental Setup for measurement of CTDI [Field work, 2016]

3.3 ORGAN AND EFFECTIVE DOSE ESTIMATION

Organ and effective doses were obtained using the CT-Expo software V2.3 (George et al., 2014) that calculates the dose for irradiation of a mathematical phantom shown in Figure 3.6. The CT-Expo V 2.3 is an MS Excel application written in Visual Basic for the calculation of patient dose in CT examinations. Dosimetry data were obtained from scans of the head and body phantoms used. These were used as input data into the CT- Expo software. The information extracted include; CT scan manufacture, model, patient age group, typical scanning parameters includes; the kV, mA acquisition time, total collimation, table feed, reconstructed slice thickness, number of scan series, scan length, $CTDI_{vol}$ (mGy) and DLP (mGy.cm). The effective dose calculation was done by using the organ dose conversion factors of ICRP 103.

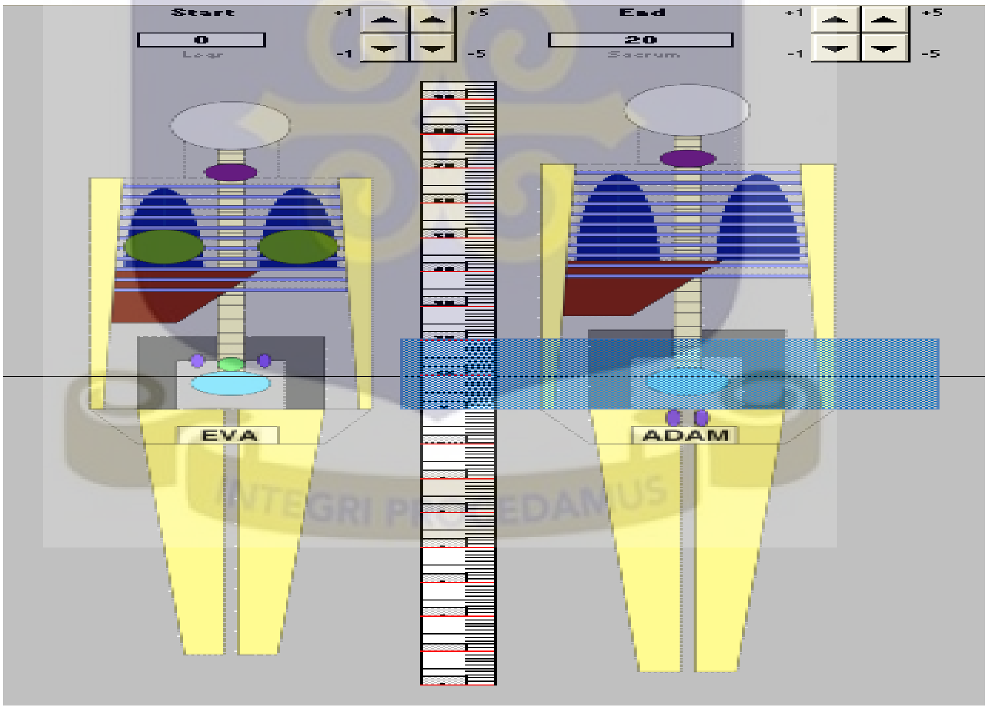

Figure 3.6: The phantom models used in the CT-Expo for calculation of the organs and Effective dose in the head, chest, abdomen and pelvis scans. The effective Dose can be selected using the organ weighting scheme of ICRP60 or ICRP 103. (G.Stamm., Hanover. German)

3.4 IMAGE QUALITY EVALUATION

Image quality is a characteristic used to assess the imaging performance of a medical diagnostic modality. The imaging performance of a system does not only relates to how an image is resolved, but how well it conveys the anatomical and functional information to the requested physician (Bushberg, 2002). The image quality was evaluated on a Siemens Somatom Emotion 16 - slice multi detector row CT scanner using a Catphan 700 phantom. The catphan 700 is a diagnostic imaging tool designed to test the image quality and system performance of CT scanners. It is divided into five different test modules each specific for a different image quality test. Figure 3.7 shows an illustration of the catphan 700 with the different test modules within the phantom. The catphan can be used to test different parameters regarding the performance of CT system. But those test that are pertinent to this study include; spatial resolution, low contrast detectability and contrast to noise ratio.

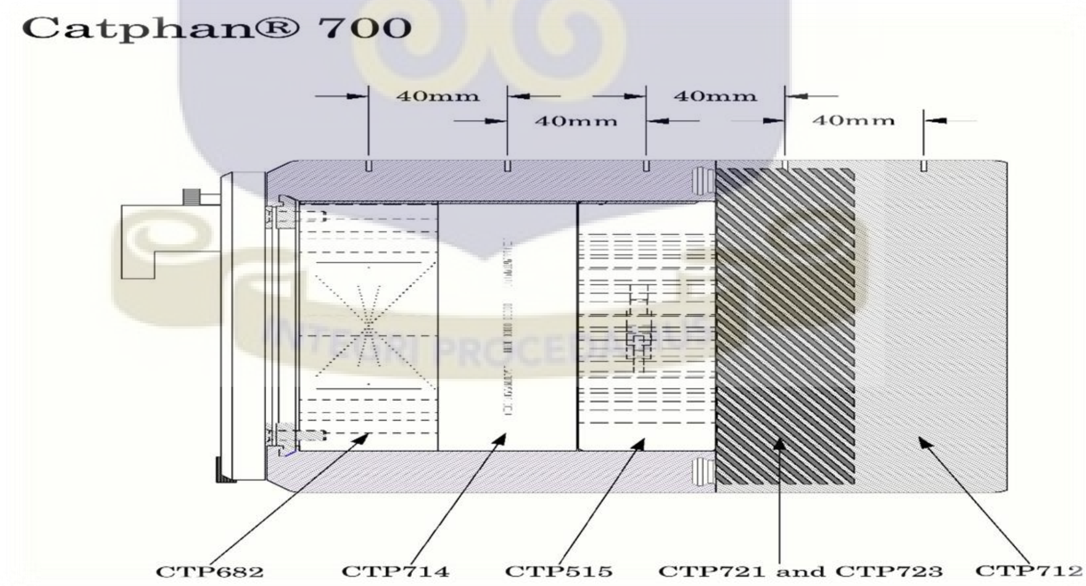

Figure 3.7: An illustration of the Catphan 700 used to evaluate the image quality performance of the CT scanner (Goodenough, D., 2013; The Phantom Laboratory Inc, Greenwich NY).

The module CTP714 of the catphan was used to evaluate the spatial or high contrast resolution and the module CTP515 been used to evaluate the low contrast detectability and the contrast to noise ratio. CT images obtained using automatic tube current modulation and manual selection of fixed tube current techniques were taken using routine exposure parameters on patients with the Siemens Somatom emotion CT scanner. The Catphan images from both techniques were then evaluated and compared in terms of spatial resolution, low contrast detectability and contrast to noise ratio to determine the difference in image quality at similar patient imaging protocols. Five different routine scan protocols were used to scan the phantom. These are default routine scan protocols on the machine used for the various examinations and provide the best estimate in evaluating the system image quality. Tables 3.4 and 3.5 shows the routine scan protocols used in performing the different examinations of this study.

The phantom was aligned in the gantry using the system's external lasers. The BB's located on the phantom were used to correctly align the phantom with the lasers in the axial, sagittal and longitudinal directions. The axial laser coincided with the last axial BB nearest to the phantom mount. Once the phantom was correctly aligned, it was imaged with different routine scan protocols. To compare the image quality obtained using automatic exposure control technique and fixed tube current technique, CT images of the spatial and low contrast resolutions modules of the catphan 700 phantom were obtained from each technique using the default routine patient scan protocols.

Table 3.4: List of routine patient imaging protocols with the use automatic exposure control

PROTOCOL	EXAMINATION Head helical	Thorax	Abdomen	Pelvis	Spine
KVp	130	130	130	130	130
mAs	81	33	57	53	26
Rotation Time (s)	1.5	0.6	0.6	1.0	1.0
Slice Thickness (mm)	4.0	5.0	5.0	5.0	3.0
Pitch	0.55	0.8	0.8	1.5	0.65
Collimation (mm)	16 x 1.2	16 x 1.2	16 x 1.2	16 x 1.2	16 x 0.6
Kernel	H31S	B41S	B41S	B41S	B31S
FOV (cm)	213	213	213	213	213

Table 3.5: List of routine patient imaging protocol with the use of manual fixed tube current technique (FTC).

PROTOCOL	EXAMINATION Head helical	Thorax	Abdomen	Pelvis	Spine
KVp	130	130	130	130	130
mAs	220	100	120	120	190
Rotation Time (s)	1.5	0.6	0.6	1.0	1.0
Slice Thickness (mm)	4.0	5.0	5.0	5.0	3.0
Pitch	0.55	0.8	0.8	1.5	0.65
Collimation (mm)	I6 x 1.2	16 x 1.2	16 x 1.2	16 x 1.2	16 x 0.6
Kernel	H31S	B41S	B41S	B41S	B31S
FOV (cm)	214	214	214	214	214

3.4.1 Evaluation of Catphan Images for AEC and FTC Techniques

The method used to evaluate and measure the images obtained with the use of automatic exposure control (AEC) and fixed tube current techniques were the same in order to determine the overall image quality for each patient protocol. A series of images from both techniques were transported into an ImageJ software to evaluate the spatial resolution, low contrast detectability and contrast to noise ratio module of the catphan phantom. Each module was evaluated using the methods presented in the catphan 700 manual (Phantom Laboratory Inc.). The purpose of the image quality evaluation was to quantitatively measure the overall image quality produced by the two scanning techniques on the CT system and compare the quality of the resulting images. The methods by which the images were evaluated are presented below.

3.4.1.1 Spatial Resolution

The spatial resolution is defined as the ability of a CT imaging system to distinguish as separate entities two objects that are very small and close to each other. The closer the objects are with the image depicting them as separate objects, the better the resolution of the imaging system. In this study, spatial resolution was measured using the CTP 714 module in the catphan. This module contains a 30 line pair per cm gauge cut from 2 mm thick aluminium sheets and cast into epoxy. The resolution was determine by the number of lines one could visualize out of the total number of line pair per centimetre. A score of 0 to 30 lp/cm was recorded depending on the number of line pairs one could see, where a higher value means better image resolution. Figure 3.8 shows the CTP 714 module together with data relating to the gap size between each line pair. Table 3.6 presents associated line pair per cm and gap sizes for the CTP 714 module.

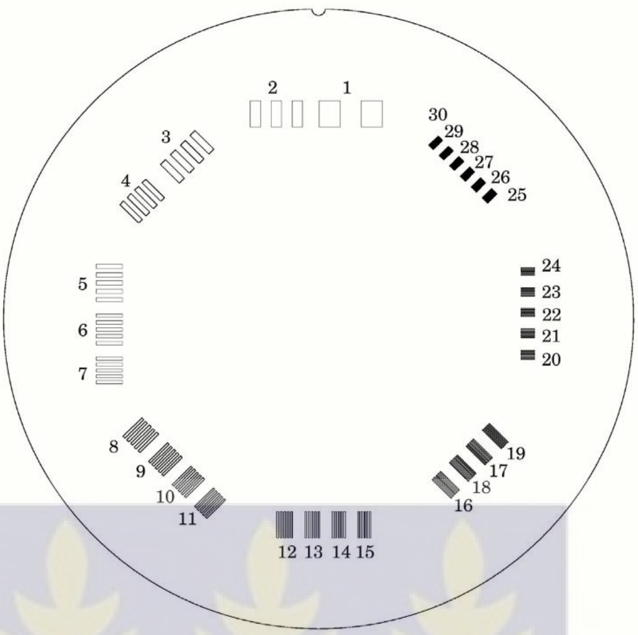

30 Line pair per centimetre high resolution gauge

Figure 3.8: CTP 714 Module used to evaluate the high contrast spatial resolution on the CT scanner (Goodenough, D., 2013; The Phantom Laboratory Inc, Greenwich NY).

Table 3.6: shows line pair per cm and gap sizes for the CTP 714 module.

Line Pair/cm	Gap Size	Line Pair/cm	Gap Size	Line Pair/cm	Gap Size
1	0.500 cm	11	0.045 cm	21	0.024 cm
2	0.250 cm	12	0.042 cm	22	0.023 cm
3	0.167 cm	13	0.038 cm	23	0.022 cm
4	0.125 cm	14	0.036 cm	24	0.021 cm
5	0.100 cm	15	0.033 cm	25	0.020 cm
6	0.083 cm	16	0.031 cm	26	0.019 cm
7	0.071 cm	17	0.029 cm	27	0.0185 cm
8	0.063 cm	18	0.028 cm	28	0.0178 cm
9	0.056 cm	19	0.026 cm	29	0.0172 cm
10	0.050 cm	20	0.025 cm	30	0.0167 cm

3.4.1.2 Low Contrast Detectability

In CT imaging systems, low contrast detectability is the ability of the imaging system to display as distinct images areas that differ in density by a very small amount. The catphan phantom low contrast module CTP515 contains various targets which are used to evaluate the CT system low contrast detectability performance. There are a total of six different contrast target areas within the module CTP515. There are three supra-slice targets located in the peripheral of the phantom with contrast levels of 1.0 %, 0.5 %, and 0.3 %. The supra-slice targets are cylindrical objects that are arranged round the entire length of the CTP515 module. At each of the three supra-slice contrast level, a total of 9 targets with varying diameters from 15 mm to 2 mm as shown in figure 3.9. Also three sub slice target areas located are in the center of the phantom with contrast levels of 1.0 % each. With each area containing four targets with varying diameters from 9 mm to 3 mm. The lengths of the cylindrical targets in the sub slice do not cover the entire length of the CTP515 module as in the case of the supra – slice and therefore have typically a z-axis length smaller than clinical slice thicknesses. The evaluation of the sub slice targets is helpful in understanding the scanner's different spiral imaging settings and the partial volume averaging techniques.

Low contrast performance evaluation in CT systems is done by visual analysis. In this study, the supra-slice and sub-slice target areas were evaluated independently of each another. The Supra-slice contrast was measured by determining the total number of visible targets at 1.0 %, 0.5 % and 0.3 % contrast levels with each image scored on a scale of 0-27 depending on the number of targets visualized. Similarly, the sup-slice contrast was determined by the total number of targets in the 3 mm, 5 mm, and 7 mm sections each at 1.0 % contrast level with a score of 0-12 for the sub-slice contrast.

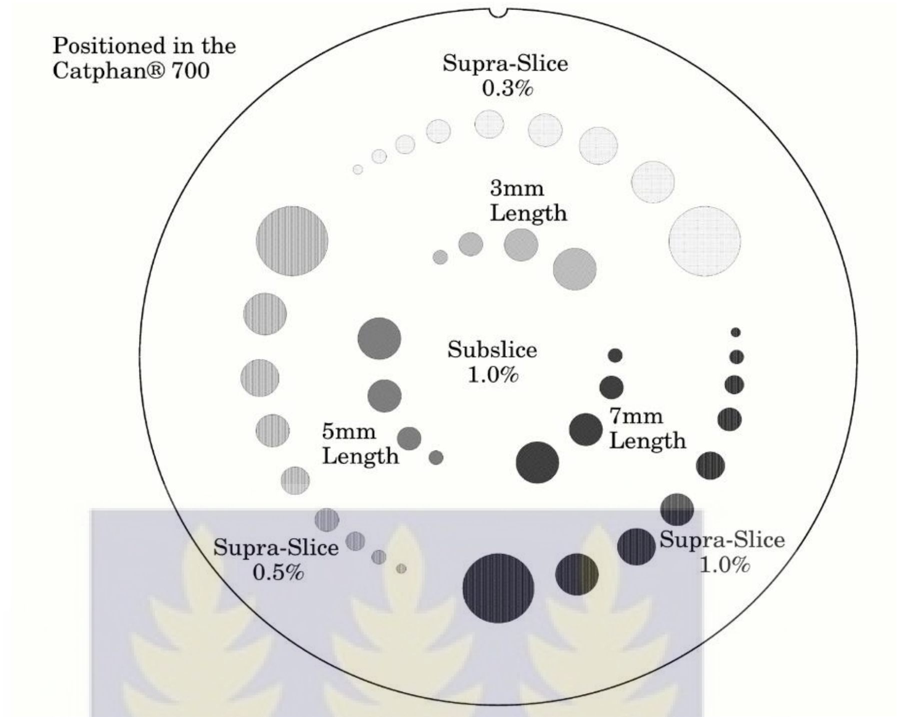

CTP515 low contrast module with supra-slice and sub-slice contrast targets

Figure 3.9: CTP515 low contrast module with phantom specifications (Goodenough, D., 2013: The Phantom Laboratory Inc, Greenwich NY)

Table 3.7: Shows diameters of the low contrast module for the supra and sub slice Targets.

Supra-slice target diameters (Outer circle of targets)	Sub-slice target diameters (Inner circle of targets)
2.0 mm	3.0 mm
3.0 mm	5.0 mm
4.0 mm	7.0 mm
5.0 mm	9.0 mm
6.0 mm	
7.0 mm	Nominal target contrast levels (±.05 %)
8.0 mm	0.3 %
9.0 mm	0.5 %
15.0 mm	1.0 %

3.4.1.3 Contrast-to-Noise Ratio (CNR)

The ability to see low contrast lesions in an image depends on how much noise is in the image. The greater the image noise the lower the low contrast visibility of lesions in an image and verse versa. However, one way of quantifying the contrast in an image is determining the contrast-to-noise ratio (CNR), which provides a value describing the quality of an image (Eq. 3-1). The CTP515 low contrast module was exported into ImageJ software after reading the obtained image on a DICOM viewer and used to determine the contrast to noise ratio. The contrast to noise ratio was measured by placing a region of interest (ROI) of 5.4 cm^2 in the 15 mm diameter target in the 1.0 % contrast level. The mean CT value for each target image was recorded. Similarly, a second ROI of the same area was placed on the background adjacent to the target and the mean background CT value was recorded. With this same background ROI, the standard deviation was also determined. The CNR was calculated using the relation;

$$CNR = \frac{Target\ mean\ value - Background\ mean\ value}{Background\ standard\ deviation} \tag{3.1}$$

The *CNR* was recorded for each imaging protocol with AEC activated and selection of fixed tube current technique and compared. Figure 3.10 show detail on how the *CNR* is calculated.

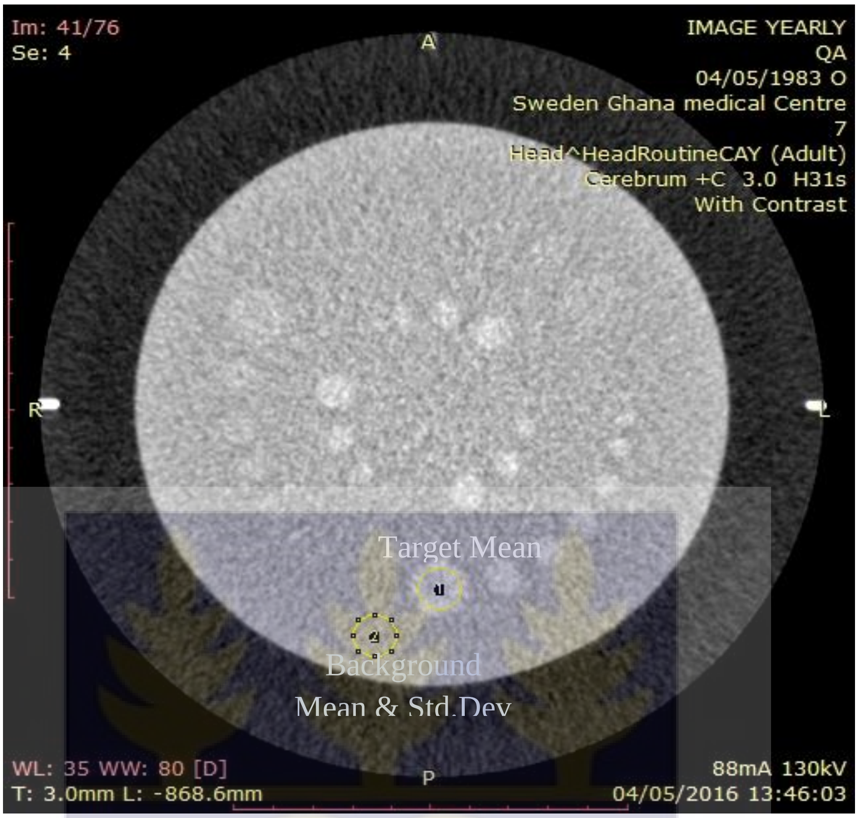

Figure 3.10: ROI evaluation for determining the CNR in each contrast target levels

3.5 DETERMINATION OF DOSE REDUCTION

The $CTDI_{vol}$ and DLP were obtained to represent the radiation dose delivered for each CT scan for the AEC and FTC techniques. From the $CTDI_{vol}$ and DLP values it was possible to estimate the reduction in radiation dose by calculating the difference of the $CTDI_{vol}$ and DLP values of the AEC in percent relative to the $CTDI_{vol}$ and DLP values for the fixed tube current technique as shown in Eq. 3-2 and 3-3. Thus, in terms of $CTDI_{vol}$ the;

$$Dose\ reduction = \frac{CTDI_{vol\ Fix\ m\ A} - CTDI_{vol\ AEC}}{CTDI_{vol\ Fix\ mA}} \times 100\% \qquad (3.2)$$

In terms of the DLP, the dose reduction is calculated as;

$$Dose\ reduction = \frac{DLP_{Fix\ mA} - DLP_{AEC}}{DLP_{Fix\ mA}} \times 100\% \qquad (3.3)$$

3.6 DATA ANALYSIS

The data collected were analysed using the Statistical Package for the Social Sciences (SPSS) version 20.0. The SPSS was used to conduct relevant statistical analysis of the results obtained. This was selected mainly because of its proven track record as an excellent software tool for statistical analysis in most research areas. The paired *t*-test was used to compare the DLP, and CTDIvol between the AEC and FTC imaging techniques as well as the overall image quality test for spatial resolution, low contrast detectability and contrast to noise ratio. A value of $P < 0.05$ indicates a statistically significant difference.

3.7 THEORY

3.7.1 Dose Measurements in CT

Theoretically, the amount of dose delivered to the patient during a CT scan is usually measured using a standardized index called computed tomography dose index (CTDI). The CTDI is defined as the integral along a line Z perpendicular to the tomographic plane of the dose profile D(z) for a single axial scan, divided by the product of the number of tomographic sections N and the nominal section thickness T (Shope, et al., 1981). $CTDI_{100}$ is commonly used when measuring radiation dose in CT and refers to the absorbed dose integrated over a length of 100 mm. In order to measure $CTDI_{100}$, a 3-cc active volume CT pencil ionization chamber with an active length of 100 mm is used, often in a cylindrical PMMA phantom (15 cm in length), with a diameter of 32 cm (body) or 16 cm (head) (Galanski, et al., 2002). The $CTDI_{100}$ is given by the equation (Eq. 3.4).

$$CTDI_{100} = \frac{1}{nt} \int_{-50\,mm}^{+50\,mm} D(z)dz \tag{3.4}$$

The measurements is normally performed with a stationary patient table. In dose measurement, charges produced are converted in to exposure in roentgen (R) or air kerma in milligray (mGy) with an exposure meter. The meter reading thus represent the average exposure reading over the length of the chamber given by the relation (Eq 3. 5);

$$Meter\ reading = \int_{-\ell/2}^{\ell/2} X(z) \frac{1}{f.\ell} \int_{-\ell/2}^{\ell/2} D(z)dz \tag{3.5}$$

Where *f* is the exposure to dose conversion factor, *D* = *f. X*

From equation (3-4) the CTDI is calculated using the relation;

$$CTDI = \frac{f\left(\frac{rad}{R}\right) * (mm) * meter\ reading(R)}{N * T(mm)} \tag{3.6}$$

Thus, from the definition of $CTDI_{100}$ above, equation (3.6) can be simplify to obtain the relation;

$$CTDI_{100}(rad) = \frac{C * f\left(\frac{rad}{R}\right) * 100\ mm * meter\ reading(R)}{N * T(mm)} \tag{3.7}$$

Where *C* is the unitless chamber correction factor which is required to correct the meter reading for temperature and pressure and into true exposure reading which is *1.06* for dose to tissue is usually and *f* value been *0.94 rad/R* for tissue dose estimates (McCollough et al., 2008).

3.7.2 Effective Dose Estimation

Theoretically, effective dose can be estimated using conversion factors (E_{DLP}) which has been published by European Commission (European Commission 1999) for a general anatomic region. This value is the normalized effective dose per dose length product over various body regions such as head, neck, chest, abdomen and pelvis for different sizes of patient. In this approach, $CTDI_{vol}$ and distance (scan length) are used to estimate the dose length product (DLP) and then multiplied with the conversion factor value to obtained the effective dose (E) using the equation (3.8) below.

$$E = E_{DLP} * DLP \tag{3.8}$$

Where, E_{DLP} is the *DLP* to effective dose conversion factor.

3.7.3 Organ dose determination

Doses to radiosensitive organs in CT examinations can be determined by measuring CT dose in air ($CTDI_{air}$) and organ dose conversion coefficients (Jones & Shrimpton, 1993). Most often organ dose data are expressed in terms of absorbed dose to tissue, this measured values of dose in air ($CTDI_{air}$) are converted to dose to tissue ($CTDI_{tissue}$) using the ratio of the mass-energy absorption coefficients $\left({}^{\mu_{en}}/_{\rho}\right)$ of tissue to air. The $CTDI_{tissue}$ is calculated using equation (3.9);

$$CTDI_{tissue} = \frac{\left({}^{\mu_{en}}/_{\rho}\right)tissue}{(\mu_{en}/\rho)air} * CTDI_{air} \tag{3.9}$$

However, the mass-energy absorption coefficient depends on the photon energy with it ratio for soft tissue to air assumed to be constant for all typical X-ray spectra produced by the CT scanners examined with a value of 1.06 (with an error of no more than ±1%). Hence, using scanner-specific organ dose conversion coefficient, the average organ dose,

$D_{org,\,T}$ for individual examination can be estimated using the relation (Eq.3.10);

$$D_{org,T} = CTDI_{tissue} \sum_{z_1}^{z_2} f(organ, z). \tag{3.10}$$

Where z_1 and z_2 are the start and end region of the scanned position respectively.

CHAPTER FOUR

4.0 RESULTS AND DISCUSSION

This chapter outlines and discusses the results obtained from measurements made on acrylic head and body PMMA phantoms for comparison of radiation dose and image quality when an AEC and FTC techniques are used. The results for the estimation of effective and organ doses for the most radiation sensitive organs in the head and trunk regions are also presented.

4.1 RESULTS

4.1.1 Measurements of $CTDI_{vol}$, $CTDI_w$ and DLP with the use of AEC and FTC

The results of $CTDI_{vol}$, $CTDI_w$ and DLP values were obtained from an average of three measurements in the head and body phantoms scan with AEC activated and comparison made with European MDCT DRLs (Bongartz et al., 2004) and IAEA - study (Tsapaki et al., 2006). The results are presented in Tables 4.1 and 4.2. The obtained dose descriptors; weighted computed tomography dose index ($CTDI_w$), volume computed tomography dose index ($CTDI_{vol}$), and dose-length product (DLP) are shown in Tables 4.1 and 4.3.

Table 4-1: Measurements of CTDIvol, CTDIw and DLP values for head and body examination with AEC

Examination	CTDIvol (mGy)	CTDIw (mGy)	DLP (mGy.cm)
Head	32.8	18.0	593.0
Chest	6.7	6.0	108.0
Abdomen	14.3	11.0	240.0
Pelvis	11.7	17.0	190.0

Table 4-2: comparison of average CTDIvol and DLP values with AEC and other studies

Examination	This Study		IAEA study, Tsapaki et al., 2006		European DRL, Bongartz et al., 2004	
	CTDIvol (mGy) and DLP (mGy.cm)					
	$CTDI_{vol}$	DLP	$CTDI_{vol}$	DLP	$CTDI_{vol}$	DLP
Head	32.8	593.0	47.0	527.0	64.0	337.0
Chest	6.7	108.0	9.5	447.0	7.8	267.0
Abdomen	14.3	240.0	10.9	696.0	14.5	724.0
Pelvis	11.7	190.0	-	-	14.5	724.0

Note: (-) means no data was available

Similarly, the results of $CTDI_{vol}$ and DLP values for the fixed mAs technique were obtained from an average of three measurements in the head and body phantom with varied fixed mAs values as presented in Tables 4.3- 4.4.

Table 4-3: Measurements of CTDIvol, CTDIw and DLP values for head phantom examination with fixed mAs.

Fixed mAs	CTDIvol (mGy)	CTDIw (mGy)	DLP (mGy.cm)
140	32.9	17.60	571.0
160	33.4	18.50	602.0
180	34.5	18.95	615.0
200	37.2	20.44	664.0
220	41.0	22.53	731.0
240	44.6	24.55	797.0
260	50.7	27.86	904.0
280	51.4	26.40	922.0
300	53.0	29.12	946.0

Table 4-4: Measurements of CTDIvol, CTDIw and DLP values for body phantom examination with fixed mAs.

Fixed	CTDIvol (mGy)			CTDIw (mGy)			DLP (mGy.cm)		
mAs	C	A	P	C	A	P	C	A	P
80	9.5	9.5	9.5	8	8	14	284	165	250
100	11.0	11.2	11.9	11	9	18	354	181	314
120	14.3	13.5	14.3	13	11	21	426	197	376
140	16.7	15.6	16.7	15	13	25	497	251	439
160	19.0	18.0	19.0	17	14	28	568	290	502
180	21.4	20.0	21.1	19	16	32	639	327	565
200	23.8	22.8	24.0	21	19	35	710	357	658
210	25.0	23.5	25.0	22	19	37	745	327	627
220	26.2	24.2	26.2	23	21	39	780	543	690

Note: C, A and P represent Chest, Abdomen and Pelvis examinations respectively.

The $CTDI_{vol}$ and the dose length product (DLP) values determined in this study are presented in Table 4.5 for both, head and body phantoms between the two imaging techniques along with proposed recommendations and other countries diagnostic reference levels. For the head examination, the $CTDI_{vol}$ and DLP values refers to the 16 cm diameter dosimetry phantom, for the trunk regions examination the CTDIvol and the DLP values refers to the 32 cm diameter dosimetry phantom**.**

Table 4-5: Comparison of CTDIvol and DLP values for the head and body phantom examination with fixed mAs and other studies.

Fixed	CTDIvol (mGy)				DLP (mGy.cm)			
mAs	Head	Chest	Abdomen	Pelvis	Head	Chest	Abdomen	Pelvis
80	32.9	9.5	9.5	9.5	571	284	165	250
100	33.4	11.0	11.2	11.9	602	354	181	314
120	34.5	14.3	13.5	14.3	615	426	197	376
140	37.2	16.7	15.6	16.7	664	497	251	439
160	41.0	19.0	18.0	19.0	731	568	290	502
180	44.6	21.4	20.0	21.1	797	639	327	565
200	50.7	23.8	22.8	24.0	904	710	357	658
210	51.4	25.0	23.5	25.0	922	745	327	627
220	53.0	26.2	24.2	26.2	946	780	543	690
Other Studies								
Pontas et al., (2011)	**-**	**-**	**-**	**-**	**733**	**394**	**464**	**434**
Turkey (2015)	**66.4**	**11.6**	**13**	**19.4**	**810**	**389**	**204**	**421**
Ireland (2012)	**66.2**	**9.2**	**12**	**12.3**	**940**	**393**	**598**	**598**
IAEA Study; Tsapaki et al., (2006)	**47**	**9.5**	**11**	**-**	**527**	**447**	**696**	**-**

Note: (-) means no available data and H, C, A and P represents, Head, Chest, Abdomen and Pelvis examinations respectively.

An estimation of the dose reduction between the AEC and the FTC techniques for the head examination is presented in Table 4.6. Compared with fixed tube current (FTC), there was significant difference in the $CTDI_{vol}$ *($P = 0.009$)* and DLP *($P = 0.013$)* values with a mean dose reduction of 19.4% (0.3 – 38.1% for $CTDI_{vol}$) and 18.2% (-3.9-37.3 for DLP) were achieved for the head examination with the used of the AEC.

Table 4-6: Estimated dose reduction (DR) in CTDIvol and DLP for head phantom between AEC and fixed mAs.

Scanning Type	$CTDI_{vol}$ (mGy)	DR for $CTDI_{vol}$ [%]	DLP (mGy.cm)	DR for DLP [%]
AEC	32.8	-	593.0	-
140	32.9	0.3	571.0	-3.9
160	33.4	1.7	602.0	1.5
180	34.5	4.9	614.9	3.6
200	37.2	11.8	663.5	10.6
220	41.0	20.0	731.3	18.9
240	44.6	26.5	796.8	25.6
260	50.7	35.3	904.2	34.4
280	51.4	36.2	921.6	35.7
300	53.0	38.1	945.5	37.3
p-value	*0.009*	*19.4%*	*0.013*	*18.2%*

Note: The P-values indicate if there is significant difference in the $CTDI_{vol}$ and DLP values between the AEC and FTC techniques. Thus, $P < 0.05$ indicates significant difference and $P > 0.05$ indicates no significant difference between the two techniques.

Table 4-7: Estimated dose reduction (DR) in CTDIvol for body phantom between AEC and fixed mAs.

Scanning Type	$CTDI_{vol}$ (mGy)			DR [%]		
	C	A	P	C	A	P
AEC	6.7	14.0	12.0	-	-	-
80	9.5	9.5	9.5	29.5	-47.4	-26.3
100	11.0	11.2	12.0	39.1	-25.0	-1.0
120	14.3	13.5	14.0	53.1	-3.7	16.1
140	16.7	15.6	17.0	59.9	10.3	28.1
160	19.0	18.0	19.0	64.7	22.2	36.8
180	21.4	20.0	21.0	68.7	30.0	43.1
200	23.8	22.8	24.0	71.8	38.6	50.0
210	25.0	23.5	25.0	73.2	40.4	52.0
220	26.2	24.2	26.0	74.4	42.1	54.2
P-value	*3.9×10^{-4}*	*0.84*	*0.01*	*59.4%*	*12%*	*28.1%*

Note: C, A, P represents chest, abdomen and pelvis respectively. Mean dose reduction of 59.4%, 12%, 28.1% in CTDIvol was achieved with the use of AEC for chest, abdomen and pelvis examinations compared with FTC technique. There was significant difference in $CTDI_{vol}$ for chest examination *($P = 3.9x10^{-4}$)* and pelvis examination *(P = 0.013)* between AEC and FTC techniques. However, no significant difference in CTDIvol for the abdomen examination was noted *(P = 0.84)* between the two imaging techniques.

Table 4-8: Estimated dose reduction (DR) in DLP for body phantom between AEC and fixed mAs.

Scanning Type	DLP (mGy.cm)			DR [%]		
	C	**A**	**P**	**C**	**A**	**P**
AEC	108	240	190	-	-	-
80	284	165	250	62.0	-45.5	24.0
100	354	181	314	69.5	-32.6	39.5
120	426	197	376	74.6	-21.8	49.5
140	497	251	439	78.3	4.4	56.7
160	568	290	502	81.0	17.2	62.2
180	639	327	565	83.1	26.6	66.4
200	710	357	658	84.8	32.8	71.1
210	745	327	627	85.5	26.6	69.7
220	780	543	690	86.2	55.8	72.5
P-value	$6.5x10^{-5}$	*0.209*	$4.2x10^{-4}$	78.3%	7.1%	56.8%

Note: C, A, P represents chest, abdomen and pelvis respectively. Mean dose reduction of 78.3%, 7.1%, and 56.8% in DLP was achieved with the use of AEC for chest, abdomen and pelvis examinations compared with FTC technique. There was significant difference in $CTDI_{vol}$ for chest examination *($P = 6.5x10^{-5}$)* and pelvis examination *($P = 4.2x10^{-4}$)* between the two techniques. However, no significant difference in DLP for the abdomen examination was noted *(P = 0.209)* between the two imaging techniques.

4.1.2 Effective Dose

The results of the effective doses obtained in this study for the routine examinations between AEC and fixed mAs techniques are presented in Table 4.9. A comparison of the effective dose values between the two techniques and literature are depicted in table 4.10.

Table 4-9: Effective dose values calculated using CT-Expo software with AEC activated and fixed mAs techniques.

Scanning Type	Examination			
	Head	**Chest**	**Abdomen**	**Pelvis**
AEC	1.6	6.4	6.1	5.4
Fixed mAs	1.4	4.8	3.5	3.1
Fixed mAs	1.6	**[6]**	4.4	3.9
Fixed mAs	1.7	7.2	**[5.3]**	**[4.6]**
Fixed mAs	1.9	8.4	6.1	5.4
Fixed mAs	2.2	9.6	7.0	6.2
Fixed mAs	**[2.3]**	10.8	7.9	7.0
Fixed mAs	2.4	12.0	8.7	7.7
Fixed mAs	2.6	13.0	9.2	8.1
Fixed mAs	2.8	13.2	9.7	8.5

Note: the values in square brackets [ ] represents the effective dose values at quality reference mAs values used for the various examinations.

Table 4-10: Comparison of effective dose values between this study and literature. (Mean values in brackets).

Study	Head	Chest	Abdomen	Pelvis
UNSCEAR, 2008	1.6	9.7	12	9.8
Breiki et al., 2008	1.14-2.74 (1.76)	4.65-24.45(14.56)	3.86-32.53(14.56)	4.08-18.10(11.21)
Goddard & Alfarsi 1999	0.3-8.2 (2.4)	0.3-10.8(3.4)	1.4-31.2 (9.5)	2.7-13.8 (6.0)
Clark et al., 2000	0.98-2.11 (1.9)	3.84-14.58 (8.9)	3.8-13.35 (10.6)	1.13-24.8 (7.12)
NRPB-Standards, 1991	0.46-4.94 (1.78)	1.05-22.5 (7.8)	1.58-22.6 (7.58)	(10)
Inkoom et al., 2014	1.1-1.6	2.7-9.3	5.3-13.2	5.5-9.1
This study				
AEC	1.6	6.4	6.1	5.4
FTC	1.4-2.8 (2.1)	4.8-13.2(9.4)	3.5-9.7 (6.9)	3.1-8.5(6.1)

4.1.3 Organ Doses

Organ doses resulted for the various routine examinations protocols conducted with AEC activated and with FTC technique are presented in Figures (4.1-4.4). The organ doses were determined under the same acquisition parameters except with the FTC technique where the mAs values were varied both below and above reference mAs values for each routine examination conducted.

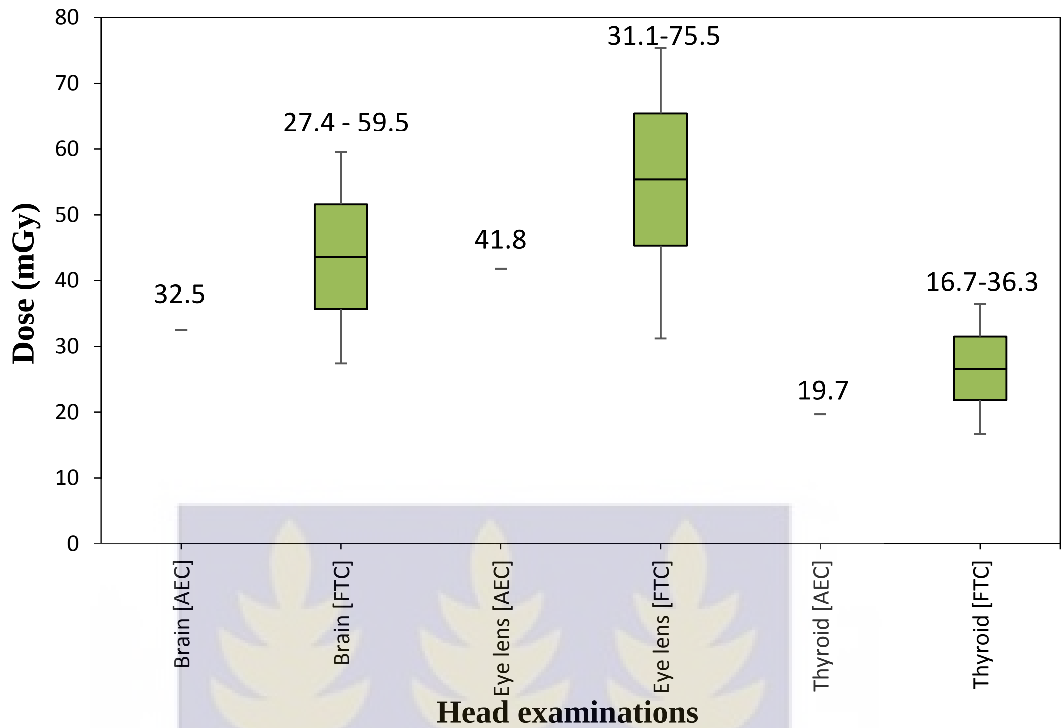

Figure 4.1: Organ doses for head examinations

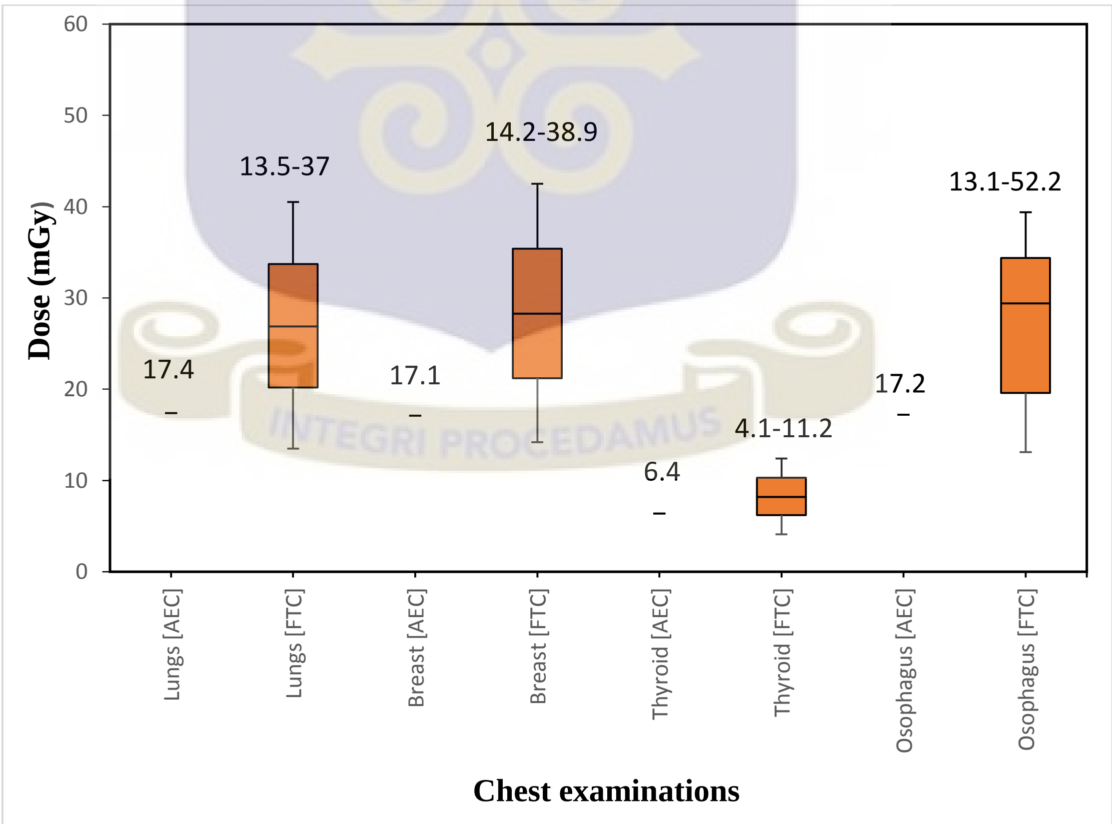

Figure 4.2: Organ doses for chest examination

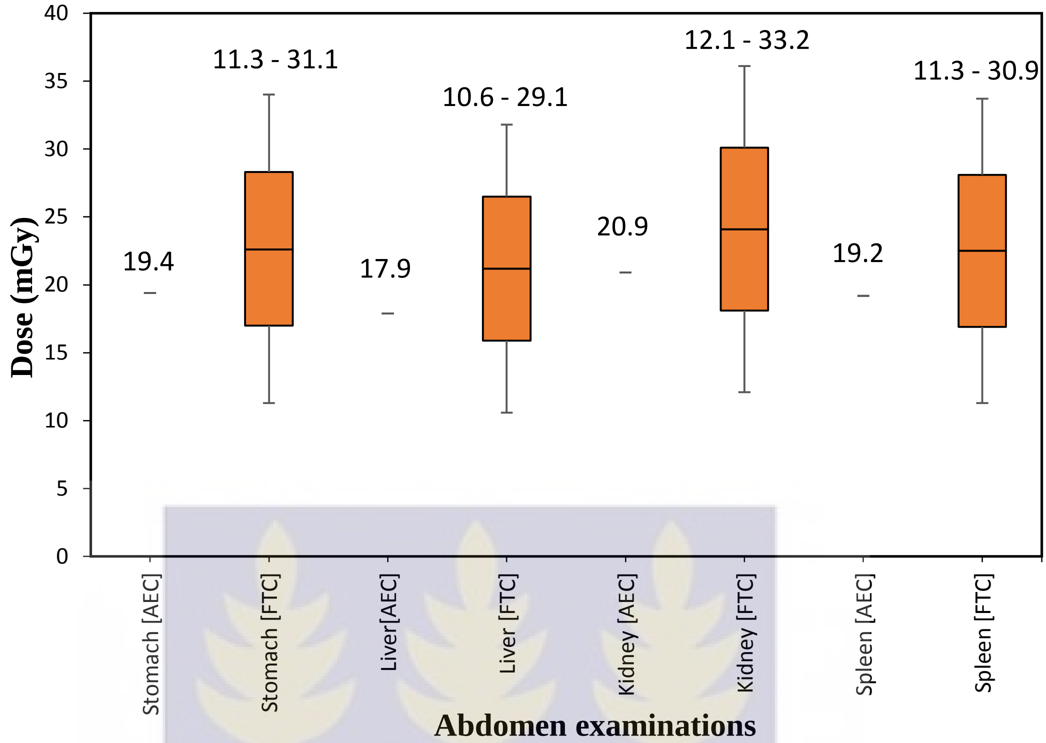

Figure 4.3: Organ doses for abdomen examinations

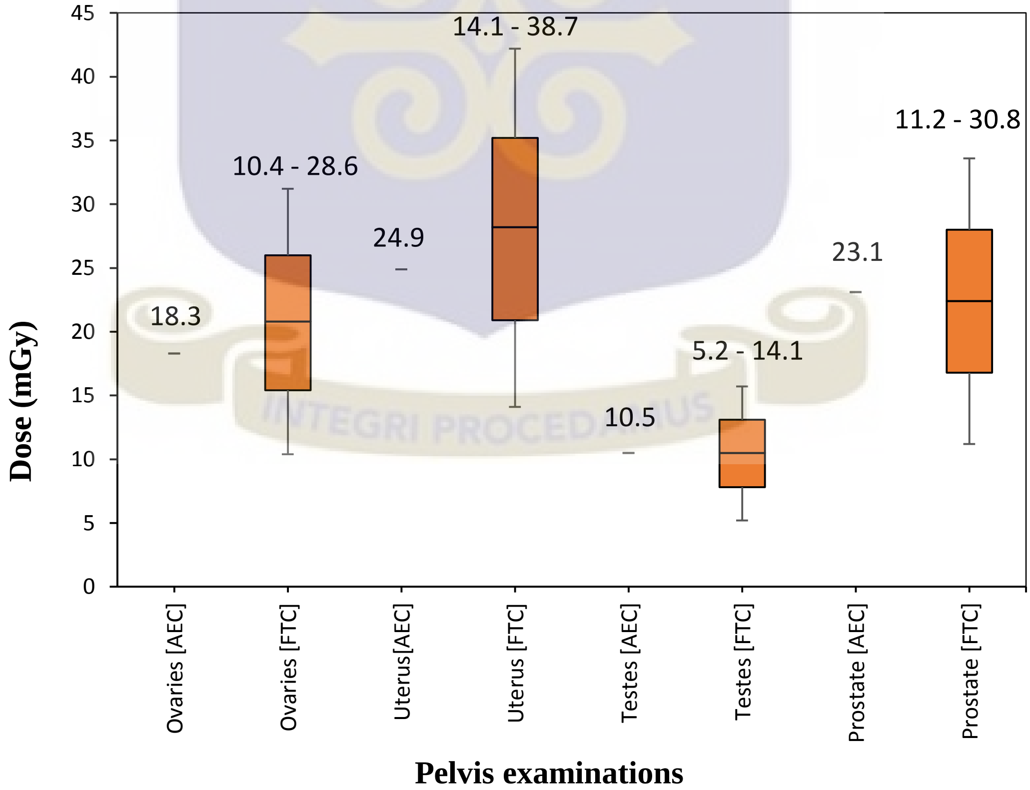

Figure 4.4: Organ doses for pelvis examinations

4.1.4 Comparison of organ doses between AEC and FTC at quality reference mAs values.

Comparison of the resultant organ doses with the AEC activated and at fixed reference mAs values for the various routine examinations considered is shown Figures 4.5 – 4.8. It is evident from the results that, the doses received by most radiation sensitive organs are much lower when the AEC was used compared with reference mAs values. However, the pelvic examination depicts a relative high organ doses with the use of the AEC system compared with the FTC technique. Similar trend was also observed for the thyroid organ in the case of abdomen examination. This variation in organ doses between the AEC technique and that of the reference mAs values may be attributed to the mAs used in each case.

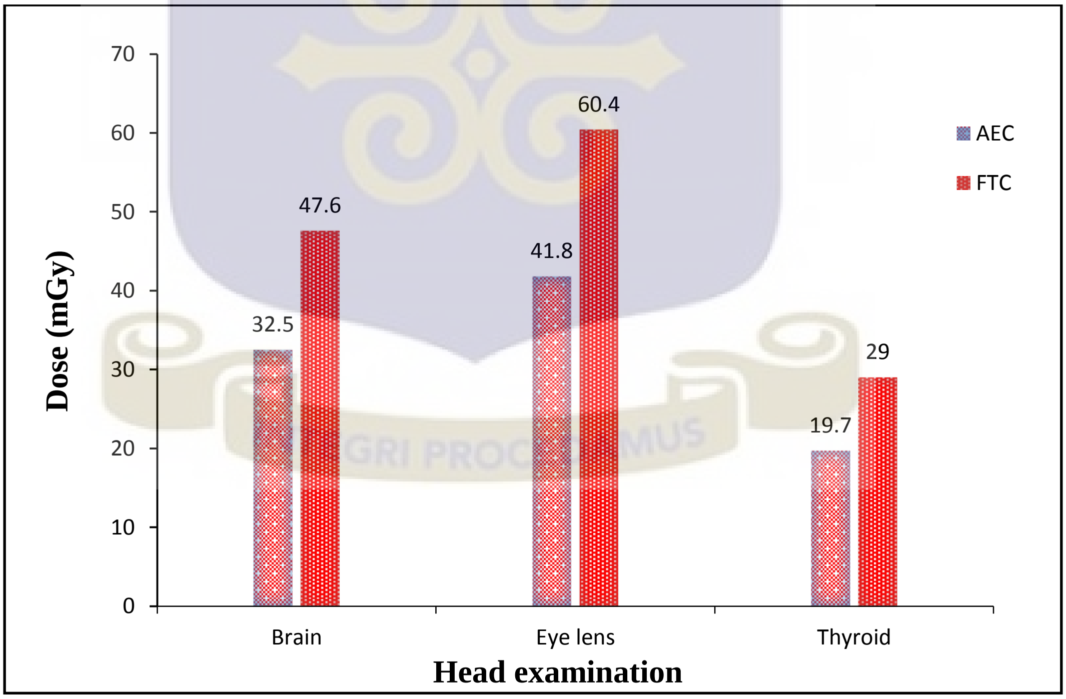

Figure 4.5: Comparison of organ doses between AEC activated and at fixed quality reference mAs (240) for head examination.

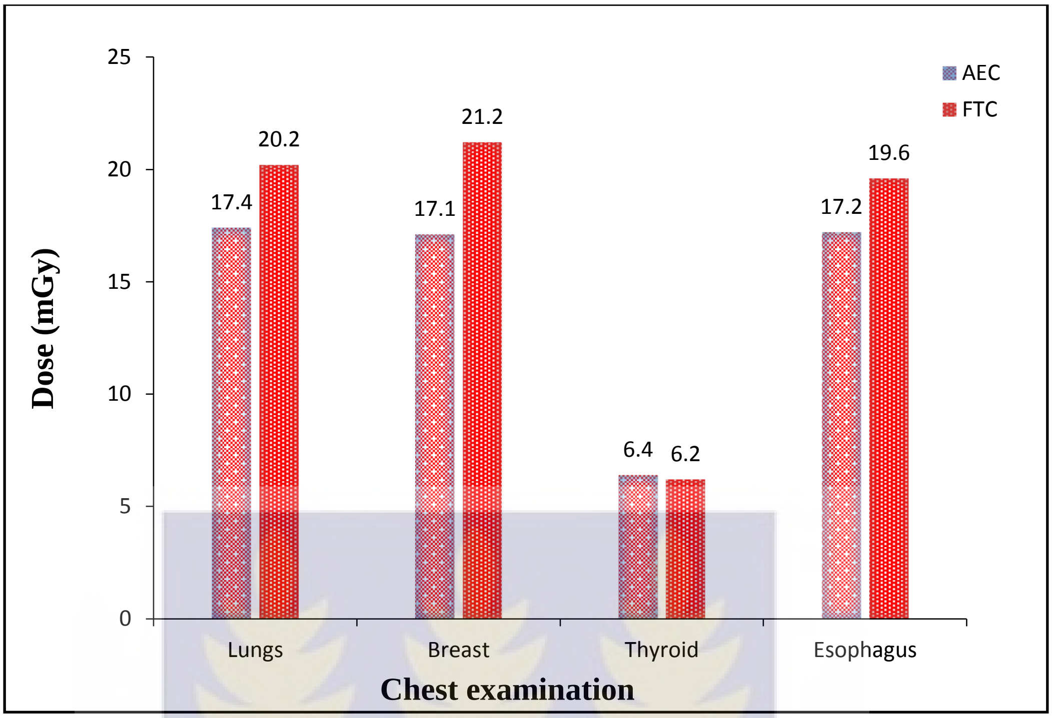

Figure 4.6: Comparison of organ doses between AEC activated and at fixed quality reference mAs (100) for chest examination.

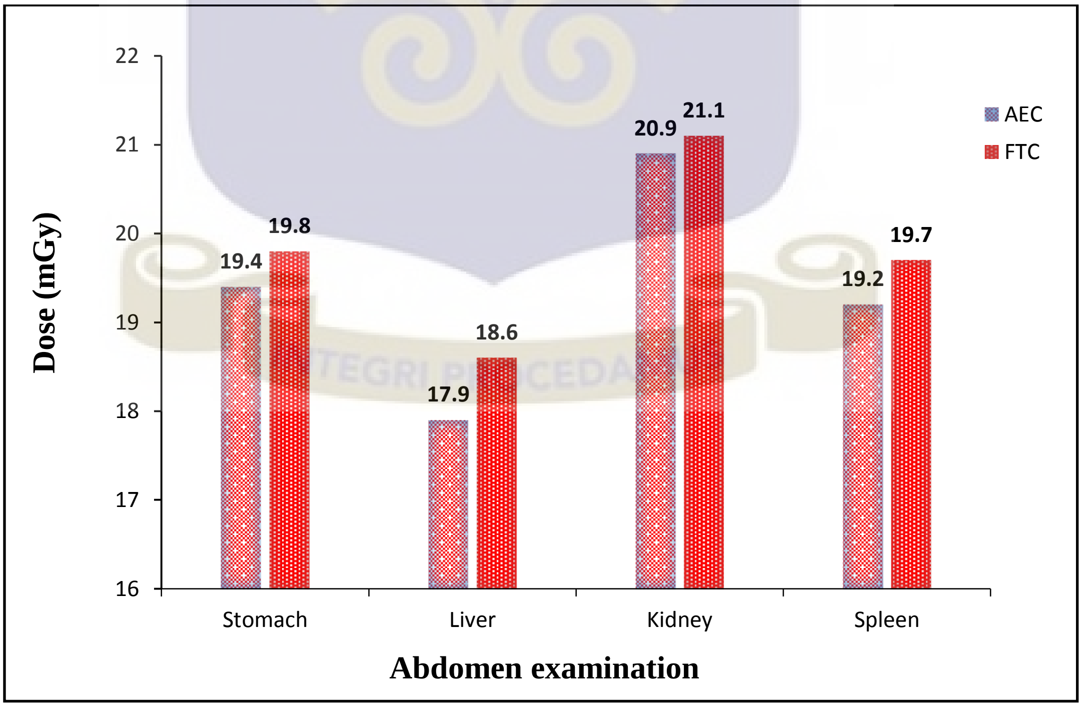

Figure 4.7: Comparison of organ doses between AEC activated and at fixed quality reference mAs (120) for abdomen examination.

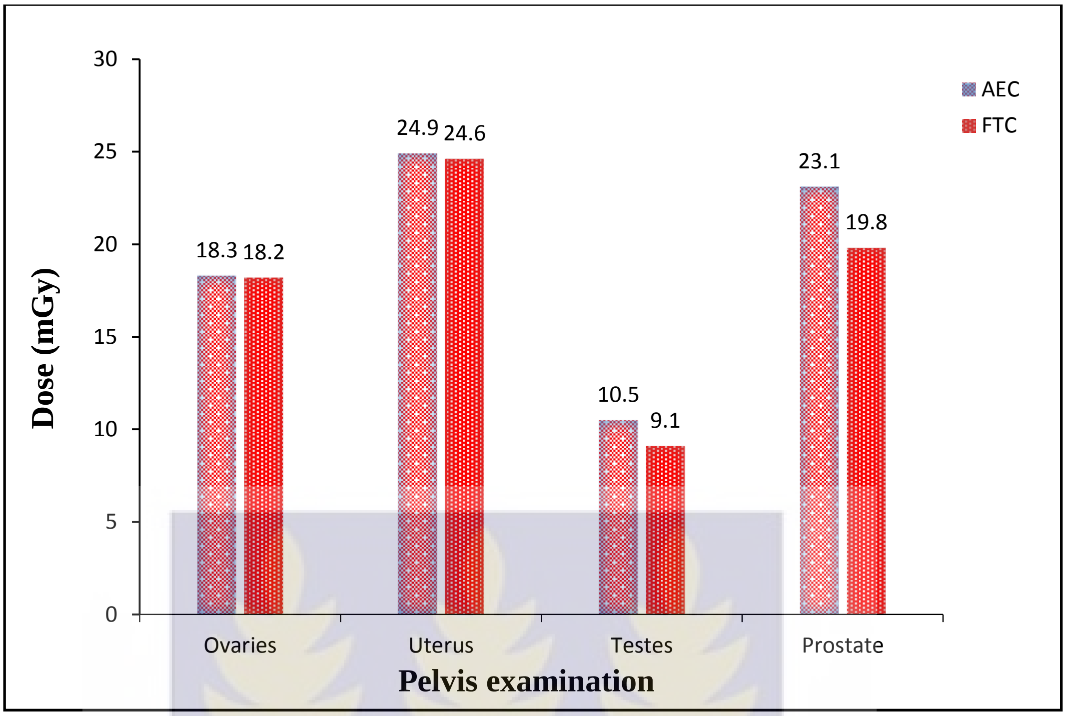

Figure 4.8: Comparison of organ doses between AEC activated and at fixed quality reference mAs (120) for pelvis examination.

Table 4-11: Comparison of mean organ doses in this study and other studies

CT Exams	Selected Organs	This Study AEC (mGy)	This Study FTC (mGy)	UK (1991) (mGy)	Japan (1991) (mGy)	Germany (1999) (mGy)	Tanzania (2006) (mGy)
Head	Eye lens	41.8	45.4 (±15.2)	-	22.4	24.8	63.9 (± 32.6)
	Thyroid	19.7	26.3 (± 6.8)	1.9	0.6	-	2.5 (± 1.3)
Chest	Lungs	17.4	26.4 (± 8.4)	22.4	19.6	20.5	31.5 (± 10.6)
	Breast	17.1	27.7 (± 8.8)	21.4	15.9	22.6	26.1 (± 10.8)
	Thyroid	6.4	8.0 (± 2.6)	2.3	1.9	-	12.3 (± 8.5)
Abdomen	Liver	17.9	20.8 (± 7.1)	20.4	27.8	15	34.1 (± 10.7)
	Stomach	19.4	22.1 (± 6.6)	22.2	26.9	15.4	35.6 (± 10.3)
Pelvis	ovaries	18.3	20.3 (± 6.5)	22.7	15.1	14.9	24 (± 17.1)
	Uterus	24.9	27.5 (± 8.8)	25.5	-	14.6	26.5 (± 18.6)
	testes	10.5	10.2 (± 3.2)	1.7	1	-	12.5 (± 19.9)

Note: (-) means no available data

4.1.5 IMAGE QUALITY

4.1.5.1 Contrast–to–Noise Ratio (CNR)

The contrast-to-noise ratio (CNR) was determined with the used of AEC and FTC techniques as shown in Tables (4.12-4.13). The CNR relates to overall image quality with respect to how much noise is seen in a particular image. Generally, the higher the CNR in an image, the lesser the noise with improved image quality. The results obtained with the AEC technique indicates that the routine head scan protocol images recorded the highest CNR (less noise) with a CNR score of 2.3. The other imaging scan protocols shows a slight varying CNR values with the thorax, abdomen, pelvis and spine having a score of 1.1, 1.0, 0.8, and 1.3 respectively. Thus the image which show the highest amount of noise is the one with the lowest CNR, which is the pelvis scan protocol image with a value of 0.8.

Comparatively, the FTC technique images shows a much higher CNR scores to that of the AEC technique. As depicted in Table 4.13, the head image recorded the highest CNR score with 2.5. The abdomen and the pelvis images have the same CNR value of 2.1 and the lowest CNR score is seen in the thorax and spine images with a value of 1.9 each. This data reflects the results seen in the low contrast detectability test where fewer targets were seen.

Table 4-12: Contrast to noise ratio with AEC technique imaging procedures

	Contrast - to - Noise Ratio With AEC				
Supra Slice @ 15mm Target Contrast level: 1.0%	**Head routine**	**Thorax routine**	**Abdomen routine**	**Pelvis routine**	**Spine**
Target Mean	186.8	140.7	143.5	145.1	142.8
Background Mean	153.4	134.0	135.7	138.9	134.5
Background Std Deviation	14.5	6.1	8.1	8.0	6.4
Contrast to Noise Ratio:	2.3	1.1	1.0	0.8	1.3

Table 4-13: Contrast to noise ratio with FTC technique imaging procedures

	Contrast - to - Noise Ratio With FTC				
Supra Slice @ 15mm Target Contrast level: 1.0%	**Head routine**	**Thorax routine**	**Abdomen routine**	**Pelvis routine**	**Spine**
Target Mean	209.7	139.9	144.0	146.3	141.7
Background Mean	175.6	133.4	135.6	138.9	135.1
Background Std Deviation	13.6	3.5	4.0	3.5	3.4
Contrast to Noise Ratio:	2.5	1.9	2.1	2.1	1.9

4.1.5.2 Spatial Resolution

The number of line pairs per centimetre (l p/cm) detected on the catphan images with the use of AEC and FTC imaging techniques are shown in Figures 4.9 and 4.10. The highest image resolution score is based on the total number of line pairs/cm gauge that can be depicted on each image. The results of the AEC technique shows that, the images with the highest spatial resolution score were the pelvis, thorax and abdomen scan protocols with scores of 6, 5 and 5 lp/cm respectively. The other AEC images scores were; 2 lp/cm for (head) and 3 lp/cm for (lumber spine). The scores for each image are as follows; head = 2, thorax = 5, abdomen = 5, pelvis = 6, and lumber spine = 3 as depicted in Figure 4.9.

Also, the FTC technique images displayed similarly resolution score to that of the AEC technique as shown in Figure 4.10. The thorax scan protocol image showed the best spatial resolution where a score of 6 lp/cm was recorded. The pelvis scan protocol showed the second best resolution score with a value of 5 lp/cm whiles the head, abdomen and lumber spine scan protocol had scores of 3, 4 and 4 lp/cm respectively.

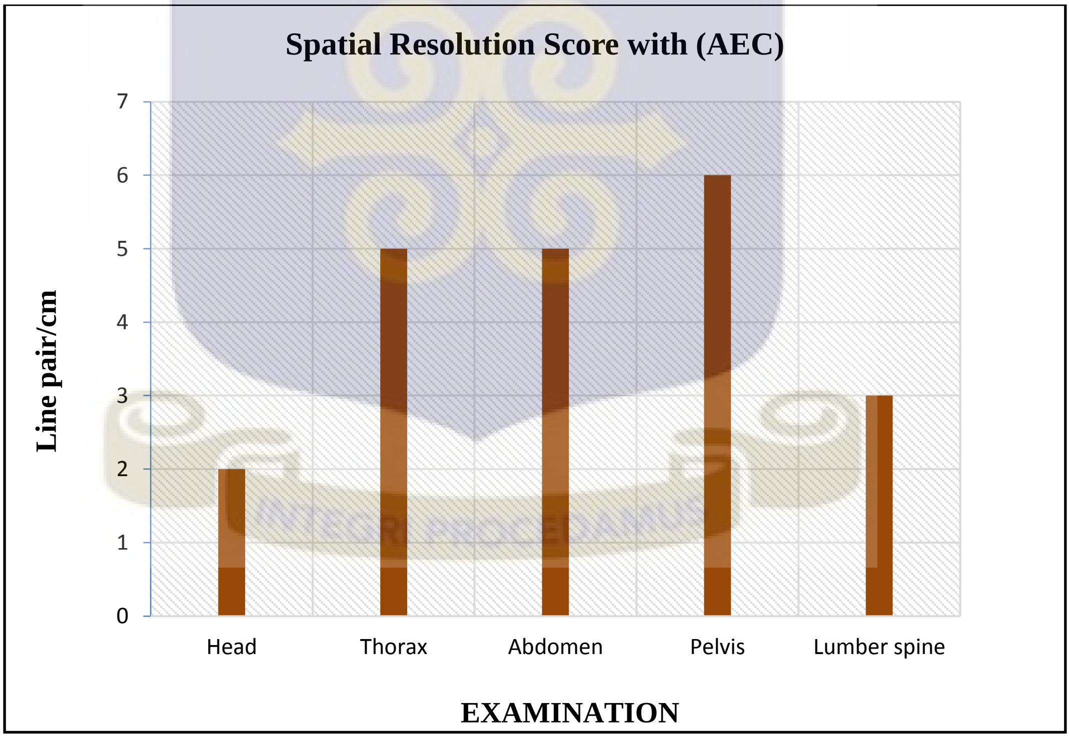

Figure 4.9: Spatial resolution (lp/cm) for AEC technique imaging procedure.

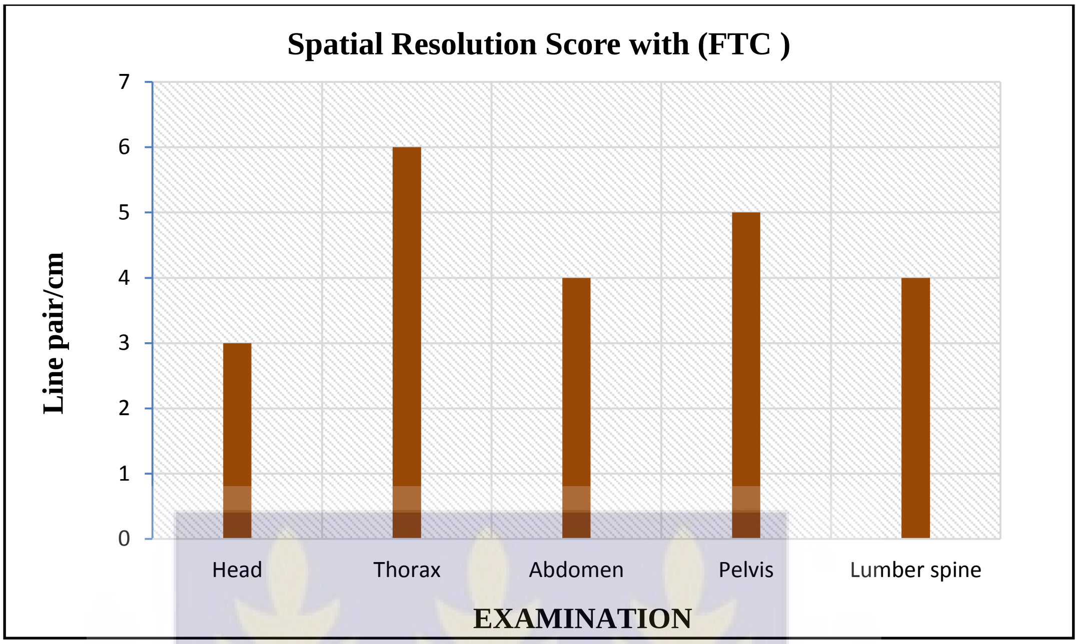

Figure 4.10: Spatial resolution (lp/cm) for FTC imaging procedure.

4.1.5.3 Low Contrast Detectability

Figures 4.11 and 4.12 show the number of visible targets in each supra-slice contrast level for the different imaging techniques. The only scan protocol image in which the 0.3% contrast level was not visible with the AEC technique is the spine scan protocol. The most targets were seen in the head and abdomen scan protocols, where a total score of 14 and 12 were recorded. However, the highest amount of targets was observed for the head and pelvis in the 1.0% contrast level. Generally, for the AEC images, the protocol that had the lowest total score is the spine routine of 8 total target score with targets scores of 5 and 3 at the 1 % and 0.5 % contrast levels respectively. The total target scores depicted by the thorax and pelvis protocol were 11 each.

Similarly with the FTC technique, the abdomen, thorax, abdomen and lumber spine images depicts the lowest score at the 0.3 % contrast level with a score of one each. The FTC image of the pelvis had the highest target count with a total of 18. The second highest total score is the head image with a target score of 16 followed by the lumber spine, thorax and abdomen with scores of 14, 13 and 13 respectively. Overall, the majority of the targets were seen in the 1.0 % contrast level in both the AEC and FTC techniques images but the FTC technique showed a much higher scores compared with the AEC technique.

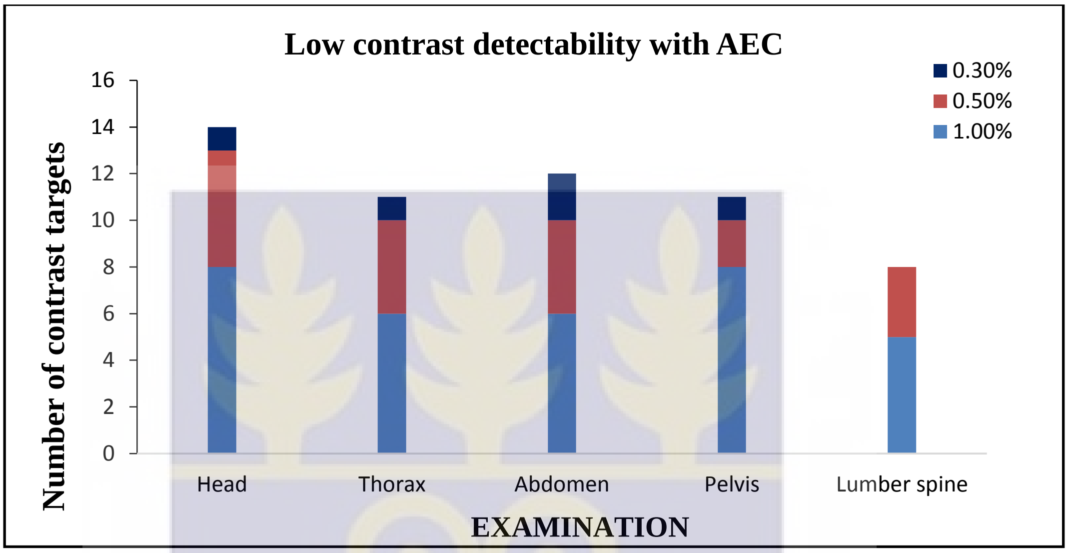

Figure 4.11: Low contrast detectability with AEC technique for the routine imaging protocols in the supra-slice contrast section.

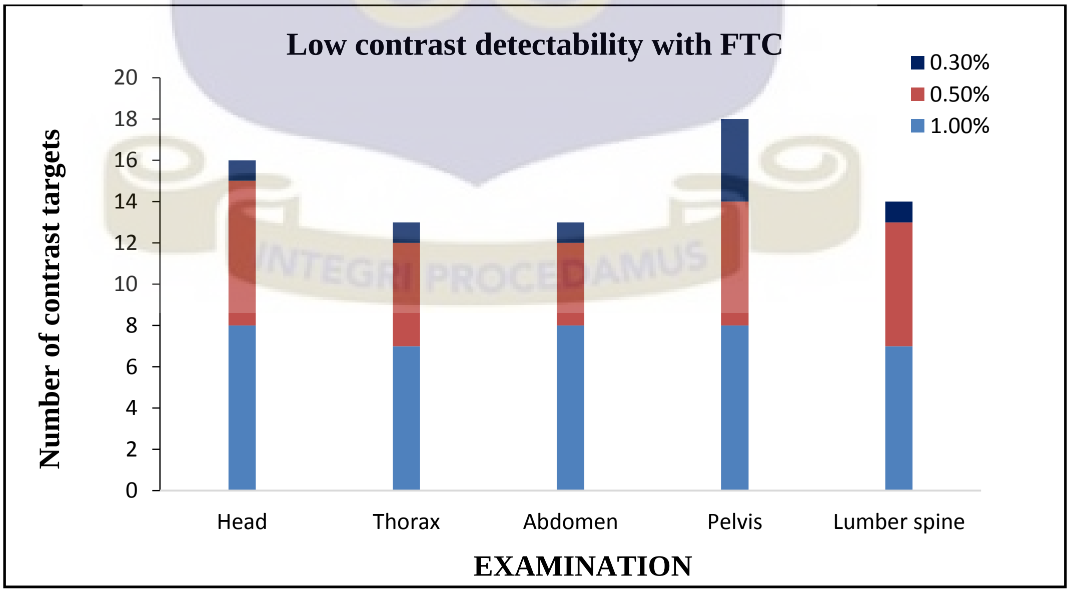

Figure 4.12: Low contrast detectability with FTC technique for the routine imaging protocols in the supra-slice contrast section.

Figures 4.13 and 4.14 depict the number of targets visible in the sub slice section of the catphan phantom for the two imaging techniques. Similar to the supra-slice low contrast evaluation, the number of targets visible in the FTC images were more than that of the AEC images. Four out of five of the 5 mm targets were visible in four of the five different AEC technique scan protocols, whereas, in the FTC technique had all the 5 mm targets visible. In the AEC technique, images of the abdomen and pelvis protocols scored 5 and 3 out of a total of 12 targets with the thorax happen to have the least score of one.

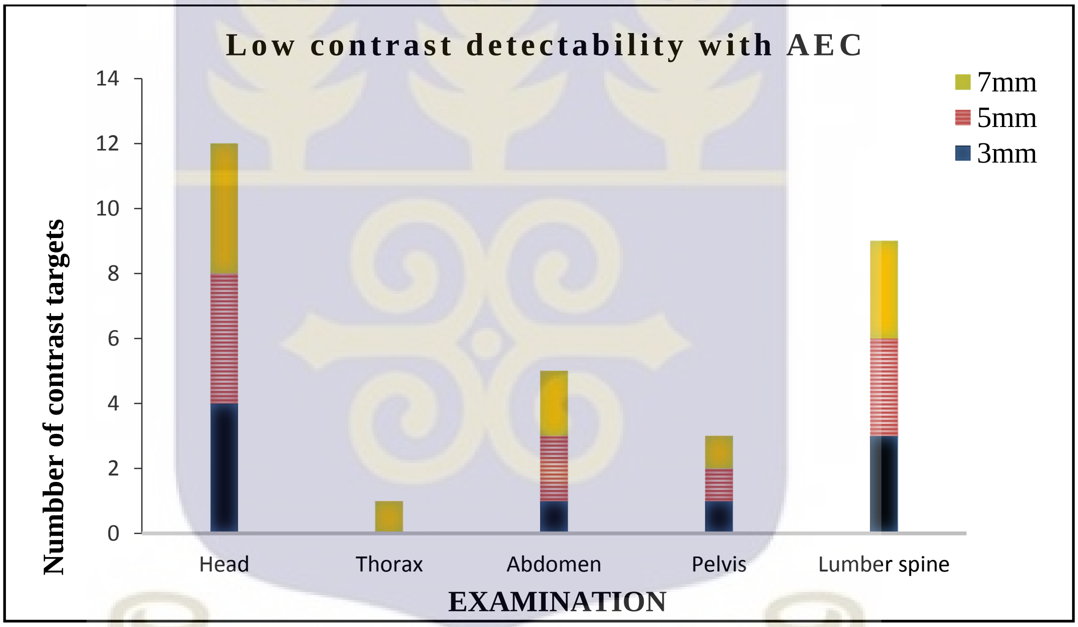

Figure 4.13: Low contrast detectability with AEC technique for the routine imaging protocols in the sub slice contrast section.

The FTC technique images had a higher number of targets visible. The head, thorax and lumber spine scored the highest with 10 each out of 12 targets, and then followed by abdomen and pelvis with 9 and 8 scores respectively. There were no targets visualised with the AEC technique thorax protocols at 3 mm and 5 mm target levels.

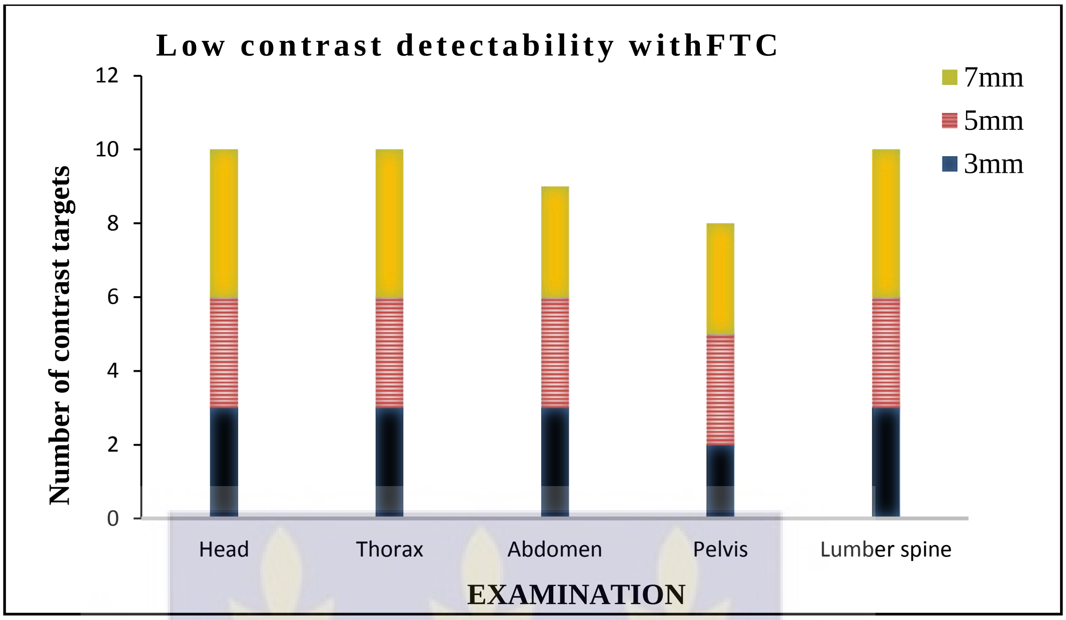

Figure 4.14: Low contrast detectability with FTC technique for the routine imaging protocols in the sub slice contrast section.

4.1.6 ANALYSIS OF IMAGE QUALITY

The scores of image-quality test, for spatial resolution, low contrast detectability, and contrast to noise ratio, for the routine examination performed with FTC and AEC techniques are summarized in appendix C. No significant difference was observed for the overall spatial resolution *(P = 0.704)* and low contrast detectability *(P = 0.187)* of image quality test for the examinations performed with the two different techniques. However, there was significant difference in the low contrast to noise ratio between the two different techniques *(P = 0.014)*. Also, the overall image noise (SD) in the images acquired showed a significant difference between the two imaging techniques *(P = 0.008)*. The background Noise (SD) level in the catphan images acquired with AEC technique were relatively higher than those with FTC technique (Tables 4.11 – 12).

4.2 DISCUSSION

In general x-ray procedures, radiation dose and image quality depends on the tube potential and tube current-time product, whiles as in CT scan they depend on tube potential, tube current, scanning time, slice thickness, scanning volume, and pitch. Changes in exposure parameters affect CT tissue attenuation values and can have similar effects on the tissue contrast. Recent CT scanners have change in their mode of operation with a wide range of facilities available on them. This called for the need to assess the dose delivered during routine CT examinations (Wade et al., 1997).

Modern CT scanners have automatic exposure control systems, which permit automatic adjustment of exposure technique factors according to the size of the patients (Huda et al., 2000). The use of fixed mAs settings would impart the same exposure to all patients, irrespective of the difference in patient sizes. If a manual protocol is used, radiation exposures to slim patients can be reduced by selecting lower exposure parameters. In contrast, AEC in CT scanners reduces patient dose by dynamic modulation of the tube current. A considerable reduction of patient dose in the range of 35-60% and 53-65% can be achieved by AEC technique in CT among young adults and paediatric patients.(Prakash, 2010; Food & Drug, 2002).

Some studies have reported substantial reduction in radiation dose with the AEC technique. A study conducted shows a 33% dose reduction for abdominal and pelvic CT examination with similar artefacts and diagnostic acceptability, using z-axis tube current modulation compared with a FTC technique (Kalra et al., 2004). Similarly, Kalra et al., 2005, reported an 18% – 26% radiation dose reduction for a chest CT study by using z-axis modulation.

The results in this study showed a mean dose reduction of 19.4% in $CTDI_{vol}$ and 18.2% in DLP for the head phantom examination with the AEC activated and manual selection of tube current. The chest examination with the body phantom, had a mean dose reduction of 59.4% in $CTDI_{vol}$ and 78.3% in DLP noted with the AEC activated and manual selection of tube current as shown in Table 4.6. The dose reduction estimated in this study for chest CT examination were quite comparable to that reported by Livingstone et al., (2010) on human subjects who underwent a contrast enhanced CT exam of the chest. Their study, which involves a 6-slice CT scanner estimated a dose reduction of up to (15% - 42%). Compared with FTC technique, a mean dose reductions of 12% in $CTDI_{vol}$ and 7.1% in DLP and 28.1% in $CTDI_{vol}$ and 56.8% in DLP were noted for abdomen and pelvis examinations using the AEC technique in this study (Table 4.7). The estimated abdomen and pelvis dose reductions compared favourably with study by Greess et al.,(2000; 1998) for abdomen and pelvic single section CT examination. Their study, reported a dose reduction of 15% and 25% which is almost similar to that reported in this study.

Estimated mean values of $CTDI_{vol}$ and DLP in this study were calculated from an average of three measurements made in the head and body phantoms for each technique. The mean values of $CTDI_{vol}$ were: 32.8 mGy, 6.7 mGy, 14.3 mGy, 11.7 mGy with the AEC technique and a range of 32.9-53 mGy, 9.5-26.2 mGy, 9.5-24.2 mGy, and 9.5-26 mGy with the FTC technique representing the head, chest, abdomen and pelvis examinations respectively. The mean values of DLP were: head (593 mGy.cm), chest (108 mGy.cm), abdomen (240 mGy.cm), and pelvis (190 mGy.cm) with the AEC technique and a range of 571-946 mGy.cm for head, 284-780 mGy.cm for chest, 165-543 mGy.cm for abdomen and 250-290 mGy.cm for pelvis with the FTC technique examinations respectively.

The $CTDI_{vol}$ and DLP values estimated with AEC activated and with FTC technique in this study show statistical significant difference for the head, chest and pelvis examinations with exception of the abdomen examination that shows no statistical significant difference (Tables 4.3-4.4). The variations in the dose metrics for the head, chest and abdomen examinations may be attributed to the imaging technique used, the mAs value and the anatomical composition of the various CT examinations conducted.

Comparison of the mean values of $CTDI_{vol}$ and DLP for the head and body phantoms obtained in this study with AEC activated was made with IAEA study-Tsapaki et al., 2006 and the European MDCT DRL, Bongartz et al., 2004 (Table 4.2). As expected, there were some variations of the dose descriptors for some of the CT examinations considered when the results in this study were compared with the reference dose levels (RDLs). With respect to the $CTDI_{vol,}$ all the examinations conducted were lower by 1-95% than RDLs of Bongartz et al., 2004 (14.5-64 mGy) and the head and chest CT of (32.8 and 6.7 mGy) were lesser than Tsapaki et al., 2006 (9.5-47 mGy) by 43% and 42% respectively except the abdomen examination which exceeds that of Tsapaki et al.,2006 (10.9 mGy) by 24% and closed to that of Bongartz et al., 2004 (14.5 mGy). The DLP values for the examinations conducted were lesser than RDLs of Bongartz et al., 2004 (267-724 mGy.cm) by 147-281% and also lesser than RDLs Tsapaki et al., 2006 (447 and 698 mGy.cm) by 313% and 190% respectively. However, the head examinations exceeds that of Tsapaki et al., 2006 (527 mGy.cm) and Bongartz et al., 2004 (337 mGy.cm) by 11% and 43% respectively. The variations in the dose descriptors between this study and the RDLs may be attributed to the exposure settings, scan length and the type of CT scanner used for the examinations.

For the FTC technique, comparison of the mean values of $CTDI_{vol}$ and DLP were made with that of Pontas et al., (2011), Turkey RDLs (2015), Ireland RDLs (2012) and

IAEA study-Tsapaki et al., 2006 (Table 4.5). From the results it's shows clearly that, the mean CTDIvol for head examinations was observed to be lesser in comparison with international RDLs reported Turkey (2015) and Ireland (2012) by up to 25% and 24.9% respectively and exceeds that of Tsapaki et al., (2006) by 11%. However, the chest, abdomen, and pelvis mean values of $CTDI_{vol}$ exceeded some of the international RDLs values reported by up to 56% and 64%, for Turkey (2015) and Tsapaki et al., (2006), 46%, 50% and 54% for Turkey (2015), Ireland RDLs (2012), and Tsapaki et al., (2006), and 26% and 53% for Ireland RDLs (2012) and Tsapaki et al., (2006) respectively.

For the DLP, the chest examinations values were higher than some RDLs reported by other studies. Some of the head DLP values were lower in comparison with those reported for the international RDLs by 0.2%, and 2% for Pantos et al., (2011), Turkey RDLs (2015) and Ireland RDLs (2012) but exceeds that of IAEA study-Tsapaki et al., (2006) RDLs by 44%. The Abdomen examination mean DLP values were lesser in comparison with Pontas et al., (2011), Ireland RDLs (2012) and IAEA study-Tsapaki et al., (2006) but were higher than RDLs for Turkey RDLs (2015) whiles the pelvis examination were slightly lower than Ireland RDLs (2012) and IAEA study-Tsapaki et al., (2006) RDLs values but exceeded that of Pontas et al., (2011), Turkey RDLs 2015. However, it is worthy of note that these findings may not imply overdosing or under dosing of patients since this study was only performed on a simple homogeneous PMMA phantom.

In CT examination, patients are exposed to high radiation dose. Therefore, the use of ordinary dose values (CTDI, or DLP) will provide less information regarding the radiation risks. Effective dose is the unit of choice in this situation and can be used for comparisons between different procedures with different imaging modalities.

Effective dose is a dosimetry quantity that takes in to accounts doses to all organs irradiated during a radiological examination as well as the radio sensitivity of each irradiated organ or tissue and also the best possible predictor of stochastic risk. In this study effective dose values for average adult has been calculated for the two different imaging techniques using CT-Expo software for some selected exams. Table 4.8 shows values of effective doses obtained for the two techniques used for the various examinations conducted.

Effective dose values with the AEC activated were; (1.6 mSv) for head, (6.4 mSv) for chest, (6.1 mSv) for abdomen and (5.4 mSv) for pelvis respectively. Whiles effective dose values with FTC technique, for head examination had values ranging between (1.4-2.8 mSv), chest exams which shows the highest had a range of (4.8-13.2 mSv), abdomen exams had a range of (3.5-9.7 mSv) and pelvis exams had a range of (3.1-8.5 mSv) respectively. The effective dose values between the two imaging technique gave variation factor ranging from 1.6 (abdomen and pelvis) to 2.0 (head and chest). Table 4.9 shows a comparison between values of effective dose of this study and values given by some institutions and researches. Considering the AEC technique, the effective dose values found in this study were all within values reported in the literature except for the chest exams which exceeded that of Goddard & Alfarsi (1999) mean reported value by 47%.

For the FTC technique, and considering only the mean values of effective doses found in this study. It is evident that the effective dose values for the head and chest exams were higher by a factor of 1.3 and 1.0 than the mean effective dose values reported by Clark et al., (2000) and Inkoom et al., (2014). Whereas the average values for the abdomen and pelvis exams were below those reported in the literature. It was observed that, the mean effective dose values for chest, abdomen and pelvis exams were below values reported by UNSCEAR, (2008) and Breiki et al., (2008) and exceeded by a factor of 1.3 and 1.2 for the head examination respectively. The effective dose values for the head are considerable less than that for the trunk regions, even though the head CTDI values for head are much higher. This could be as a result of fewer radiosensitive organs been irradiated.

For assessment of risk associated with medical diagnosis in a comprehensive manner, it is important to consider doses to different radiosensitive organs in CT examinations than evaluate the effective dose resulted. Figures (4.1-4.4) depicts the organ doses for the routine examinations conducted. For the AEC technique, organ doses obtained for the head examination were; 32.5 mGy for brain, 41.8 mGy, for eye lens and 19.7 for thyroid. The organ doses for chest examination were; 17.4 mGy for lungs, 17.1 mGy for breast, 6.4 mGy for thyroid and 17.2 mGy for oesophagus. For abdomen exams the dose to the stomach, liver, kidney and spleen were; 19.4 mGy 17.9 mGy, 20.9 mGy, and 19.2 mGy respectively. For pelvis exams the organ doses were; 18.33 mGy, 24.9 mGy, 16.5 mGy and 23.1 mGy for ovaries, uterus, testes and prostate respectively.

For the FTC technique, the dose range to the brain in the head was; 27.4-59.5 mGy, for the eye lens was 31.2-75.5 mGy and a range of 16.7-36.3 mGy for thyroid. For chest exams where somatic risk is due to doses to the lungs, breast and oesophagus which are lying directly to primary beam is possible, the range of radiation dose was 13.5-37 mGy for lungs, 14.2-38.9 mGy for breast, 4.1-11.2 for thyroid and 13.1-52.2 mGy for oesophagus. The dose range for abdomen examination was 11.3-31.1 mGy for stomach, 10.6-29.1 mGy for liver, 12.1-33.2 mGy for kidney and 11.3-30.9 mGy for spleen. In the case of pelvis exams the organ dose range was 10.4-2.6 mGy for ovaries, 14.1-38.7 mGy for uterus, 5.2-14.1 mGy for testes and 11.2-30.8 mGy for prostate.

The results of organ dose comparison between AEC activated and at fixed quality reference mAs per examination are presented in Figures 4.5 – 4.8. It is observed that, there were variation in organ doses per each examination, with the FTC technique depicting higher organ doses than the AEC activated. For instance, organ doses between the two techniques for the brain and thyroid (for head) and breast and lungs (for chest examination) varied up to a factor of 1.5 and 1.2, respectively, while for the stomach and liver (for abdomen) the variation was up to a factor of 1.0 respectively. However, organ doses obtained with the AEC activated were high up to a factor of 1.2 for the pelvic examination compared with the FTC techniques with similar trend being observed for the thyroid organ in the abdominal examination. This organ doses variations may largely be attributed to the mAs used with respect to each region anatomical built.

Comparison of organ doses with the AEC technique and the mean organ doses with the FTC technique of selected organs per examination in this study and from reported values from the literature for the United Kingdom (1991), Japan (1991), Germany (1999), and Tanzania (2006) are presented in Table 4.11. It is evident from the results that, with the exception of values reported from Tanzania, the organ doses obtained with the two imaging techniques per given examination were mostly comparable with those from other studies. For instance, the variation of organ doses between this study and reported values from the United Kingdom and Japan mostly varied by up to a factor of 1.3 (for AEC and FTC) and 1.7 (for AEC and FTC) respectively, while for Germany and Tanzania, the organ doses mostly varied by up to a factor of 1.9 for AEC, 1.8 for FTC and 1.9 for AEC, 1.6 for FTC respectively. Higher organ doses of up to a factor of 1.9 and 1.6 were observed in this study relative to that reported from Tanzania might be attributed to the different method used for estimation of organ doses whereby that of Ngaile and Msaki (2006) used the ImPACT spreadsheet based on NRPB conversion factors. Moreover, the differences in organ doses between this study and those reported in the literature for the United Kingdom, Germany, and Japan might be attributed to the variation in CT scanning protocols (i.e., kV, mAs, slice thickness, number of slices, use of contrast media, etc.) and type of scanners used.

The spatial resolution is the ability to differentiate closely located small objects. Spatial resolution was measured by viewing the images of the appropriate phantom sections. The measured spatial resolution for the AEC and FTC images for each examination considered was fairly consistent with one another, however the resolution measured in the AEC images was poorly resolved compared with the FTC technique. Figures 4.9 and 4.10 shows the number of line pair resolved for the various examinations considered using AEC and FTC techniques. For the AEC technique the number of line pairs resolved for the head, thorax, abdomen, pelvis and spine were; 2, 5, 5, 6 and 3 lp/cm respectively. For the FTC technique, 3, 6, 4, 5, and 4 lp/cm were depicted for the head, thorax, abdomen, pelvis and spine protocols respectively. A Pair t- test conducted on the overall spatial resolution scores to test the statistical significant difference between the two imaging techniques shows, no significant difference between the two imaging techniques (*P = 0.704*). In radiographic imaging, the X-ray tube focal spot size and blur occurring in the image receptor are the primary causes of reduced resolution. Although focal spot size does affect CT spatial resolution, CT resolution is generally limited by the size of the detector measurements (referred to as the aperture size) and by the spacing of detector measurements used to reconstruct the image, this concept, is known as sampling(Goldman, 2007).

Low contrast resolution in this study was measured by quantifying the smallest disc visible in each low contrast disc at 1.0%, 0.5%, and 0.3% contrast. Figures (4.11-14) depicts the low contrast detectability scores at the supra slice and sub slice sections for the two imaging techniques. Contrast resolution was measured using different slice thickness. The measured minimum resolvable low contrast target in this study for the supra slice target ranged from 5 - 2 mm at 0.5% and from 0 - 1 mm at 0.3% and 5-8 mm at 1.0% for the AEC technique respectively. For the FTC the resolvable low contrast targets range from 4-7 at 0.5%, 1-4 at 0.3% and 7- 9 at 1.0%, respectively. No statistical significant difference was noted for the supra slice low contrast detectability score between images of the two imaging techniques *($P = 0.187$).*

In the sub slice low contrast targets the resolvable targets range from 1- 4 at 3mm, 1- 4 at 5mm and 1- 4 at 7mm for the AEC technique. Whiles for the FTC technique the resolvable targets range from 2 -3 at 3mm, 3 – 5 at 5mm and 3 -4 at 7 mm targets respectively. Also, no statistical significant difference was observed in the sub slice low contrast detectability test images acquired with the two imaging techniques *($P = 0.06$).* The most significant difference between the AEC and FTC images was observed in the contrast to noise ratio test *($P = 0.0014$).* The contrast to noise ratio can be related to the overall image quality with respect to how much noise is seen in a particular image. In general, the larger it is, the less noise is viewed in an image and the quality is improved. Analysis of the results shows that the FTC technique images have the highest CNR (least noise) compared with the AEC activated images (Tables 4.13 and 4.14). This reflects the low contrast detectability results where only a few targets were visible with images that have low contrast to noise ratio.

The study has some limitations. The dose values estimated in this study were based on standard-sized PMMA phantoms and not on human subjects. As a result, there may be errors in the dose estimates due to obvious variations in patient sizes from the standard size that the phantoms assume. Also the image quality evaluation was done using a CT dosimetry Catphan phantom and not on actual patients images. It is obvious that, there may be errors in these dose values and image quality results due to obvious variations in tissue attenuation of patient to that of the Catphan. Nonetheless the dose values and the image quality results can facilitate clinical dosimetry assessment and also serve as a baseline towards establishing optimized dosimetry protocols as these doses can be compared with reference levels to assess the performance of CT scanners.

In spite of the fact that, radiation dose reduction is an important exercise, maintaining high quality of a diagnostic imaging study is also essential to provide an accurate and effective diagnosis. It is therefore worthwhile to keep a fine balance between image quality and radiation dose.

CHAPTER FIVE

5.0 CONCLUSION AND RECOMMENDATIONS

5.1 CONCLUSION

The goal of this research was to investigate the radiation doses received by patients during CT examinations and image quality with the employment of AEC and FTC techniques in Siemens 16-slice CT imaging system and state the significance of AEC when used in CT examination.

In this study, the chest examination recorded the highest dose reduction of 59.4% in $CTDI_{vol}$ and 78.3% in DLP when the AEC and FTC techniques were compared. Similarly, the head, abdomen and pelvis examinations also recorded a dose reductions in $CTDI_{vol}$ and DLP with; 19.4% and 18.2%, 12% and 7.1%, and 28.1% and 56.8% respectively. However, this is not to say that the FTC technique cannot be used for CT examinations. There was statistical significant difference observed in the $CTDI_{vol}$ and DLP values for the head, chest and pelvis examinations between the two techniques. However, in the case of abdominal examination no statistical significant difference was shown in the $CTDI_{vol}$ and DLP values between the FTC and AEC techniques. Since some FTC technique values were comparable as those obtained with AEC activated.

The effective dose values between the two imaging technique gave a variation factor ranging from 1.6 (abdomen and pelvis) to 2.0 (head and chest). The effective dose values for the AEC activated for all examinations were lower than those reported in the literature but that of the head exceeded the mean value reported by Goddard and Alfarsi (1999) by 12.5% whiles for the FTC techniques the mean values for chest, abdomen and pelvis were below those reported by UNSCEAR, (2008) and Breiki et al., (2008) except for the head which exceeded the reported values by about 31 and 19% respectively.

Dose to sensitive organs in the head, chest, abdomen and pelvis regions were estimated. There were variations of radiation dose to various organs between the two imaging techniques. The organs doses obtained with AEC technique and the mean organ doses for the FTC technique were slightly higher than reported values from United Kingdom, Germany, and Japan. However organ dose values reported from Tanzania were higher by up to a factor of 1.9 and 1.6 than that reported from this study. The main contributor for this difference is attributed to; the technique factors used, the type of CT scanners used and the scan length used in some of these countries.

In evaluating the quality of images between the two imaging techniques for the routine examinations conducted, the quality of the AEC images acquired were similar to that of the FTC in terms of spatial resolution and the supra slice low contrast detectability test scores with no statistical significant difference in the overall test results. The only major limitation in the AEC images was the presence of noise. For the sub slice low contrast detectability test and the contrast to noise ratio the FTC technique provides improved image quality over the AEC activated. The AEC images test results were much relatively lower to that of the fixed tube current technique in terms of contrast to noise ratio and sub slice low contrast detectability test scores.

Generally, we can conclude that, the results of the radiation dose and the CT images obtained for analysis shows the AEC system of the CT scanner has the potential for considerable dose reduction with improved image quality compared with the fixed tube current technique. Therefore, routine usage of the AEC techniques for CT examinations may be justify for reasonable reduction of radiation dose to the patients.

5.2 RECOMMENDATIONS

From the findings of this work, the following recommendations are made;

5.2.1 Management of Health Institutions

1. Regular training and refresher courses should be organize for CT staff to update them on current developments with regards to patients' dose management and optimization of scan protocols techniques.

2. It is recommended that, medical physicists should be assigned to CT facilities to perform regular quality control to ensure that the dose delivered are within acceptable diagnostic reference levels (DRLs) consistent with acceptable image quality to prevent excess radiation dose to patients.

5.2.2 Regulatory Authority

The Nuclear Regulatory Authority (NRA), a body responsible for supervising the use of ionizing radiation in Ghana should consider establishing national diagnostic reference in collaboration with the relevant professional bodies to serve as a benchmark for patient dose optimization in CT examinations for all CT facilities in the country.

5.2.3 Radiographers

The use of AEC systems for CT examinations should be encouraged since; it usage reduces the dose delivered to patient substantially without compromise of the image quality.

5.2.4 Further Work by the research community

1. Similar works should be conducted at health care institutions using other CT scanners from other manufacturers to investigate their dose reduction potentials since CT scanners are manufactured from different vendors with different mode of operations of the AEC system. This can serve as a base line towards establishing optimized local diagnostic reference levels.

2. A continuation of this work based on the findings should be extended to human subjects undergoing various routine CT examinations. This can be useful towards establishing standardize dosimetry scan protocols.

REFERENCES

AAPM, (2008). The Measurement, Reporting, and Management of Radiation Dose in CT (AAPM Report no.69). Report of AAPM Task Group 23 of the Diagnostic Imaging Council CT Committee.

Akbari, S. M., Ay, M. R., Asl, A. R. K., Ghadiri, H., and Zaidi, H., (2010). Experimental measurement of Modulation Transfer Function (MTF) in five commercial CT scanners. *IFMBE Proceedings* (Vol. 29).

Ataç, G. K., Parmaksız, A., İnal, T., Bulur, E., Bulgurlu, F., Öncü, T., and Gündoğdu, S., (2015). Patient doses from CT examinations in Turkey. *Diagn Interv Radiol,* 21, 428–434. http://doi.org/DOI 10.5152/dir.2015.14306.

Aweda, M., and Arogundade, R., (2007). Patient dose reduction methods in computerized tomography procedures: A review. *International Journal of Physical Sciences*, *2*(1), 1–9.

Bongartz, G., Golding, S.J., Jurik, A.G., Leonardi, M., Van Persijn, E., Van Meer ten., Rodríguez, R., Schneider, K., Calzado, A., Geleijns, J., Jessen, K.A., Panzer, W., Shrimpton, P.C., and Tosi, G., (2004). European Guidelines for Multislice Computed Tomography. Funded by the European Commission. Contract number FIGM-CT 2000-20078-CT-TIP.

Breiki, G., Abbas, Y., El-Ashry, M., and Diyab, H., (2008). Evaluation of Radiation Dose and Image Quality for Patients Undergoing Computed Tomography (CT) Examinations. *In IX Radiation Physics & Protection Conference*, 15-19 November Nasr City - Cairo, Egypt.

Brenner, D. ., McCollough, C., and Orton, C., (2006). It is time to retire the computed tomography dose index (CTDI) for CT quality assurance and dose optimisation. *Med Phys*, *33*(11),89-91.

Brix, G., Nissen-Meyer, S., Lechel, U., Nissen-Meyer, J., Griebel, J., Nekolla, E. A., … Reiser, M., (2009). Radiation exposures of cancer patients from medical X-rays: How relevant are they for individual patients and population exposure? *EuropeanJournalofRadiology*,*72*(2),342–347. http://doi.org/10.1016/j.ejrad.2008.07.009.

Bushberg, J. T., Seibert, J. A., Leidholdt, E. M., and Boone, J. M., (2012a). The essential physics of medical imaging. Lippincott Williams & Wilkins (1st ed.). Hall, New York.

Bushberg, J. T. Seibert, J. A., Leidholdt, E. M., and Boone, J. M., (2012b). The essential physics of medical imaging. Lippincott Williams & Wilkins (second edi).

Bushberg, J. T. (2012c). The essential physics of medical imaging. Lippincott Williams & Wilkins (2nd ed.). USA: Lippincott.

Bushberg, J. T. (2002). Computed Tomography." The Essential Physics of Medical. (Lippincott Williams & Wilkins, Ed.). Philadelphia:

Callstrom, M. R., Johnson, C. D., Fletcher, J. G., Reed, J. E., Ahlquist, D. A., Harmsen, W. S., … Corcoran, K. E., (2001). CT colonography without cathartic preparation: feasibility study. *Radiology*, *219*(3), 693–8.

Carlton, R. R., Adler, A. M., and Bushong, S., (2005). Principles of radiographic imaging.

Catalano, C., Francone, M., Ascarelli, A., Mangia, M., Iacucci, I., and Passariello, R., (2007). Optimizing radiation dose and image quality. *European Radiology, Supplement*, *17*(SUPPL. 6), 26–32. http://doi.org/10.1007/s10406-007-0225-6.

Clarke, J., Cranley, K., and Robinsion, J., (2000). Application of draft European commission reference levels to a regional CT dose survey. The British Journal of Radiology, 73, 43–50.

Cody, D. D., Pfieffer, D., McNitt-Gray, M. F., Ruckdeschel, T. G., and Strauss, K. J. (2012). Computed Tomography: Quality Control Manual. Jacksonville. http://doi.org/10.1016/B978-1-4160-9979-6.00377-9.

Crawley, M. T., Booth, A., and Wainwright, A., (2001). A practical approach to the first iteration in the optimization of radiation dose and image quality in CT: estimates of the collective dose savings achieved. *The British Journal of Radiology*, *74*(883), 607–614. http://doi.org/10.1259/bjr.74.883.740607

Cunningham, I. A., and Judy, P. F. (2000). Computed Tomography J. D. Bronzino (2nd Ed.)*The Biomedical Engineering Handbook*. (J. D. Bronzino, Ed.) (Second Edi).

Danthi, S. N. (2013). Computed Tomography (CT). *National Institute of Biomedical Imaging and Bioengineering*, (July).

Deak, P.D., Smal, Y., and Kalender, W. (2010). Multi section CT protocols: sex- and age specific conversion factors used to determine effective dose from dose-length product. *Radiology*, 257, 158–166.

Edyvean, S., Lewis, M. A., Keat, N., and Jones, A. P. (2003). Measurement of the performance characteristics of diagnostic X-ray system used in medicine Part III (CT). York: York publisher.

Fishman, E. K., and Jeffrey, R. B. (1998). Spiral CT: principles, techniques, and clinical applications: Lippincott-Raven Philadelphia.

Foley, S., Mcentee, M., and Rainford, L. (2012). Establishment of CT diagnostic reference levels in Ireland. *Br J Radiol*, 85, 1390–1397.

Food and Drug Administration (2006). Provision for Alternate Measure of the Computed Tomography Dose Index (CTDI) to Assure Compliance with the Dose Information Requirements of the Federal Performance Standard for Computed Tomography. Retrieved from http://www.fda.gov/MedicalDevices.

Food and Drug, Administration. (2002). FDA public health notification: Reducing radiation risk from computed tomography for pediatric and small adult patients. *Pediatric Radiology*, *32*(4), 314–316. http://doi.org/10.1007/s00247-002-0687-6

Fujii, K., Aoyama, T., Yamauchi-Kawaura, C., Koyama, S., Yamauchi, M., Ko, S., … Nishizawa, K. (2009). Radiation dose evaluation in 64-slice CT examinations with adult and paediatric anthropomorphic phantoms. *British Journal of Radiology*, *82*(984), 1010–1018. http://doi.org/10.1259/bjr/13320880.

G. Marchal, T.J., Vogl, J P., and Heiken, G. D. R. (2005). Multidetector-Row Computed Tomography*: Scanning and Contrast Protocols Barnes & Noble*. *Springer*. Springer Verlag. http://doi.org/9788847003057.

Geleijns, J., Salvadó Artells, M., de Bruin, P. W., Matter, R., Muramatsu, Y., and McNitt-Gray, M. F. (2009). Computed tomography dose assessment for a 160 mm wide, 320 detector row, cone beam CT scanner. *Physics in Medicine and Biology*, *54*(10), 3141–59. http://doi.org/10.1088/0031-9155/54/10/012.

General Electric Company. (2004). Brochure: LightSpeed Serien 2369740-142.

Georg, S., Dieter, H., and Nagel. (2014). CT-Expo:A Tool for Dose Evaluation in Computed Tomography; user's guide. *Manual*. Germany.

Goddard, C., and Alfarsi, A. (1999). Radiation doses from CT in the Sultanate of Oman. *British Journal of Radiology.*, 72, 1073–1077.

Goergen, S., Revell, A., and Walker, C. (2009). Computed Tomography (CT). *Inside Radiology*. Retrieved from http://www.nibib.nih.gov/science-education/science-topics/computed-tomography-CT.

Goldman, L. W. (2007). Principles of CT: radiation dose and image quality. *Journal of Nuclear Medicine Technology*, *35*(4), 213–225; quiz 226–228. http://doi.org/10.2967/jnmt.106.037846.

Goldman, L. W. (2008). Principles of CT: multislice CT. *Journal of Nuclear Medicine Technology*, *36*(2), 57–68; quiz 75–76. http://doi.org/10.2967/jnmt.107.044826.

Goodenough, D. (2013). Catphan 700 Manual." Phantom Laboratories Inc. Greenwich NY.

Greess, H., Wolf, H., and Baum, U. (2000). Dose reduction in computed tomography by attenuation-based on-line modulation of tube current: evaluation of six anatomical regions. *Eur Radiol*, *10*, 391–394.

Gutierrez, D., Schmidt, S., Denys, A., Schnyder, P., Bochud, F., and Verdun, F. (2007). CT-automatic exposure control devices: Nuclear Instruments and Methods in Physics Research Section A:Accelerators, Spectrometers, Detectors and Associated Equipment, 2580, 2990–995.

Hall, E. J., and Brenner, D. J. (2008). Cancer risks from diagnostic radiology. *British Journal of Radiology*, *81*(965), 362–378. http://doi.org/10.1259/bjr/01948454

Healthcare, Human Factor Group. (2006). Computed Tomography Radiation Safety Issues in Ontario Table of Contents. Appraisal. Toronto, ON, Canada.

Hidajat, N., Maurer, J., and Schroder, R. (1999). Relationships between physical dose quantities and patient dose in CT-Germany. *Br J Radiol*, 72, 556–561.

Hidajat, N., Maurer, J., Schroder, R. J., Wolf, M., Vogl, T., and Felix, R. (1999). Radiation exposure in spiral computed tomography. Dose distribution and dose reduction. Invest Radiol, 34(1), 51–57.

Huda, W., Scalzetti, E. M., and Levin, G. (2000). Technique factors and image quality as functions of patient weight at abdominal CT. *Radiology*, *217*(2), 430–5. http://doi.org/10.1148/radiol.12120134.

International Commission on Radiological Protection (ICRP), (2006). Assessing dose of the representative person for the purpose of radiation protection of the public and the optimisation of radiological protection: Annals of the ICRP Publication 101 Broadening the process. UK: Elsevier.

International Commission on Radiological Protection (ICRP), (2001). Diagnostic reference levels in medical imaging: review and additional advice. Annals of the ICRP, 31(4), 33–52. Retrieved from http://www.icrp.org/docs/DRL_for_web.pdf

Inkoom, S., Schandorf, C., Boadu, M., Emi-Reynolds, G., and Nkansah, A. (2014). Adult medical X-ray dose assessments for computed tomography procedures in Ghana – a review paper. *Journal of Agricultural Science and Technology*, 19(1 & 2), 1–9.

International Electrotechnical Commission. (2009). Medical Electrical Equipment. Part 2-44: Particular Requirements for the Basic Safety and Essential Performance of X-Ray Equipment for Computed Tomography (IEC Standa). (Geneva, Switzerland: IEC).

Jen-Pai, S. U., Twei-S hiun, J., C hiao-Yun, C. hen., Yu-Ting, K., TSYh-JYi, Hs. L., S hu-huei, L., and Chien-C, H. (2010). Automatic Tube Current Modulation versus Fixed Tube Current in Multi-detector Row Computed Tomography of Liver: Comparison of Image Quality and Radiation Dose. *Chin J Radiol*, *35*, 131–142.

Jones, D., and Shrimpton, P. (1991). Survey of CT practice in the UK. Part 3. Normalised organ doses calculated using Monte Carlo techniques. *National Radiological Protection Board. NRPB SR-250, 250.*

Jones, D., and Shrimpton, P. (1993). Normalised organ doses for X-ray computed tomography calculated using Monte Carlo techniques. NRPB-SR250. *National Radiological Protection Board (NRPB).* Chilton, UK.

Joseph, N., and Rose, T. (2013). Quality Assurance and the Helical (Spiral) Scanner, *Online Rad*. Retrieved from Retrieved from <http://www.ceessentials.net.

Jurik, A.G., Jessen, K.A., and Hansen, J. (1997). Image quality and dose in computed tomography.*EuropeanRadiology*,*7*(1),77–81. http://doi.org/10.1007/s003300050114.

Kalender, W., Wolf, H., and Suess, C. (1999). Dose reduction in CT by anatomically adapted tube current modulation: phantom measurements. *Med Phys*, *26*, 2248–2253.

Kalender, W. A. (2005). CT: the unexpected evolution of an imaging modality. *European Radiology*, *15*(Suppl 4), D21–4. http://doi.org/10.1007/s10406-005-0128-3.

Kalra, M. K., Maher, M. M., Toth, T. L., Hamberg, L. M., Blake, M. A, Shepard, J.-A., and Saini, S. (2004a). Strategies for CT radiation dose optimization. *Radiology*, *230*(3), 619–628. http://doi.org/10.1148/radiol.2303021726.

Kalra, M. K., Naz, N., Rizzo, S. M. R., and Blake, M.A. (2005a). Computed tomography radiation dose optimization: Scanning protocols and clinical applications of automatic exposure control. *Current Problems in Diagnostic Radiology*, *34*(5), 171–181. http://doi.org/10.1067/j.cpradiol.2005.06.002.

Kalra, M. K., Rizzo, S. M. R., and Novelline, R. A. (2005b). Reducing radiation dose in emergency computed tomography with automatic exposure control techniques. *Emergency Radiology*, *11*(5), 267–274. http://doi.org/10.1007/s10140-004-0395-7.

Kalra, M. K., Rizzo, S., Maher, M. M., Halpern, E. F., Toth, T. L., Shepard, J.-A. O., and Aquino, S. L. (2005c). Chest CT performed with z-axis modulation: scanning protocol and radiation dose. *Radiology*, *237*(1), 303–308. http://doi.org/10.1148/radiol.2371041227.

Kalra, M., Maher, M., and Toth, T. (2004b). Comparison of Z-axis automatic tube current modulation technique with fixed tube current CT scanning of abdomen and pelvis. *Radiology*, *232*, 347–53.

Katada, K. (2002). Characteristics of Multislice CT (Vol. 125).

Keat, N. (2005). Report 05016 CT scanner automatic exposure control systems. Medicines and Healthcare Products Regulatory Agency. London, England: ImPACT, 2005. Available at: http://www.impactscan. Org/reports/Report 05016. Accessed October 3, 2015.

Kulama, E. (2004). Scanning protocols for multislice CT scanners. *British Journal of Radiology*, *77*(SPEC. ISS.). http://doi.org/10.1259/bjr/28755689.

Lee, E. J., Lee, S. K., Agid, R., Howard, P., Bae, J. M., and TerBrugge, K. (2009). Comparison of image quality and radiation dose between fixed tube current and combined automatic tube current modulation in craniocervical CT angiography. *AmericanJournalofNeuroradiology*,*30*(9),1754–1759. http://doi.org/10.3174/ajnr.A1675.

Lewis, M. (2005). Radiation dose issues in multi-slice CT scanning. *Medicines and Healthcare Products Regulatory Agency*, 1–14.

Lewis, M. A and Edyvean, S. (2005). Patient dose reduction in CT. *The British Journal of Radiology*, *78*(934), 880–883. http://doi.org/10.1259/bjr/75960844.

Li, Y., Poulos, A., McLean, D., and Rickard, M. (2010). A review of methods of clinical image quality evaluation in mammography. *European Journal of Radiology*,*74*(3),e122e131.http://doi.org/http://dx.doi.org/10.1016/j.ejrad.2009.04.069.

Livingstone, R., Dinakaran, P., Cherian, R., and Eapen, A. (2009). A Comparison of radiation doses using weight-based protocol and dose modulation techniques for patients undergoing biphasic abdominal computed tomography examinations. *The Official Journal of Association of Medical Physicists of India*, *34*(4), 217–222.

Livingstone, R. S., Pradip, J., Dinakran, P. M., and Srikanth, B. (2010). Radiation doses during chest examinations using dose modulation techniques in multislice CT scanner. *The Indian Journal of Radiology & Imaging*, *20*(2), 154–157. http://doi.org/10.4103/0971-3026.63036.

Lois, R. (2013). CT image quality.

Mahesh, M. (2009). MDCT Physics: The Basics--Technology, Image Quality and Radiation Dose. Lippincott Williams & Wilkins.

Månsson, L. G. (2000). Methods for the Evaluation of Image Quality: A Review. *Radiation Protection Dosimetry*, *90*(1-2), 89–99.

Marchal, G., Vogl, T.J., Heiken, J.P., and Rubin, G.D., (2005). Multidetector-Row Computed Tomography: Scanning and Contrast Protocols Barnes & Noble. *Springer*. Springer Verlag. pp 141, http://doi.org/9788847003057.

McCollough, C., Cody, D., Edyvean, S., and Geise, R. (2008). The measurement, reporting, and management of radiation dose in CT. *Report of AAPM Task Group*, 1–34. http://doi.org/ISBN: 978-1-888340-73-0 ISSN: 0271-7344.

McCollough, C. H., Bruesewitz, M. R., and Kofler, J. M. (2006). CT dose reduction and dose management tools: overview of available options. *Radiographics : A Review Publication of the Radiological Society of North America, Inc*, *26*(2), 503–512. http://doi.org/10.1148/rg.262055138.

McCollough, C. H., Primak, A. N., Braun, N., Kofler, J., Yu, L., & Christner, J. (2009). Strategies for Reducing Radiation Dose in CT. *Radiologic Clinics of North America*, *47*(1), 27–40. http://doi.org/10.1016/j.rcl.2008.10.006.

McCollough, C., Guimaraes, L., and Fletcher, J. (2009b). In defence of body CT. *AJR Am J Roentgenol*, 193, 28 - 39.

McCollough, C. H., and Zink, F. E. (1999c). Performance evaluation of a multi-slice {CT} system. *Medical Physics*, 26(11), 2223–2230.

McNitt-Gray, M. F., and Geffen, D. (2006). Tradeoffs in Image Quality and Radiation Dose for CT. *Medical Physics*, *33*(6). http://doi.org/doi: 10.1118/1.2241390

Mettler, F., Weist, P., and Locken, J. (2000). CT Scanning:Patterns of use and dose. *J. Radiol Prot*, *20*(4), 353–359.

Morin, R. L., Gerber, T. C., and McCollough, C. H. (2003). Radiation dose in computed tomography of the heart. Circulation, *107*(6), 917.

Nagel, H., and Huda, W. (2002). Radiation exposure in computed tomography. *Medical Physics*.

Namasivayam, S., Kalra, M. K., Pottala, K. M., Waldrop, S. M., and Hudgins, P. a. (2006). Optimization of Z-axis automatic exposure control for multidetector row CT evaluation of neck and comparison with fixed tube current technique for image quality and radiation dose. *American Journal of Neuroradiology*, *27*(10), 2221–2225.

Ngaile, J. E., and Msaki, P. K. (2006). Estimation of patient organ doses from CT examinations in Tanzania. *Journal of Applied Clinical Medical Physics*, 7(3), 80–94.

Nishizawa, K Maruyama, T., Takayama, M., Okada, M., Hachiya, J., and Furuya, Y. (1991). Determination of organ doses and effective dose equivalents from computed tomographic examination-Japan. *Br J Radiol*, 64, 20–28.

Pantos, I., Thalassinou, S., Argentos, S., Kelekis, N., Panayiotakis, G., and Efstathopoulos, E.P (2011). Adult patient radiation doses from non cardiac examinations: a review of published results. *Br J Radiol*, 84, 293–303.

PhilipsMedicalSystems. (2008).Z-Axis Dose Modulation (Z DOM)) [online document].

Prakash, P. (2010). Modifid Chest CT Technique Reduces Patient Radiation Exposure. Paper presented in Annual meeting,. American Roentgen Ray Society *(ARRS)*. San Diego, CA, USA.

Primak, A. N., McCollough, C. H., Bruesewitz, M. R., Zhang, J., and Fletcher, J. G. (2006). Relationship between noise, dose, and pitch in cardiac multi-detector row CT. *Radiographics : A Review Publication of the Radiological Society of North America, Inc*, *26*(6), 1785–1794. http://doi.org/10.1148/rg.266065063.

Rizzo, S., Kalra, M., Schmidt, B., Dalal, T., Suess, C., Flohr, T., … Saini, S. (2006). Comparison of angular and combined automatic tube current modulation techniques with constant tube current CT of the abdomen and pelvis. *American Journal of Roentgenology*, *186*(3), 673–679. http://doi.org/10.2214/AJR.04.1513

Sabri, A. H., Ali, A., Daud, N. ., Ha, M. ., and Nasir, F.(2015). Comparison of Image Quality and Radiation Dose between Angular Automatic Tube Current Modulation and Fixed Tube Current CT Scanning of Thorax: Phantom Study. *Global Journal Of Engineering Science And Researches*, *2*(7), 183–188.

Seerman, E. (2009). Computed Tomograpy: Physical Principles, Clinical Applications, and Quality Control (third ed). USA.

Shope, T. B., Morgan, T. J., Showalter, C. K., Pentlow, K. S., Rothenberg, L. N., White, D. R., and Speller, R. D. (1982). Radiation dosimetry survey of computed tomography systems from ten manufacturers. *British Journal of Radiology*, *55*(649), 60–69. http://doi.org/10.1259/0007-1285-55-649-60.

Shope, T., Gagne, R., and Johnson, G. (1981). A method for describing the doses delivered by tranamission x-rays computed tomography. *Medical Physics*, *8*(4), 488–495.

Shrimpton, P., Hart, D., Hiller, M., Wall, B., and Faulkner, K. (1991). Survey of CT practice in the UK. part 2: Dosimetric aspects, NRPB-R249. Chilton: National Radiological Protection Board.

Shrimpton, P. C. (2004). Assessment of Patient Dose in CT. *National Radiological Protection Board*, *5*, 1–36.

Siemens. (2010). Computed Tomography; Its History and Technology. *Siemens Medical*, 1–36.

Siemens.(2004). Somatom Sensation 64 Application Guide. Siemens AG Medical Solutions.

Söderberg, M., and Gunnarsson, S. M. (2008). Master of Science Thesis Automatic exposure control in CT : an investigation between different manufacturers considering radiation dose and image quality. Physics. Lund University., Lund, Sweden.

Sookpeng, S. (2014). Investigation of CT dosimetry techniques for use in optimisation of Automatic Tube Current Modulation (ATCM) performance. University of Glasgow, Glasgow, uk.

Sookpeng, S., Martin, C. J., Gentle, D. J., and Phantom, A. (2013). A Study of Dose Distribution and Image Quality under an Automatic Tube Current Modulation (ATCM) System for a Toshiba Aquilion 64 CT Scanner Using a New Design of Phantom. *World Academy of Science, Engineering and Technology*, *7*(73), 82–88.

Su, J.-P., Jaw, T.-S., Chen, C.-Y., Kuo, Y.-T., Hsieh, T.-J., Lee, S.-H., and Lin, C.-C. (2010). Automatic tube current modulation versus fixed tube current in multi-detector row computed tomography of liver: Comparison of image quality and radiation dose. *Chinese Journal of Radiology*, *35*(3), 131–142.

Tsalafoutas, I. A., and Koukourakis, G. V. (2010). Patient dose considerations in computed tomography examinations. *World Journal of Radiology*, *2*(7), 262–268. http://doi.org/10.4329/wjr.v2.i7.262.

Tsapaki, V., and Rehani, M. (2007). Dose management in CT facility. *Biomedical Imaging and Intervention Journal*, *3*(2), e43. http://doi.org/10.2349/biij.3.2.e43.

Tsapaki, V., John E, A., Raju, S., Maria Anna, S., Anchali, K., Madan, R., … Mathias, P. (2006). Dose reduction in CT while maintaining diagnostic confidence: Diagnostic reference levels at routine head, chest, and abdominal CT – IAEA Coordinated Research Project. *Radiology*, 240, 828– 834.

United Nations Scientific Committee on the effects of Atomic Radiation (2008).UNSEAR 2008 Report to the General Assembly on Medical Radiation Exposures. *New York, NY:UnitedNations*,(Vol.I Annexes Aand B). Retrieved from http://www.unscear.org/unscear/en/publications.html.

Wade, J. P., Weyman, J. C., and Goldstone, K. E. (1997). CT standard protocols are of limited value in assessing actual patient dose. *British Journal of Radiology*, *70*(NOV.), 1146–1151.

www.rti.se, RTI Electronics, Sweden.

Yoshinori, F., Kazuo, A., Masahiro, H., Masamitchi, Shimamura Yumi, Y., Seitaro, O., and Yasuyuki, Y. (2008). Automatic tube current modulation technique for multidetector CT, it is effective with a 64-detector CT? *Radiological Physics and Technology*, *1*(1), 33–37.

Zarb, F., Rainford, L., and McEntee, M. F. (2010). Image quality assessment tools for optimizationofCTimages.*Radiography*,*16*(2),147153.http://doi.org/10.1016/j.radi.2009.10.002.

APPENDICES

APPENDIX A

Table A. 1: Head phantom measurements

CTDIvol (mGy)										
S/N	AEC	140 mAs (FTC)	160 mAs (FTC)	180 mAs (FTC)	200 mAs (FTC)	220 mAs (FTC)	240 mAs (FTC)	260 mAs (FTC)	280 mAs (FTC)	300 mAs (FTC)
1	32.83	32.9	33.4	34.45	37.17	40.97	44.64	50.65	51.36	52.95
2	32.8	33.5	33.7	35	37.9	41.9	44.7	51.2	51.4	53.4
3	32.9	32.3	33.1	33.9	36.4	40	44.6	50.1	51.3	52.5
Average	**32.83**	**32.90**	**33.40**	**34.45**	**37.17**	**40.96**	**44.64**	**50.65**	**51.35**	**52.95**
DLP (mGy.cm)										
S/N	AEC	140 mAs (FTC)	160 mAs (FTC)	180 mAs (FTC)	200 mAs (FTC)	220 mAs (FTC)	240 mAs (FTC)	260 mAs (FTC)	280 mAs (FTC)	300 mAs (FTC)
1	592.55	571	602	614.9	663.5	731.3	796.8	904.2	921.6	945.5
2	592.8	571.1	602.8	615.2	663.8	731.9	797.4	904.3	922.4	946.1
3	592.3	570.9	601.2	614.6	663.2	730.7	796.2	904.1	920.8	944.9
Average	**592.55**	**571**	**602**	**614.9**	**663.5**	**731.3**	**796.8**	**904.2**	**921.6**	**945.5**

Table A. 2: Body phantom measurements

CHEST (CTDIvol, mGy)										
S/N	AEC	80 mAs (FTC)	100 mAs (FTC)	120 mAs (FTC)	140 mAs (FTC)	160 mAs (FTC)	180 mAs (FTC)	200mAs (FTC)	210 mAs (FTC)	220 mAs (FTC)
1	6.7	9.5	11	14.3	16.7	19	21.4	23.8	25	26.2
2	6.9	10.0	11.1	14.9	16.7	19.1	21.4	24.1	25.2	26.4
3	6.5	9.0	10.9	13.7	16.7	18.9	21.4	23.5	24.8	26.0
Average	**6.7**	**9.5**	**11.0**	**14.3**	**16.7**	**19.0**	**21.4**	**23.8**	**25.0**	**26.2**
ABDOMEN (CTDIvol, mGy)										
S/N	AEC	80 mAs (FTC)	100 mAs (FTC)	120 mAs (FTC)	140 mAs (FTC)	160 mAs (FTC)	180 mAs (FTC)	200 mAs (FTC)	210 mAs (FTC)	220 mAs (FTC)
1	14	9.5	11.2	13.5	15.6	18	20	22.8	23.5	24.2
2	15.0	10.4	11.5	13.8	15.7	18.8	20.1	23.1	23.6	24.5
3	13.6	8.6	10.9	13.2	15.5	17.2	19.9	22.5	23.4	23.9
Average	**14.3**	**9.5**	**11.2**	**13.5**	**15.6**	**18.0**	**20.0**	**22.8**	**23.5**	**24.2**
PELVIS (CTDIvol, mGy)										
S/N	AEC	80 mAs(FTC)	100 mAs (FTC)	120 mAs (FTC)	140 mAs (FTC)	160 mAs (FTC)	180 mAs (FTC)	200 mAs (FTC)	210 mAs (FTC)	220 mAs (FTC)
1	11.7	9.5	11.9	14.3	16.7	19.0	21.4	23.8	25.0	26.2
2	12.3	10.1	12.1	14.4	17.1	19.8	22.0	24.1	25.9	26.9
3	11.0	8.9	11.7	14.2	16.3	18.2	20.8	23.5	24.1	25.5
Average	**11.7**	**9.5**	**11.9**	**14.3**	**16.7**	**19.0**	**21.4**	**23.8**	**25.0**	**26.2**

Table A. 3: Body phantom measurements

CHEST (DLP, mGy.cm)										
S/N	AEC	80 mAs (FTC)	100 mAs (FTC)	120 mAs (FTC)	140 mAs (FTC)	160 mAs (FTC)	180 mAs (FTC)	200 mAs (FTC)	210 mAs (FTC)	220 mAs (FTC)
1	108	284	354	426	497	568	639	710	745	780
2	108.9	284.3	354.5	426.0	497.2	568.9	639.6	710.0	745.4	780.9
3	107.2	283.7	353.5	426.0	496.8	567.1	638.4	710.0	744.6	779.1
Average	**108.1**	**284.0**	**354.0**	**426.0**	**497.0**	**568.0**	**639.0**	**710.0**	**745.0**	**780.0**
ABDOMEN (DLP, mGy.cm)										
S/N	AEC	80 mAs (FTC)	100 mAs (FTC)	120 mAs (FTC)	140 mAs (FTC)	160 mAs (FTC)	180 mAs (FTC)	200 mAs (FTC)	210 mAs (FTC)	220 mAs (FTC)
1	240	165	181	197	251	290	327	357	327	543
2	239.9	165.8	181.2	197.0	251.0	290.0	327.6	357.7	327.9	543.0
3	239.6	164.2	180.8	197	251	290	326.4	356.3	326.1	543
Average	**239.8**	**165.0**	**181.0**	**197.0**	**251.0**	**290.0**	**327.0**	**357.0**	**327.0**	**543.0**
PELVIS (DLP, mGy.cm)										
S/N	AEC	80 mAs (FTC)	100 mAs (FTC)	120 mAs (FTC)	140 mAs (FTC)	160 mAs (FTC)	180 mAs (FTC)	200 mAs (FTC)	210 mAs (FTC)	220 mAs (FTC)
1	190	250	314	376	439	502	565	658	627	690
2	190.3	250.5	314.1	376.3	439.7	502.5	565.0	658.6	627.2	690.2
3	188.9	249.5	313.9	375.7	438.3	501.5	565.0	657.4	626.8	689.8
Average	**189.6**	**250.0**	**314.0**	**376.0**	**439.0**	**502.0**	**565.0**	**658.0**	**627.0**	**690.0**

APPENDIX B

CATPHAN PHANTOM IMAGES

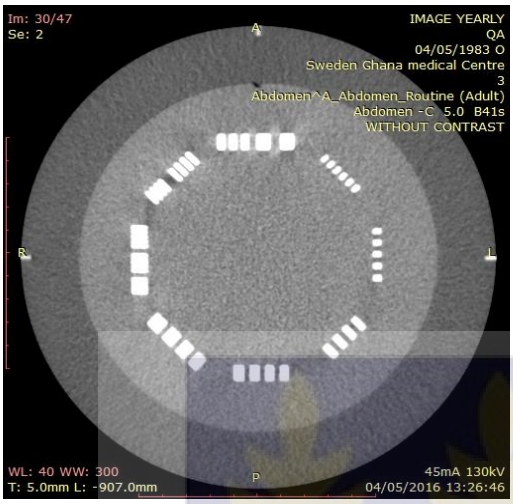

(a) Sample AEC image

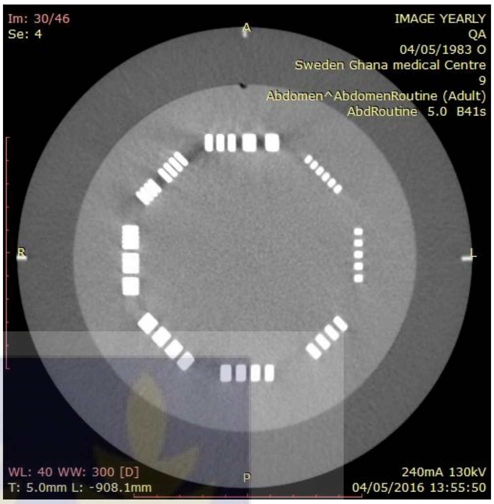

(b) Sample FTC image

Figure B. 1: Catphan image of spatial resolution module

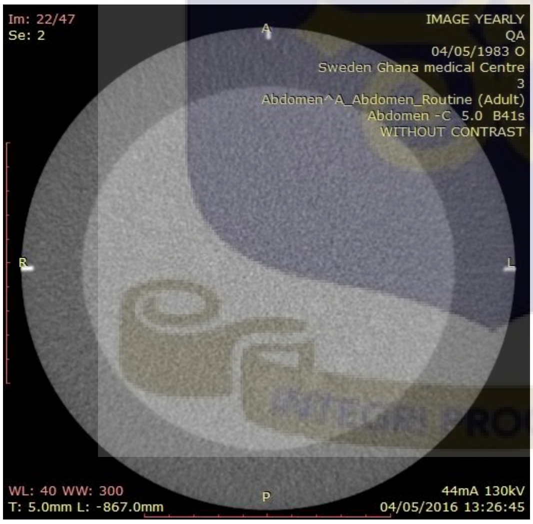

(a) Sample AEC image

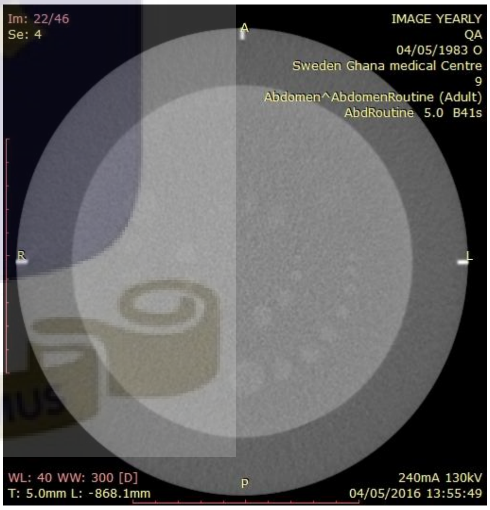

(b) Sample FTC image

Figure B. 2: Catphan image of low contrast detectability module

APPENDIX C

Table C. 1: P-values of pair t-test between the two different imaging techniques

Examination	AEC	FTC	*P - Value*
Head			
$CTDI_{vol}$ (mGy)	32.83 (± 1.02)	42.05 (± 8.12)	0.009
DLP (mGy.cm)	593 (± 18.46)	750.0 (± 147.34)	0.013
Chest			
$CTDI_{vol}$ (mGy)	6.70 (± 0.13)	18.54 (± 6.09)	3.9×10^{-4}
DLP (mGy.cm)	108 (± 2.05)	511.10 (± 177)	6.5×10^{-5}
Abdomen			
$CTDI_{vol}$ (mGy)	14.32 (± 0.02)	17.59 (± 5.46)	0.84
DLP (mGy.cm)	240.0 (± 0.35)	287.80 (± 117)	0.209
Pelvis			
$CTDI_{vol}$ (mGy)	11.70 (± 0.07)	18.63 (± 6.0)	0.01
DLP (mGy.cm)	190.0 (± 0.85)	461.10 (± 157)	4.2 x10-4

Table C. 2: P-values of pair t-test (at 95% confidence interval) on image quality between the two different imaging techniques

Image quality score	AEC	FTC	*P-Value*
Spatial resolution	4.20 (±1.64)	4.4 (±1.14)	0.704
low contrast detectability			
Supra Slice contrast level	11.20 (±2.17)	14.60(±2.07)	0.060
Sub slice contrast level	9.4 (±0.89)	6.0 (± 4.47)	0.187
contrast- to - noise ratio	1.30 (±0.59)	2.10 (0.24)	0.014
Standard deviation (noise)	8.62 (±3.41)	5.58 (±4.40)	0.008